Spring 5-15-2016

Modulation of Human and Malarial Glucose Transporter Activity by Lipids and Small Molecules

Thomas E. Kraft
Washington University in St. Louis

WASHINGTON UNIVERSITY IN ST. LOUIS

Division of Biology and Biomedical Sciences
Biochemistry

Dissertation Examination Committee
Paul W. Hruz, Chair
Colin G. Nichols, Co-Chair
Katherine Henzler-Wildman
Weikai Li
Paul H. Schlesinger

Modulation of Human and Malarial Glucose Transporter Activity by Lipids and Small Molecules

by
Thomas E. Kraft

A dissertation presented to the
Graduate School of Arts & Sciences
of Washington University in
partial fulfillment of the
requirements for the degree
of Doctor of Philosophy

May 2016
St. Louis, Missouri

Table of contents

List of figures

List of Tables

List of Abbreviations

^{3}H-2DG - ^{3}H-2-deoxy-glucose

AcGFP- Aequorea coerulescens green fluorescent protein

ATB-BMPA - 4-1-azi-2,2,2-trifluoroethyl-benzoyl-1, 3-bisd-mannos-4-yloxy-2-propylamine

CB – cytochalasin B

CFP - cyan fluorescent protein

CHS - cholesteryl hemisuccinate

compound 3361- [3-O-undec-10-en-yl-D-glucose]

DAG - palmitoyl-oleoyl-glycerol

eggPC - egg phosphatidylcholine

EPR - electron paramagnetic resonance

EPR DEER - electron paramagnetic resonance double electron-electron resonance

FC14 - Fos-Choline 14

FLIP - FLII^{12}Pglu-700μδ6

FRET- fluorescence resonance energy transfer

FSEC – fluorescence size exclusion chromatography

GLUT - glucose transport protein

IC_{50} - inhibitory concentration

IMAC- immobilized metal-affinity chromatography

LMNG - lauryl maltose neopentyl glycol

MBCD - methyl-beta-cyclodextrin

MD - molecular dynamics

MFS - major facilitator superfamily

MMV - Medicines for Malaria Venture

NMR - nuclear magnetic resonance

PA - phosphatidic acid

PE - phosphatidylethanolamine

PfHT - *Plasmodium falciparum* hexose transporter

PI - phosphatidylinositol

PIP_2 - phosphatidylinositol bisphosphate

PIs - protease inhibitors

PM - plasma membrane

POPA - palmitoyl-oleoyl-phosphatidic acid

POPE - palmitoyl-oleoyl-phosphatidylethanolamine

POPG - palmitoyl-oleoyl-phosphatidylglycerol

POPS - palmitoyl-oleoyl-phosphatidylserine

PS - phosphatidylserine

SEC – size exclusion chromatography

SLCs - solute carriers

SM - sphingomyelin

smFRET - single molecule FRET

SPR - surface plasmon resonance

TEV - tobacco etch virus

YFP - yellow fluorescent protein

Acknowledgements

I'd like to thank my mentor Paul Hruz for being always supportive of my ideas, helping me to advance my career in numerous ways, giving me so much independence and ownership of my work and just being a wonderful and most pleasant boss and colleague. I also want to thank my colleagues Maria Payne, Monique Heitmeier and Rich Hresko for their substantial work that made this dissertation and the many publications herein possible, for being my intellectual sparring partners, for career advice, for their friendship and for being the most fun colleagues I could imagine. I want to thank my collaborators Marina Putanko, Chris Armstrong, Audrey Odom, Paul Schlesinger, Colin Nichols, Katie Henzler-Wildman, Rachel Edwards, Ma. Xenia Ilagan, Andrew Quigley, Liz Carpenter, Weikai Li, Mike Autry, Kurt Peterson, Prachi Bawaskar, and David Thomas for constructive discussions, providing expertise and access to instruments, and their experimental contributions to this dissertation.

I'd like to thank my family for their support. Especially my parents Gregor and Halina for instilling a general curiosity in me and keeping me focused on my scientific career that led to this dissertation, my grandparents Alexander and Katharina for allowing me to nearly burn down their house several times during my scientific quests and for teaching me what it means to be an experimenter, and my grandparents Rudolf and Traudel for their financial support and genuine interest in my research.

ABSTRACT OF THE DISSERTATION

Modulation of Human and Malarial Glucose Transporter Activity by Lipids and Small Molecules

by

Thomas E. Kraft

Doctor of Philosophy in Biology and Biomedical Sciences

Biochemistry

Washington University in St. Louis, 2016

Professor Paul W. Hruz, Chair

Professor Colin G. Nichols, Co-Chair

Glucose transport is a fundamentally important process for maintenance and regulation of cellular metabolism in all kingdoms of life. Despite their high importance, detailed examination of glucose transport proteins in humans and parasites through biochemical, biophysical and structural properties was greatly hampered by the inability to express, purify and reconstitute sufficient amounts of active transporters. This dissertation describes strategies that led to the first successful expression, purification, stabilization and functional reconstitution of active insulin-responsive GLUT4 transport protein. Furthermore, the work described herein establishes a requirement of anionic and conical lipids for full activity of the mammalian glucose transporters GLUT3 and GLUT4, thereby extending the field of known membrane protein-lipid interactions to the family of structurally and functionally related human solute carriers. Because of its crucial role in parasite survival, the malarial glucose transporter PfHT has been extensively validated as drug target for different parasitic life stages *in vitro* and in animal models. The emergence of parasites with resistance to even the most potent existing anti-malarial drugs has made paramount the development of novel drugs that target essential

pathways for parasite survival. We identified PfHT as molecular target of the antimalarial activity of the clinically used HIV inhibitor lopinavir which had been shown previously to decrease parasite viability *in vitro*, *in vivo*, and in patients. In order to find novel PfHT inhibitors with increased potency and selectivity over human orthologs, a high-throughput assay was developed that uses fluorescence as direct readout of PfHT mediated glucose transport inhibition. Validation of this approach was demonstrated by our success in identifying several verified hits in a screen of the MMV malaria box compound library. Importantly, we identified a potent PfHT inhibitor with >10 fold higher selectivity for PfHT over its human orthologs. These findings have high potential for direct application in large-scale screens and new drug development. Taken together, this work provides a novel framework for ongoing efforts to directly target glucose transporters in the treatment of human disease.

Chapter 1 - Introduction

1.1 Sugars are used to store, transport and provide energy in all forms of life

Sugars provide energy and building blocks to all living cells. Light energy is converted into chemical energy by plants and algae through photosynthesis through conversion of carbon dioxide and water into mainly sugars which are consumed by all forms of life ranging from bacteria to fungi to multicellular organisms. In higher organisms, sugars are synthesized through gluconeogenesis. Therefore, sugars can be regarded as the predominant energetic currency and source of carbon for all non-photosynthetic forms of life. Sugar transport is an essential step in cellular metabolism. Carrier proteins mediate the regulated movement of hydrophilic sugar molecules over the hydrophobic cell membrane barrier. Most sugar transporters show high specificity for mono- and disaccharides and mediate transport either through facilitated diffusion or through proton or sodium coupled cotransport[1]. Facilitative sugar carriers of uniporters transport their substrate along a concentration gradient thereby equilibrating the intra- and extracellular concentration. Electrochemical gradients of counter-ions allow cotransporters or secondary active transporters to move substrates against concentration gradients. This process is particular important in concentrating sugar inside specific cells as observed in the reabsorption of glucose from glomerular filtrate to the blood by kidney cells[2] or in the accumulation of nutrients by bacteria[3].

1.2 Sugar transporters are part of the major facilitator superfamily

The major facilitator superfamily (MFS) encompasses structurally and functionally related facilitative and secondary active sugar transporters that share a common fold comprising 12 transmembrane helices with intracellular amino- and carboxy-termini. These sugar carriers are evolutionary conserved and can be found in different forms of life ranging from mono- and disaccharide transporters in plants[4,5], monosaccharide transporters like the recently crystallized proteins GlcP and XylE[6,7], the large family of hexose transporters in yeast[8], glucose transporters in the infectious stages of several parasites[9] or the Glucose Transport protein (GLUT) family of membrane transporters expressed in various tissues and cells of mammals[10]. Bacterial sugar transporters have been characterized in great detail using mutational and functional analysis of their substrate specificity, key residues for transport and substrate binding, and transport mechanism[11]. The most prominent example is the bacterial lactose permease LacY. Its architecture and conformational transitions have been closely examined using various structural techniques including X-ray crystallography[12], electron paramagnetic resonance double electron-electron resonance (EPR DEER) and molecular dynamics (MD) simulations. Prior to the structure determination of human GLUTs, much of the knowledge about MFS fold transporters was derived from this model protein; however, bacterial and mammalian sugar transporters differ in several important aspects. Most bacterial MFS sugar transporters function as proton coupled symporters[7,13–16] while all mammalian GLUTs with the exception of HMIT are uniporters. Additionally, they share less than 35% sequence identity[7,13,17], which complicates extrapolation from bacterial to mammalian transporters. Finally, the lipid bilayer in which these transporters are embedded in, playing an important role in regulating their activity, differs

significantly in composition and bilayer thickness between bacteria and mammals[18–20]. Therefore, it is crucial to directly study the mammalian orthologues in order to understand their function in human health and disease. The work described in this dissertation focuses on the mammalian glucose transporters GLUT3 and GLUT4 (Chapters 2 and 3) and the hexose transporter of the parasite, causing malaria in humans, *Plasmodium falciparum*, PfHT (Chapters 4 and 5).

1.3 The human GLUT glucose transporters

GLUT proteins facilitate the selective diffusion of hexose and pentose sugars down a concentration gradient in and out of cells. However, some GLUTs also transport other substrates including ascorbic acid, urea, glucosamine or myoinositol and for several GLUTs the physiological substrate is currently unknown[10,21]. The 14 GLUTs can be divided into three classes based on sequence similarity. GLUT3 and GLUT4 belong to class 1 of the GLUT family, together with GLUT1, GLUT2 and GLUT14. Class two is comprised of GLUTs 5, 7, 9 and 11 whereas GLUTs 6, 8, 10, 12 and HMIT belong to class 3. Class three can be further subdivided based on comparative genomic analyses[22]. GLUTs are fundamentally important to human metabolism as they provide a pathway for regulated cellular influx and efflux of glucose. Every human cell expresses at least one but most often a combination of several GLUT isoforms[10]. The reason for the abundance of these transporter isoforms is most likely the importance of sugar as an energy source and the need of specialized cells for transporters with specific substrate affinities, transport capacity or regulation[10]. The importance of these transporters becomes apparent by examining human diseases which are caused or aggravated by impaired GLUT

function. Class 1 transporters of have been studied in great detail and several related diseases have been identified. Several dozen mutations of the gene encoding GLUT1 (SLC2A1) cause mild to severe developmental and metabolic perturbations in individuals diagnosed with GLUT1 deficiency syndrome[23]. Gene defects in the SLC2A2 gene, affecting the function of GLUT2 result in hepatomegaly and impaired renal function, known as Fanconi-Bickel syndrome[10]. Finally, although not directly caused by mutations in the transporter, impaired GLUT4 function is the main reason for diabetes related pathology. The pathogenesis of type 2 diabetes relates to the inability of cells to respond to insulin signaling by initiating GLUT4 translocation to the cell surface.

GLUTs are encoded by the SLC2A gene family which is part of the superfamily of solute carriers (SLCs). The SLC family consists of over 400 members that are responsible for nutrient uptake, drug transport and waste removal[24]. Although, a quarter of these transporters are associated with disease in humans, they are relatively understudied[24] with crystal structures of only three members available, all belonging to the GLUT family[25–27]. SLCs are only half as often the focus of publications compared to the average over all protein families while showing by far the most uneven distribution of papers over the group members of all gene families[24]. This discrepancy can be explained by the fact that only few members were primarily studied due to their abundance in easily isolated cell types, which greatly facilitated their examination in the time before molecular biology techniques were readily available, as well as the difficulty of purifying milligram quantities of most active mammalian membrane proteins, a requirement for their biochemical and structural characterization. However, in recent years, technological advances and the development of new methodologies laid the groundwork for research aiming to close

this gap. In this dissertation, I describe the first purification of active GLUT4 transporter protein and its biochemical characterization in various lipid mimetics using several state of the art techniques to express, purify and stabilize mammalian membrane proteins (Chapter 2). GLUT4 is mainly expressed in skeletal muscle and adipose tissue. It is responsible for depositing glucose into skeletal muscle, thereby maintaining serum glucose concentrations[28]. Its activity is tightly regulated through the translocation between intracellular storage vesicles and the cell surface. Upon binding of the hormone insulin, an intracellular signaling cascade is activated that leads to the fusion of GLUT4 containing vesicles with the plasma membrane (PM)[28]. In Chapter 3, I describe an additional mechanism for modulation of GLUT4 activity. We determined that glucose transporters GLUT3 and GLUT4 require the presence of anionic phospholipids in the PM for activity and that conical lipids increase the activity of these transporters up to 6-fold in the presence of anionic lipids. This study is the first comprehensive analysis of the effect of lipids on the activity of two member of the mammalian SLC family and provides a model for the mechanism of lipid activation. By providing novel insights into the function of this class of membrane proteins, we have laid the ground work for pharmacological manipulation of their activity.

1.4 Inhibition of glucose transporter function

Transporter function is commonly manipulated using small molecules that bind the protein with high affinity and inhibit its function. Cancer metabolism and sugar uptake through human GLUTs are promising targets for cancer therapy as specific GLUT isoforms are highly expressed in certain cancer types. Cancer cells consume increased amounts of glucose which is used as

the predominant source of energy through high rates of glycolysis followed by lactic acid fermentation (Warburg effect)[29–31]. GLUT1 in particular has been targeted in preclinical studies for its high abundance in many cancer cells[32,33]. Beyond cancer, sugars are an important energy source in all cellular organisms. Therefore, glucose transport is an essential process that can be exploited for pharmacological targeting also in pathogens like protozoan parasites. Previous studies demonstrated that glucose transport is essential for the viability of infectious stages of *Trypanosoma brucei*[34–37], *Leishmania mexicana*[38,39], and *P. falciparum*[40]. Indeed, compounds that inhibit the glucose transporters of *T. brucei*[41] and *P. falciparum*[40] have been identified. The malarial glucose transporter PfHT has been extensively validated as drug target and the glucose analogue, compound 3361, has been found to inhibit viability of the parasite in different life stages *in vitro* and in animal models[42,43]. In the intraerythrocytic stage of infection, glucose is transported from blood into the erythrocyte via the abundantly expressed transporter GLUT1 where it passes freely into the parasitophorous vacuole before reaching the parasite surface. Finally, glucose uptake into the parasite is mediated through PfHT[44]. We identified PfHT as an antimalarial target of the HIV protease inhibitor lopinavir (Chapter 3) which had been shown previously to decrease parasite viability *in vitro*, *in vivo*, and in patients[45–50]. However, its mechanism of action remained unknown. Additionally, we developed a high throughput screening assay directed at identifying PfHT inhibitors with high selectivity over its human orthologues (Chapter 4). The assay has several advantages over conventional uptake assays employing radiolabeled substrates. It uses fluorescence as a direct readout of glucose uptake inhibition and can be easily adapted for other glucose transport proteins.

In summary, the work described in this dissertation helps to better understand the basic mechanism of mammalian glucose transport and provides a novel way to pharmacologically target transporters that play important roles in human diseases.

Chapter 2 – Expression, Purification, and Functional Characterization of the Insulin-Responsive Facilitative Glucose Transporter GLUT4

Thomas E. Kraft[1], Richard C. Hresko[1], Paul W. Hruz[1,2,†]

[1]Department of Pediatrics, and [2]Department of Cell Biology and Physiology, Washington University School of Medicine, St Louis MO 63110

[†]corresponding author

2.1 Abstract

The insulin-responsive facilitative glucose transporter GLUT4 is of fundamental importance for maintenance of glucose homeostasis. Despite intensive effort, the ability to express and purify sufficient quantities of structurally and functionally intact protein for biophysical analysis has previously been exceedingly difficult. We report here the development of novel methods to express, purify and functionally reconstitute GLUT4 into detergent micelles and proteoliposomes. Rat GLUT4 containing FLAG and His tags at the amino and carboxy termini, respectively, was engineered and stably transfected into HEK-293 cells. Over-expression in suspension culture yielded over 1.5 mg of protein per liter of culture. Systematic screening of detergent solubilized GLUT4-GFP fusion protein via fluorescent-detection size exclusion chromatography identified lauryl maltose neopentyl glycol (LMNG) as highly effective for isolating monomeric GLUT4 micelles. Preservation of structural integrity and ligand binding was demonstrated via quenching of tryptophan fluorescence and competition of ATB-BMPA photolabeling by cytochalasin B. GLUT4 was reconstituted into lipid nanodiscs and proper folding was confirmed. Reconstitution of purified GLUT4 with amphipol A8-35 stabilized the transporter at elevated temperatures for extended periods of time. Functional activity of purified GLUT4 was confirmed by reconstitution of LMNG-purified GLUT4 into proteoliposomes and measurement of saturable uptake of D-glucose over L-glucose. Taken together, these data validate the development of an efficient means to generate milligram quantities of stable and functionally intact GLUT4 that is suitable for a wide array of biochemical and biophysical analyses.

2.2 Introduction

The regulated glucose transport across biological membranes is of fundamental importance to maintenance of glucose homeostasis. Defects in this process contribute to several human diseases including diabetes mellitus[28]. Mammalian glucose transport is mediated by a family of membrane glycoproteins (GLUTs) that serve as passive uniporters, facilitating glucose permeation down a concentration gradient by alternating access to its glucose binding site via a proposed rocker-switch mechanism[51]. The GLUTs are members of the sugar porter subfamily of the major facilitator superfamily (MFS), one of the largest and most ubiquitous secondary transporter superfamilies[52,53]. Both the amino and carboxy termini are located on the intracellular side together with a large loop connecting helices six and seven (Fig. 2.1). GLUT1 (SLC2A1) is the most extensively characterized of the GLUTs, largely due to the abundance of expression of this protein in the erythrocyte membrane. Initially cloned by Mueckler et al in 1985[54], GLUT1 has been studied by a variety of traditional biochemical techniques including cysteine-scanning mutagenesis[55,56]. The insulin-responsive transporter GLUT4 (SLC2A4) is highly expressed in skeletal and cardiac muscle, brown and white adipose tissue and mediates the rate limiting step in regulated transport in these tissues. Although GLUT4 thus plays a key role in controlling whole body glucose homeostasis, the structure of this protein remains poorly characterized. This has been due in part to the inherent difficulties in isolating GLUT4 with retention of functional activity.

Purification of this transporter is the prerequisite for all structural and dynamic studies like X-ray crystallography, NMR, EPR or single molecule FRET. Additionally, experiments studying the effect of different membrane lipids on GLUT4 function are difficult without reliable purification

and reconstitution of active protein. Most of these approaches require hundreds of microgram to milligram quantities of this protein. Additionally, reconstituting the protein into membrane mimetics like detergent micelles, amphipols, nanodiscs and liposomes that stabilize the protein for several days in its properly folded, active conformation is crucial for subsequent biochemical and structural experiments. In spite of the availability of various expression systems and purification techniques, mammalian membrane proteins continue to pose a considerable challenge for large scale, functional purification due to their instability once isolated from their native lipid environment. Another major hurdle for the purification of mammalian membrane proteins is successful solubilization by detergents. The choice of detergent is critical as it needs to be harsh enough to solubilize the protein from its native lipid environment but mild enough to stabilize its three-dimensional structure and preserve activity. Here we report the first successful large scale expression, purification, stability optimization and functional reconstitution of the mammalian insulin responsive glucose transporter GLUT4.

2.3 Results and Discussion

Expression

We tested several expression systems in our laboratory including *E.coli, S. cerevisiae* and insect SF9 cells for over-expression of GLUT4 with only limited success. Difficulties encountered in these systems have included poor transporter expression, protein misfolding with generation of inclusion bodies, and production of GLUT4 lacking detectable glucose transport activity. Although GLUT4 has previously been expressed in *P. pastoris*, presence of protein in a monomeric state and functional activity could not be demonstrated[57]. Prokaryotes lack post-translational modifications and differ in the membrane lipid composition from eukaryotes, two important characteristics that often determine the successful use of a heterologous expression system[58]. In general, these hosts either do not express sufficient quantities or yield poorly folded protein. We utilized the mammalian cell line HEK293 to expresses over 1.5 mg of functional GLUT4 per liter of culture. Using a modification of the protocol previously reported by the Stroud lab[59], we created a stably GLUT4 expressing, tetracycline inducible HEK293S GnTI$^-$ cell lines. After selecting the highest expressing cell line from 10 individual clones, expression was verified by western blot analysis (Fig. 2.2A). Functional activity of the expressed transporter was tested by comparing radiolabeled ^{3}H-2-deoxy-glucose (^{3}H-2DG) uptake into tetracycline induced and uninduced cells as well as untrasfected control HEK293 GnTI$^-$ cells (Fig. 2.2B). Induced cells overexpressing GLUT4 showed a more than two-fold increase in glucose uptake over background (uninduced and untransfected). This uptake could be completely inhibited by the GLUT specific inhibitor cytochalasin B (CB). We further analyzed intracellular protein localization by expressing GLUT4 tagged with AcGFP at the protein carboxy-terminus. In

addition to the plasma membrane, large amounts of the protein were found in intracellular vesicles, resembling the native state of the protein[28]. The transporter is known to undergo significant post-translational processing[60,61]. GLUT4 expression levels were monitored over time using western blot analysis of whole cell lysates which peaked at 72h post induction (Supplementary figure 2.1). The HEK293S GnTI- clone showing the highest GLUT4 expression was grown up in adherent culture and transferred to suspension culture. Cells in suspension culture were grown at 1-4x10^6 cells/ml in square bottles on an orbital shaker and harvested 72h post induction with tetracycline.

Detergent screening

It is imperative to find a detergent that solubilizes GLUT4 efficiently from its lipid environment while maintaining native three-dimensional fold and function. Currently, large libraries of detergents have to be screened to empirically identify suitable candidates as there is no way to predicting *a priori* the best detergent for a newly purified membrane protein. We used fluorescent-detection size exclusion chromatography (FSEC) to rapidly detect oligo-or monomeric state, stability and overall homogeneity to rank different detergents for downstream purification and biochemical studies of the protein. HEK293S GnTI$^-$ cells, transiently expressing AcGFP, linked to GLUT4's C-terminus were harvested, homogenized and split into several aliquots. Each aliquot containing whole cell homogenate was treated with 1% detergent and subjected to size exclusion chromatography following detection of whole protein absorption and AcGFP fluorescence. Large void volume peaks are indicative of detergents leading to protein aggregation and misfolding. Shape and peak area of the monomer peak are excellent indicators of protein quality. Detergents with high solubilization efficiency that

stabilize a homogeneous population of GLUT4 will result in monodisperse, symmetric peaks whereas detergents that lead to multiple conformations or aggregated states will result in polydisperse, asymmetric peaks, often at higher stokes diameter. We screened 29 detergents from different classes using the FSEC method and identified LMNG and the fos-choline 13-16 family as suitable detergents for the detection of monomeric, symmetric peaks with minimal void peaks (Fig. 2.3A-C). We further tested GLUT4 stability in commonly used detergents like DDM, DM and Triton X-100. DDM had previously been identified as the detergent of choice for purifying GLUT4[57]. We found LMNG to be superior compared to the other tested detergents in stabilizing GLUT4 over several days (Fig. 2.4). This stability is crucial for successful protein crystallization trials, which require maintenance of homogenous protein for several days to weeks to facilitate crystal formation. Detergents that lead to heterogeneous protein populations will have a low likelihood of yielding highly diffracting crystals. LMNG belongs to a novel class of detergents that have shown great potential in solubilizing and stabilizing membrane proteins compared to conventional detergents[62,63]. In order to further increase stability of GLUT4 in detergent we screened several additives that were previously reported to stabilize membrane proteins. Non-detergent sulfobetaines in particular have been shown to prevent protein aggregation and help protein folding[64,65]. Glycerol is also well known for its stabilizing effect on both soluble and membrane proteins[66,67]. Additionally, we tested several compounds that are known to bind to the transporter and possibly lock it into a single conformational state[68,69]. Cytochalasin B is a tightly binding glucose transport inhibitor, locking GLUT4 into its inward facing conformation[69], thus stabilizing it. We found that glycerol has a similar beneficial effect on transporter stability while allowing free movement between

different conformations (Supplementary Fig. 2.2). These results correlate with the findings of Boulter *et al.* on GLUT1 stability[70]. We have observed that using glycerol in all purification and subsequent characterization steps allows for increased flexibility in temperature and analysis time.

Purification

We tested several purification strategies with various tags on GLUT4. The protein is largely tolerant of modification at both the N- and C-terminus as well as the extracellular loop between helix 1 and 2[71–73]. We tested purification using a 9x-His tag, a Strep-tag, a Twin-Strep-tag and a FLAG tag at both the N- and C-termini. All experiments described in this manuscript were conducted using the FLAG and His-tagged constructed depicted in Fig. 2.1. Use of anti-FLAG affinity gel produced highly concentrated, nearly homogenous protein that could be further purified to greater than 95% purity in a single size exclusion chromatography (SEC) step (Fig. 2.5A, B). Due to the high affinity of the resin to the FLAG tag, more than 90% of the GLUT4 in whole-cell lysate were bound after a three hour incubation time. In contrast, having tested various Strep-Tactin resins and optimized conditions for binding of the strep-tag II and twin-strep tagged GLUT4 also in combination with prior IMAC purification, we found only 5-10% of total GLUT4 in whole cell lysate to be bound which is a loss of 90-95% of protein. However, the eluted protein showed high purity. We conclude that because FLAG affinity gel has an over 300 times higher affinity for the FLAG tag compared to Strep-Tactin for the strep-tag II[74,75], it is therefore better suited to purify proteins of low abundance like membrane proteins expressed in mammalian culture systems.

Using the immobilized metal-affinity chromatography (IMAC) with His-tagged GLUT4 more than 60% of the tagged protein was bound but even stringent washing steps or binding in the presence of imidazole led to an elution product insufficient purity for further isolation using SEC. Mammalian cells have a high natural abundance of proteins containing consecutive histidine residues that often lead to contaminations in IMAC purifications[76]. Additionally, the IMAC system is often not suitable for purifications of proteins with low abundance that require greater than 100-fold enrichment[77] as we experienced in the case of GLUT4 expressed in HEK293S cells.

The only disadvantage to using anti-FLAG affinity gel compared to the other tested methods is the greatly increased cost, especially as the affinity of the gel decreased significantly after one use in whole cell lysate. Purification using anti-FLAG affinity resin and one SEC step routinely yields 600-700µg of >95% pure protein per liter of cell culture with recovery of ~50% of expressed protein after all purification steps. Both N- and C-terminal tags could be cleaved completely within three hours using TEV protease.

Testing correct protein folding by ligand binding

To verify that GLUT4 was correctly folded after purification and to test the ability of the detergents identified in the FSEC screen to maintain functional activity, we first determined the binding of known GLUT4 inhibitors by fluorescence quenching and a competition binding assay. All class 1 (GLUT1-4) and class 3 (GLUT6, 8, 10, 12) share two conserved tryptophan residues (W404 and W428) located within the glucose permeation path that are involved in binding of inhibitors like CB and conferring substrate specificity[78]. Cytochalasin B binds to and locks GLUT4

in its inward facing conformation[79]. To explore the binding site of CB we created a model of GLUT4 in the inward open conformation based on the crystal structure of GLUT1 and docked CB to it. In this model CB binds to GLUT4 in direct contact of the two tryptophan residues and possibly quenches their fluorescence by changing the polarity of their environment (Fig. 2.6A, B). Binding of CB has been shown to quench the fluorescence of these residues in GLUT1, both in intact membranes and in detergent indicating proper folding of the transporter as all twelve helices have come together in the correct geometry to create the CB binding site within the glucose permeation path[70,80]. In Figure 2.6D, we show for the first time that GLUT4 tryptophan fluorescence is quenched by CB with a dissociation constant K_{ds} of 1.4 μM. The emission maximum at 345nm shifts to a lower wavelength and its intensity is reduced by roughly 20% (Fig. 2.6C). These observations are in agreement with CB quenching for purified GLUT1[70] and indicate correct folding of the LMNG purified GLUT4. Additionally, we determined ligand binding and competition of GLUT4 in LMNG by testing the binding of the photolabel ATB-BMPA and the ability of CB to compete for ATB-BMPA binding[81]. ATB-BMPA contains the glucose analogue bis-mannose and is known to bind at the glucose binding site of class 1 transporters[68] (Fig 2.7A). ATB-BMPA binds to folded GLUT4 in LMNG in comparison to heat denatured GLUT4 (Fig 2.7B) and the amount of CB competition is comparable to GLUT4 in native lipid membranes[82].

We also measured tryptophan quenching of GLUT4 purified in Fos-Choline 14 (FC14). The SEC peak of purified GLUT4 in FC14 shifts towards a higher molecular weight, indicating dimerization, aggregation or partial misfolding of the protein (Supplementary Fig. 2.3A). Titration of CB confirmed this observation as tryptophan fluorescence could not be quenched

for GLUT4 in FC14 micelles compared to LMNG (Supplementary Fig. 2.2B). Since in contrast to the observed effect of CB on GLUT4 in LMNG micelles the transporter in FC14 micelles does not appear to bind this ligand, we conclude that the protein is most likely misfolded in this detergent environment.

Increased stability in different membrane mimetics

Various molecules like detergents, amphipols, nanodiscs or liposomes have been identified to mimic the lipid bilayer environment surrounding a membrane protein in the cell. Each mimetic exhibits specific advantageous properties: Detergents envelop membrane proteins in micelles and are generally inexpensive, available with various chemical modifications like deuteration and are the number one mimetic for crystallization studies[83]. Amphipols do not form micelles but wrap around the hydrophobic core of the membrane protein thereby stabilizing it while eliminating problems like phase separation or viscosity increase due to a lack of free polymer in solution[84]. Nanodiscs are formed by a scaffold protein belt that envelopes a lipid bilayer disc in which a membrane protein is inserted. A major advantage of nanodiscs is their similarity to the cellular lipid bilayer. This can allow investigation of the membrane protein in a near native environment with determination of direct effects of lipids on protein structure, function and dynamics. The ability to modulate nanodisc size by varying the scaffold protein used provides a platform for many different applications including nuclear magnetic resonance (NMR), electron paramagnetic resonance (EPR), surface plasmon resonance (SPR) or single molecule FRET (smFRET). An important feature of nanodiscs is that simultaneous access is provided to both sides of the membrane surface. While facilitating investigation of protein and small molecule

interactions, this system does not allow for the direct measurement of transport activity. Liposomes are the closest to a native environment for membrane proteins, allowing lateral diffusion and generating curvature. The most important application for liposomes are functional studies as they generate an outside and an inside compartment for the membrane protein, allowing uptake studies for transporters and channels. Several recent reviews have presented additional details on the relative strengths and limitations of different membrane mimetics[85,86]. We developed reconstitution protocols for GLUT4 in these membrane mimetics to increase stability and allow studying of this transporter using various techniques. The SEC profile of GLUT4 has been a good indicator of stability and aggregation and correlates with the ability of the protein to bind inhibitors and take up glucose. Reconstituting GLUT4 in the amphipol A8-35 greatly increased the protein stability at elevated temperature (Fig. 2.8A) and increased the possible NMR acquisition time at 35°C from 2 to 36 hours without detecting protein aggregation by comparing peak intensity and chemical shifts over time. A8-35 was even able to refold GLUT4 after high pH-induced partial unfolding (Fig. 2.8B). To test correct protein folding and function we tested CB binding by tryptophan fluorescence quenching and confirmed a similar K_{ds} as already shown for GLUT4 and GLUT1 in detergent (Fig. 2.8C). Nanodiscs can be used to study the influence of lipid composition on the structure and dynamics of GLUT4 by NMR, EPR and smFRET. To demonstrate that GLUT4 could be successfully reconstituted into nanodiscs, we tested two different detergents to solubilize the lipid for the nanodisc assembly step and compared GLUT4 binding to known ligands as described in Fig. 2.7A using ATB-BMPA. Reconstitution using either cholate of Triton X-100 yielded monomeric SEC peaks (Fig. 2.9A). GLUT4-nanodiscs reconstituted using Triton X-100 bound approximately 70%

of ATB-BMPA per total GLUT4 compared to cholate, indicating a higher percentage of correctly folded transporter in cholate reconstituted nanodiscs (Fig. 2.9B).

To truly measure GLUT4 function, the purified transporter needs to be reconstituted into a lipid membrane that separates two distinct compartments allowing quantification of glucose transport. We reconstituted LMNG purified GLUT4 into liposomes and measured zero-trans specific uptake of radiolabeled ^{3}H-D- and nonspecific ^{3}H-L-glucose (Fig. 2.10). We conclude that purified GLUT4 is functional and shows characteristic saturable uptake of D-glucose over L-glucose in liposomes. Beyond proving function of purified GLUT4, this assay allows us to determine the effect of individual lipid properties like chain length, charge and headgroup on GLUT4 function and correlate that data with disease phenotypes where an altered lipid composition is observed.

2.4 Conclusion

Major technical advances including the growing availability of novel detergents, improved cell expression systems, the development of artificial membrane mimetics more closely resembling native lipid environments, and expanding knowledge of the utility of small molecules to stabilize protein conformation have greatly contributed to the successful isolation and biophysical characterization of mammalian membrane transporters. Building upon this foundation, we have developed a highly robust and reliable system to generate sufficient quantities of homogenous functionally intact GLUT4 for biophysical analysis and have provided a framework for future characterization of the structure and dynamics of this protein. Thus, the most significant roadblock to the determination of membrane protein structure has been

largely overcome for GLUT4. With this success in hand, an accelerated pace of discovery both in elucidation of the structural and dynamic underpinning of glucose transport and the development of innovative means to manipulate transporter activity are now on the immediate horizon.

2.5 Materials and Methods

Cell Culture

DMEM and calcium-free DMEM were purchased from US Biological (Salem, MA). Adherent HEK293 cells were grown in DMEM at 5% CO_2 in a humidified incubator and split before they reached confluency. Suspension culture HEK293S GntI$^-$ cells were grown in 2 liter square bottles on orbital shakers (220rpm) in custom made DMEM medium according to[59] with the addition of 60 mg/l dextran sulfate (M_r 5000). Cells were grown at a density of 0.5-4.5*10^6 cells/ml and spun and resuspended into fresh media every 3 days. Stable cell lines expressing GLUT4 under a tet-on-promotor were induced 72h before harvest according to[59]. Cells were spun and resuspended at 2-3*10^6 cells/ml in fresh medium with the addition of 3g/l Primatone RL (Sigma-Aldrich), 2g/l D-glucose (Sigma-Aldrich), 5mM sodium butyrate and 2mg/l doxycycline hyclate (Sigma-Aldrich).

Molecular Biology

Purification tags and protease cleavage sites were introduced via PCR according to[87] using Phusion Hot Start II High-Fidelity DNA Polymerase from Fisher Scientific. We used GLUT4 from *R. norvegicus* as template and added a FLAG tag (DYKDDDDK) followed by a triple glycine linker

and a TEV protease site (ENLYFQS) followed by a triple glycine linker to the N'-terminus as well as a triple glycine linker followed by a TEV protease site, a triple glycine linker and a deca histidine tag to the C-terminus. This construct was placed within the multiple cloning site of the pACMV-tetO vector[88] using SalI and NotI restriction enzymes to create the pACMV-tetO-FT-G4-TH plasmid. To create a GLUT4-AcGFP fusion protein, we attached the AcGFP gene (Clontech) to the carboxy-terminus of GLUT4, separated by a triple glycine linker in the pACMV-tetO plasmid via PCR according to[87].

Generation of stable cell lines

Stable cell lines were generated according to[59]. HEK293 GnTI$^-$ cells (ATCC® CRL-3022) were stably transfected, first with the SapI linearized pcDNA6/TR vector (life Technologies) to create a tetracycline inducible cell line, then with the SmaI linearized plasmid pACMV-tetO-FT-G4-TH using the Optifect Transfection Reagent (life Technologies) according to the manufacturer's instructions. Cells that stably incorporated the plasmid into their genome were selected using 5 µg/ml blasticidin (pcDNA6/TR) and 2 mg/ml geneticin (pACMV-tetO-FT-G4-TH). Ten single colonies were isolated using cloning cylinders (Sigma Aldrich CLS31668) and expanded to 6-well plates. 72 hours after induction with 2 µg/ml doxycycline, cells were harvested, lysed and solubilized using 1% (v/v) Triton X-100. Highest expressing clones were identified using western blot analysis of cell lysate against polyclonal GLUT4 antibody (custom produced by Invitrogen using a peptide corresponding to the 16 carboxyl-terminal residues of GLUT4).

2-DOG uptake into HEK293 cells

Uptake of [^{3}H]-2DOG into HEK293 cells was measured in HEPES buffered saline solution at room temperature for 4 min as described previously[68]. Cells were previously glucose starved for 30 min at room temperature in HEPES buffered saline solution.

Detergent and additive screening

We screened several detergent families (Anatrace) and the additives glycerol (Sigma Aldrich), cytochalasin B (Enzo Life Sciences), D-glucose (Sigma Aldrich), indinavir sulfate (Fisher) and NDSB-256 (VWR) using the fluorescent size exclusion method according to Kawate and Gouaux[89]. HEK293 GnTI$^-$ cells were transiently transfected using pACMV-tetO-FT-GLUT4-GFP plasmid using the Optifect Transfection Reagent (life Technologies) according to the manufacturer's instructions. Cells were lysed in PBS buffer with 30 strokes of a dounce homogenizer, split into multiple aliquots and solubilized for 1.5h at 4°C by addition of various detergents to 1% (w/v). After ultracentrifugation, the supernatant was injected on a Superdex 200 10/300 GL column (GE Lifesciences) with buffer A (50 mM potassium phosphate, 150 mM NaCl, 0.1% (w/v) DDM, pH 7.4) and GLUT4-AcGFP fluorescence was detected using a Waters 474 scanning fluorescence detector (Ex = 475nm, Em = 505nm).

Purification

Frozen cell pellets were thawed in a 30°C water bath and resuspended in buffer B (50 mM potassium phosphate, 150 mM NaCl, 15 % (vol/vol) glycerol, 3 mM EDTA, protease inhibitor (Sigma Aldrich), 1 µg/ml DNAse I (Roche) and 1mM PMSF (Fisher)). Cells were broken by passing them through a microfluidizer at 13,000 psi four times. Membrane proteins were solubilized by addition of 0.75% (w/v) LMNG (Anatrace) and rotated at 4°C for 1h. Cell lysate was spun at

75,000 x g for 45min at 4°C and the supernatant was filtered through a 0.45 µm filter to remove insoluble matter. The filtered supernatant was incubated with washed M2 anti-FLAG affinity gel (Sigma Aldrich) according to the manufacturer's instructions for 3h with rotation. GLUT4 bound FLAG affinity gel was collected in a column and subjected to extensive washing with 30 column volumes of buffer C (50 mM potassium phosphate, 150 mM NaCl, 15 % (vol/vol) glycerol, 3 mM EDTA, complete protease inhibitor (Roche), 0.1% (w/v) LMNG, pH 7.0. GLUT4 protein was eluted with six subsequent additions of 0.5 column volumes elution buffer (buffer C containing 200 µg/ml FLAG peptide, 100 µg/ml 3x FLAG peptide (ApexBio)). Protein containing fractions were pooled and tags were cleaved with TEV protease (plasmid purchased from Addgene) at a ratio of 1:20 TEV:GLUT4 over night at 4°C in the presence of 1mM DTT. The cleaved protein was concentrated using a VIVASPIN 6 PES 10000 MWCO concentrator (Sartorius Stedim) and purified via size exclusion chromatography (SEC) using a Superdex 200 10/300 GL column (GE Lifesciences) with buffer D (50 mM potassium phosphate, 150 mM NaCl, 0.1% (w/v) LMNG, pH 7.0). Purity was assessed via SDS gel electrophoresis with IRDye Blue protein staining (LI-COR).

Modeling and docking

GLUT4 structure was predicted using the I-TASSER webserver[90–92]. We chose a model that resembled the inward open conformation based on the crystal structure on the close homologue GLUT1[13]. Docking was performed using AutoDock Vina[93]. The receptor was prepared using MGLTools version 1.5.6 and the ligand CB was prepared using ArgusLab. The docking process was completed with number of modes of 50 and exhaustiveness of 50. The results in each attempt were 20 similar docked poses. Docked poses were displayed using PyMOL version 1.7.4.0.

Fluorescence quenching

Cytochalasin B binding to GLUT4 was measured by tryptophan quenching according to[70]. SEC purified protein was equilibrated in a 50µl quartz fluorometer cell (Starna Cells, 16.50F) for 10min at 25°C in a Cary Eclipse Fluorescence Spectrophotometer (Varian) with circulating water bath. CB was added from a stock solution in DMSO.

Ligand binding assay

Binding of the biotinylated bis-mannose compound ATB-BMPA in the presence and absence of 20µM CB was determined according to[68]. After photolabeling, GLUT4 was repurified using M2 anti FLAG antibody (Sigma Aldrich) and analyzed by western blot using fluorescently labeled streptavidin (IRDye 800CW, LI-COR).

Reconstitution into membrane mimetics

Amphipol- GLUT4 was eluted in elution buffer at pH 8.0 to stabilize the amphipol. After the addition of A8-35 amphipol (Anatrace) at a ratio of 1:4 (w/w) GLUT4:amphipol the protein was rotated for 15 minutes at room temperature. After addition of Amberlite XAD-2 (Sigma Aldrich) in excess to remove detergent and TEV protease as described before we incubated the protein on a rotator at 4°C overnight. GLUT4 in amphipol was separated from Amberlite beads using a column and purified by SEC with buffer E (50 mM potassium phosphate, 150 mM NaCl, pH 8.0).

Nanodiscs- GLUT4 nanodiscs were assembled according to Sligar and coworkers[94]. Briefly, lipids dissolved in chloroform (Avanti Polar Lipids) were dried down (EggPC:POPE:POPA 70:15:15 molar ratio) and resuspended in buffer C containing either 100mM sodium cholate or 100mM triton X-100 to a final lipid concentration of 50mM. The sample was purged with argon and

vortexed/sonicated until the solution was clear. Lipid, MSP1E3D1 scaffold protein and purified GLUT4 in LMNG were combined at a molar ratio of 130:1:0.1 and rotated for 30 min at 4°C. Detergents were removed by the overnight addition of Amberlite XAD-2. After removal of Amberlite XAD-2, GLUT4 containing nanodiscs were separated from empty discs by purification using M2 anti-FLAG affinity gel and SEC as described above.

Liposomes-GLUT4 containing liposomes were assembled according to Knol *et al*.[95]. Briefly, lipids were mixed in chloroform (EggPC:POPE:POPS 70:15:15 molar ratio), dried down under nitrogen and residual chloroform was removed under vacuum for 4h. The dried lipid film was resuspended in buffer C with rigorous vortexing followed by five freeze/thaw cycles in liquid nitrogen and room temperature. The lipids emulsion was extruded eleven times through 200 nm polycarbonate filters (Whatman) to form large unilamellar vesicles. Triton X-100 destabilized liposomes were incubated with purified GLUT4 for 45 min 4°C followed by detergent removal using Amberlite XAD-2 beads. After removal of all beads, liposomes were collected by ultracentrifugation at 4°C for 1 h at 267,000 x g and resuspended in buffer containing 50 mM potassium phosphate (pH 7.4) and 130 mM KCl. Samples could be stored after this step at -80°C after flash freezing in liquid nitrogen. Glucose uptake assay

Liposome ^{3}H-2DG uptake

Frozen liposomes containing purified GLUT4 were thawed at room temperature and subjected to three freeze/thaw cycles (liquid nitrogen/room temperature) followed by extrusion through a 200 nm polycarbonate filter. Uptake was started by adding ^{3}H-D-glucose (200 µM) (American Radiolabeled Chemicals) to GLUT4 proteoliposomes. Transport was stopped at different times

with ice-cold phosphate buffer containing 100 µM phloretin and then filtered by vacuum on a 0.2 µm mixed cellulose ester filters (Avantec). Scintillation fluid was added to the filters and the radioactivity counted. ^{3}H-L-glucose (200 µM) was used to determine nonspecific transport.

2.8 Figures

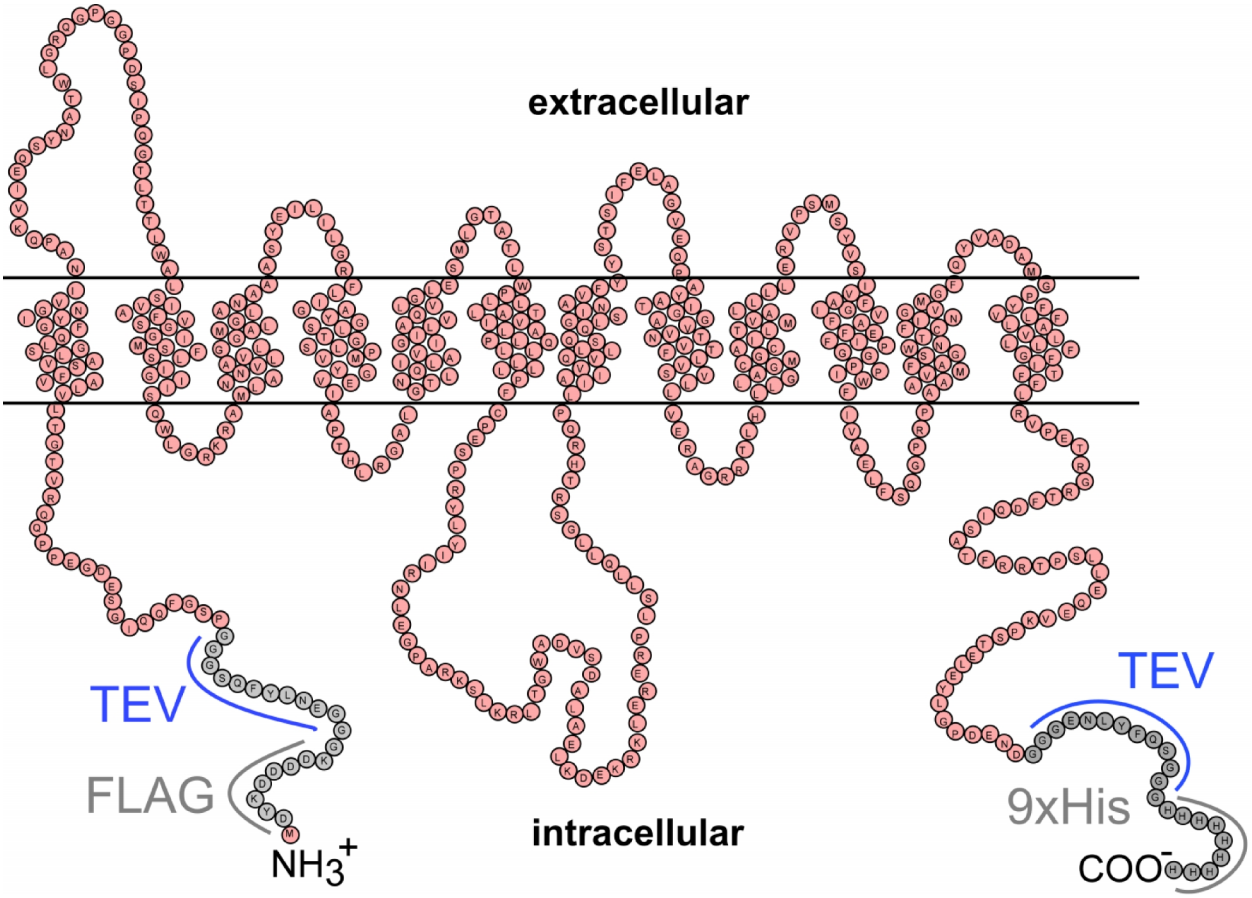

Figure 2.1. Predicted topology map of GLUT4. The membrane topology was predicted using the TOPCONS web server for consensus prediction of membrane protein topology and signal peptides[96]. Grey amino acids were added for aiding purification and removal of purification tags.

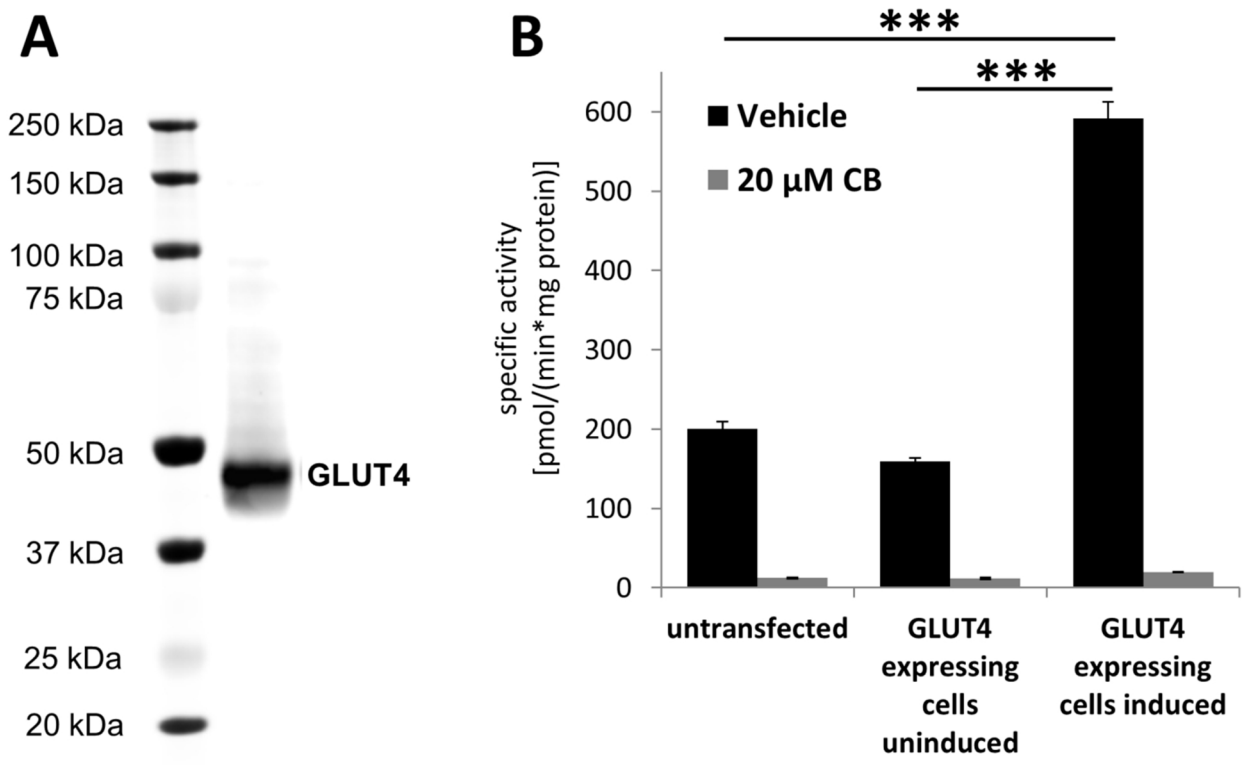

Figure 2.2. Functional expression of GLUT4 in HEK293 GnTI- cells determined by western blot and glucose uptake. Expression of FLAG and 10xHis tagged GLUT4 was determined using western blot analysis via anti GLUT4 antibody (A). Function of the protein was assessed by measuring zero-trans influx and accumulation of ^{3}H-2-Deoxy-glucose in cells before and after induction of GLUT4 expression by doxycycline (B). Uptake in the presence of vehicle (EtOH) was compared to the GLUT specific inhibitor cytochalasin B (CB). Glucose uptake in the absence of doxycycline can be attributed to basal glucose uptake for energy homeostasis as indicated by similar levels of uptake in untransfected control cells. Data is expressed as mean ±SEM (***P<0.001; one-way ANOVA analysis).

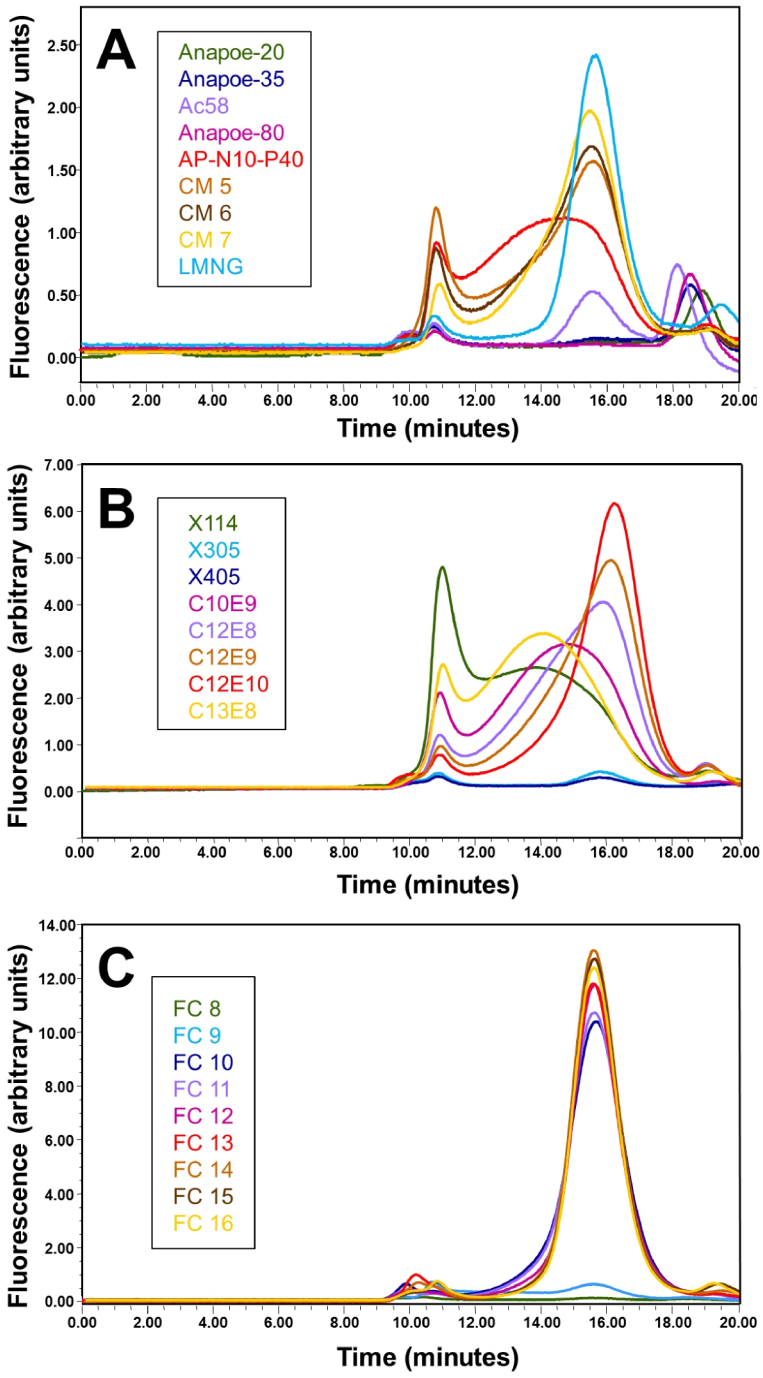

Figure 2.3. FSEC elution profiles of detergent solubilized GLUT4-AcGFP. Several detergents were used to solubilize HEK293 cells containing AcGFP tagged GLUT4. Peak shape, size and

elution volume of GLUT4-AcGFP were analyzed using fluorescent size exclusion chromatography (FSEC). The flow rate was 0.55 ml/min.

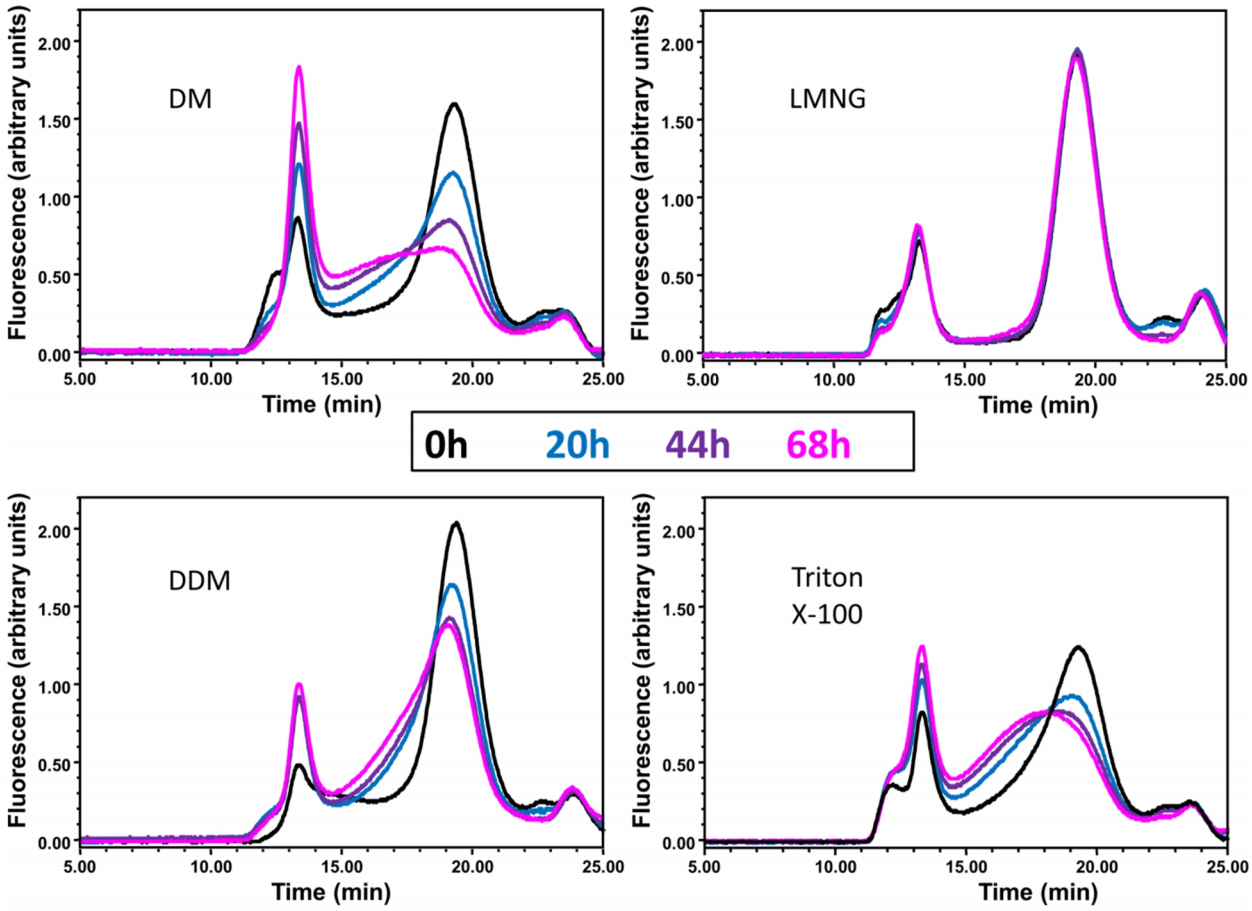

Figure 2.4. Stability of GLUT4 in various detergents over time determined by FSEC. GLUT4-AcGFP was solubilized in DDM, DM, LMNG and Triton X-100 and incubated at 4°C for 68 hours. Aliquots were analyzed by FSEC after 0h, 20h, 44h and 68h. The flow rate was 0.55 ml/min.

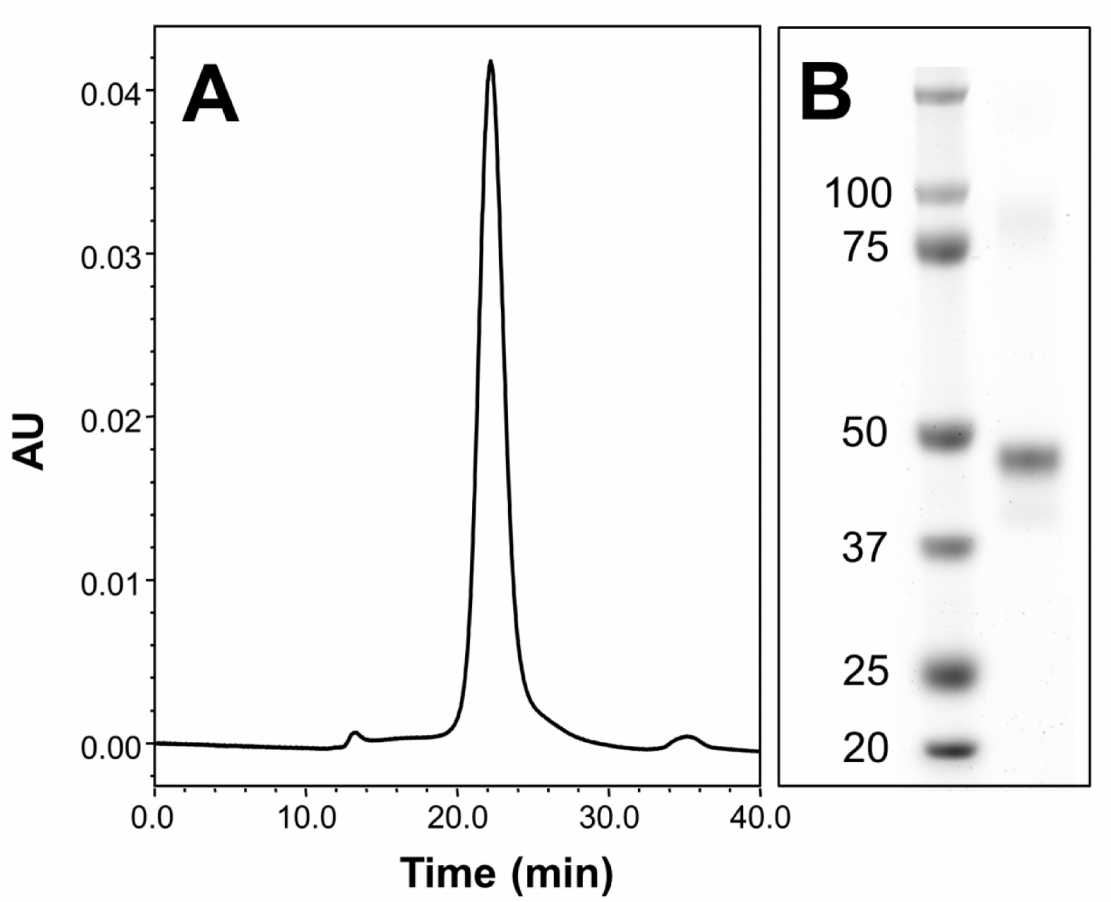

Figure 2.5. Purity assessment of FLAG and SEC purified GLUT4 by SEC and SDS-PAGE. FT-GLUT4-TH in LMNG micelles was analyzed for purity after purification via anti FLAG affinity gel and size exclusion chromatography (SEC) by SEC (A) and by IRDye Blue protein staining of polyacrylamide gel after SDS-PAGE (B). GLUT4 elutes as a sharp, single, symmetric peak from the SEC column. The flow rate was 0.55 ml/min.

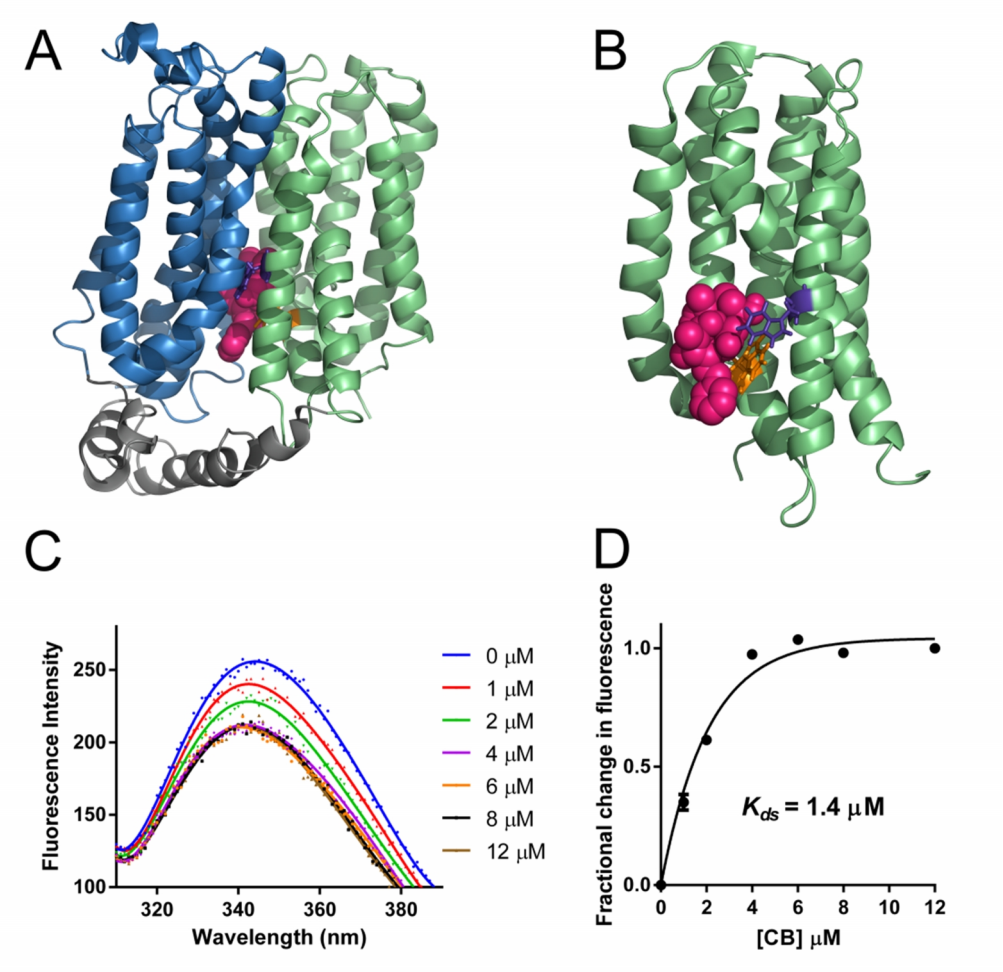

Figure 2.6. CB binding to GLUT4 analyzed by tryptophan fluorescence quenching. CB (pink) binds within the glucose permeation path formed by the N-terminal (blue) and C-terminal half (green) of the transporter in the inward facing conformation in all docked poses (A). Representative pose of CB shows binding in direct proximity of two tryptophan residues lining the glucose permeation path that were previously identified to be the target of fluorescence quenching by CB[70,97,98] (B). Fluorescence intensity was scanned between 310-390nm with excitation at 295nm for increasing concentrations of CB (C). Fractional change of fluorescence was plotted against CB concentrations (D) and K_{ds} was calculated using non-linear regression analysis (GraphPad 6.0). Data is expressed as mean ±SEM.

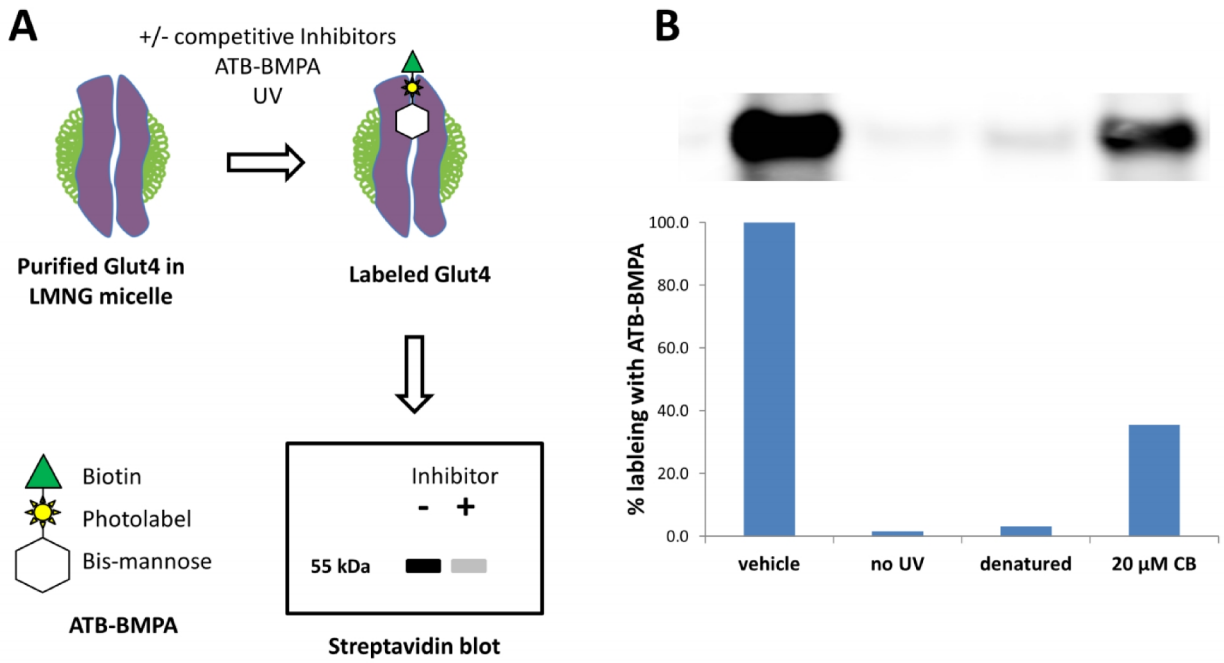

Figure 2.7. Assessment of binding of the glucose analogue ATB-BMPA in the presence and absence of the inhibitor CB. Biotinylated ATB-BMPA contains the glucose analogue bis-mannose and is known to bind at the glucose binding site of GLUT4. GLUT4 in LMNG micelles was photo-labeled with ATB-BMPA and analyzed by western blot using fluorescently labeled streptavidin (A). Vehicle treated transporter labeling was compared to CB treated and negative controls including no photolabeling (no UV) and heat denatured GLUT4 (B).

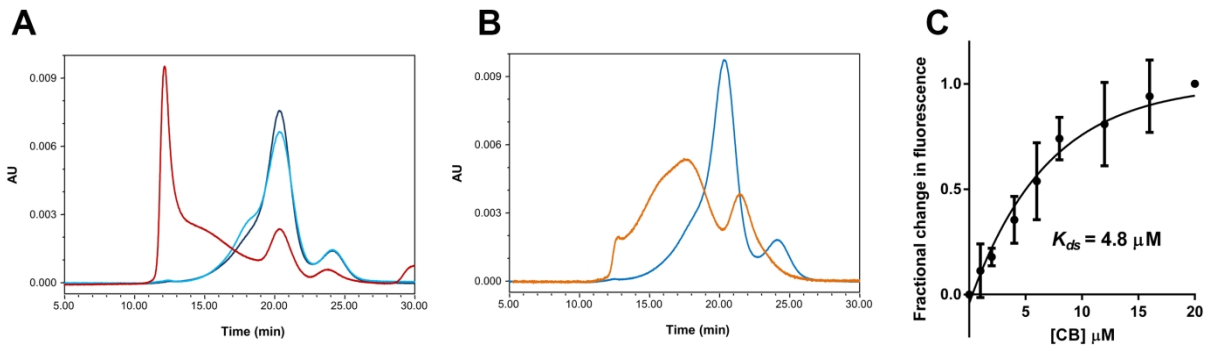

Figure 2.8. Stabilizing effect of amphipol A8-35 on GLUT4 determined by SEC and fluorescence quenching. (A) Reconstitution of GLUT4 into amphipol preserves the structure of the protein as assayed by SEC before (dark blue) and after (light blue) incubation at 40°C for 2 hours compared to LMNG after incubation at 40°C for 2 hours (red). (B) Amphipol was able to refold GLUT4 (blue) after partial, basic pH induced (pH 10) induced misfolding in LMNG (orange). (C) GLUT4 reconstituted in amphipol is binding the known inhibitor CB as assayed by tryptophan fluorescence quenching. K_{ds} was calculated using non-linear regression analysis (GraphPad 6.0). Data is expressed as mean ±SEM.

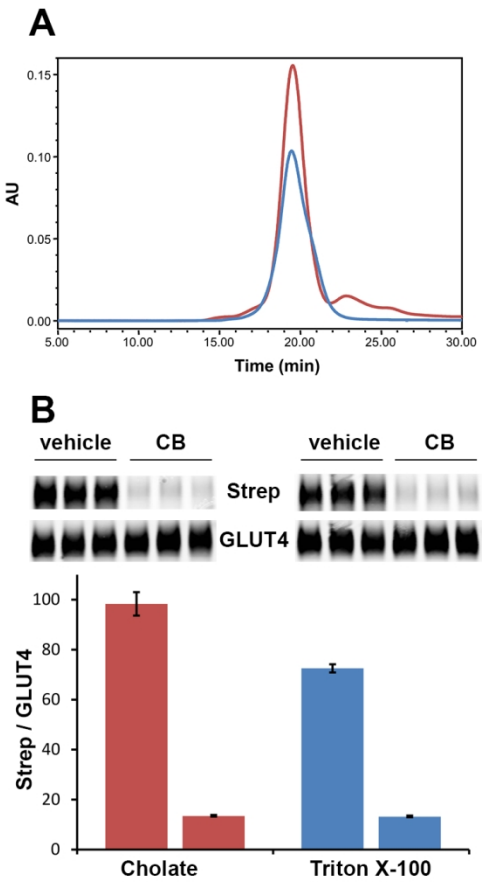

Figure 2.9. SEC elution profiles of GLUT4 reconstituted into nanodiscs and CB inhibitable binding of ATB-BMPA. GLUT4 reconstituted into MSP1E3D1 nanodiscs using sodium cholate (red) or triton X-100 (blue) for lipid solubilization elutes as a single, symmetrical peak from the size exclusion column indicating homogeneity of the protein population (A). GLUT4 in cholate and triton X-100 assembled nanodiscs shows reduced binding of ATB-BMPA in the presence of the competitive inhibitor CB. The ratio of Strep/GLUT4 indicates the fraction of GLUT4 labeled with ATB-BMPA. The flow rate was 0.55 ml/min.

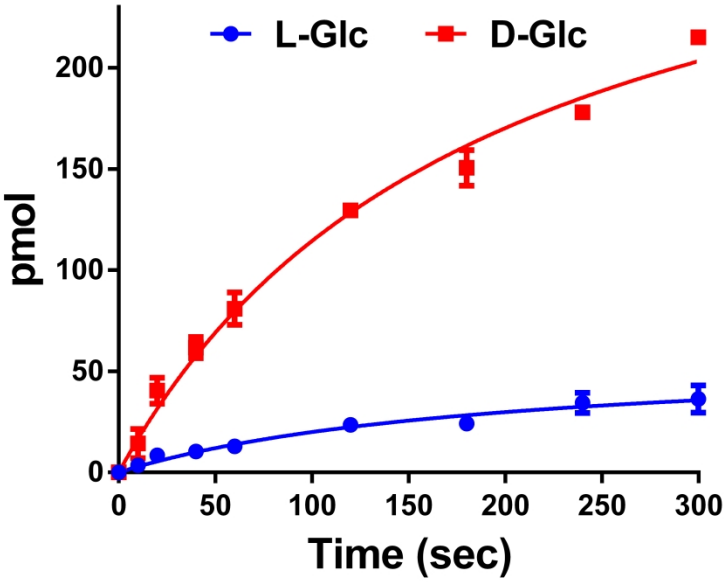

Figure 2.10. GLUT4 mediated uptake of 3H-D- and 3H-L-glucose into liposomes. Saturable, specific zero-trans uptake of ^{3}H-D-glucose into GLUT4 reconstituted liposomes (red) compared to nonspecific uptake of ^{3}H-L-glucose (blue). Uptake data was fitted using non-linear regression analysis (GraphPad 6.0). Data is expressed as mean ±SEM.

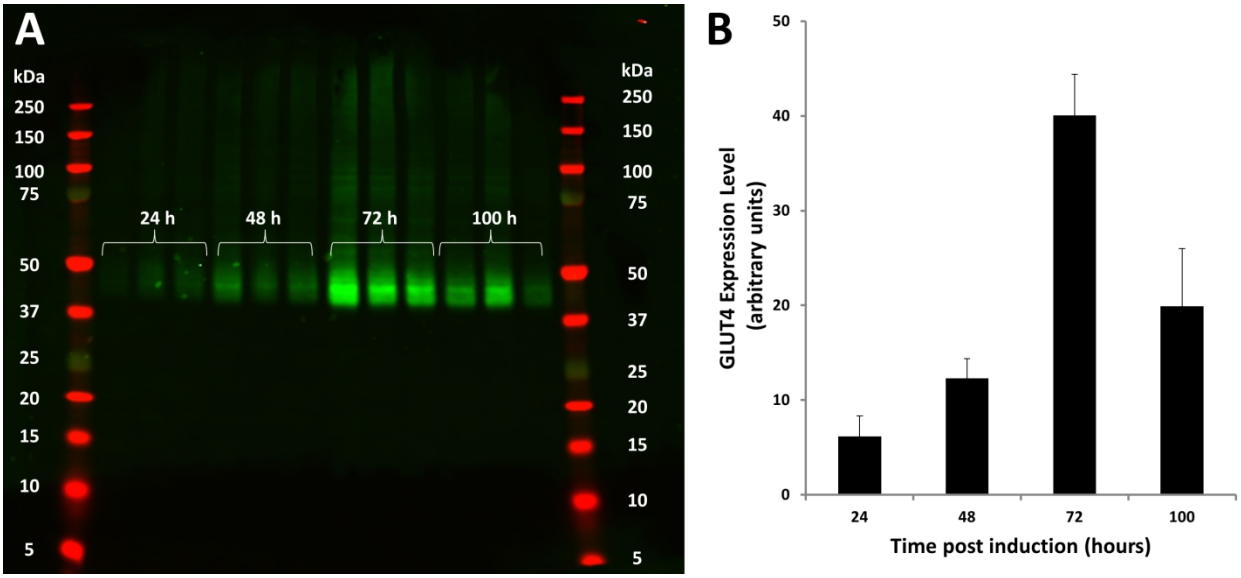

Supplementary Figure 2.1. Expression levels of GLUT4 over time post induction. HEK293 GnTI$^-$ cells stably expressing GLUT4 under a tet-on promoter were induced in triplicate with doxycycline and sodium butyrate. Cells were harvested at different time points, lysed and subjected to western blot analysis using a GLUT4 antibody (A). The intensities of the band at around 45kDa was quantified to determine the expression levels of GLUT4 at different time points (B).

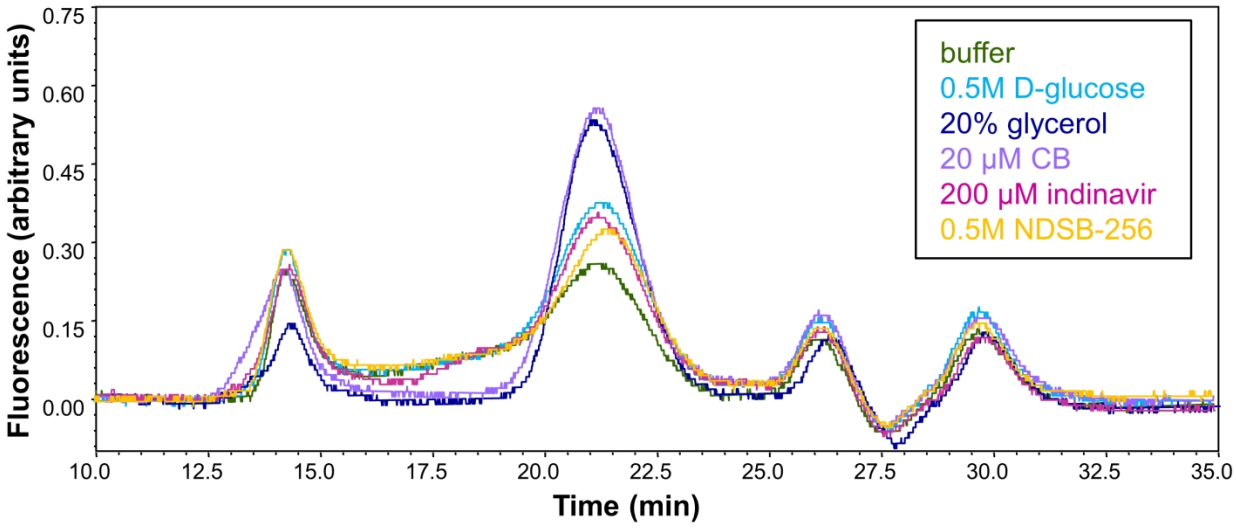

Supplementary Figure 2.2. Stabilizing effect of different additives on GLUT4 in LMNG determined by FSEC. LMNG solubilized GLUT4-AcGFP cell lysates were incubated at 37°C overnight in the presence or absence of 0.5M D-glucose, 20% (v/v) glycerol, 20µM CB, 200µM indinavir and 0.5M NDSB-256. The flow rate was 0.55 ml/min.

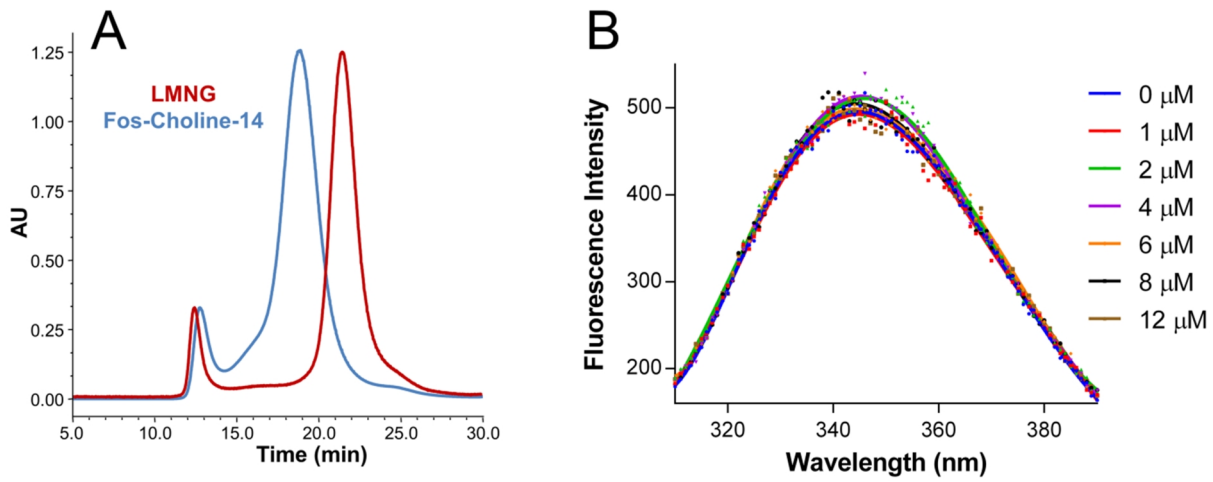

Supplementary Figure 2.3. Testing correct three-dimensional folding of GLUT4 purified in FC14 micelles. SEC elution profiles show a shift to larger stokes diameter from LMNG solubilized GLUT4 (red) to FC14 solubilized GLUT4 (blue) (A). Increasing concentration of CB does not significantly affect tryptophan fluorescence intensity of GLUT4 in FC14 (B), indicating no specific CB binding to GLUT4. Both results indicate misfolding or aggregation of the transporter.

Chapter 3 – Mammalian glucose transporter activity is dependent upon anionic and conical phospholipids

Richard C. Hresko[1,*] , Thomas E. Kraft[1,†,*], Andrew Quigley[2], Elisabeth P. Carpenter[2], Paul W. Hruz[1,3,†]

[1]Department of Pediatrics, and [3]Department of Cell Biology and Physiology, Washington University School of Medicine, St Louis MO 63110, USA

[2]Structural Genomics Consortium, University of Oxford, Oxford OX3 7DQ, UK

[†]corresponding author

[*]These authors contributed equally to this work

3.1 Abstract

The regulated movement of glucose across mammalian cell membranes is mediated by facilitative glucose transporters (GLUTs) embedded in lipid bilayers. Despite the known importance of lipids in regulating protein structure and activity, lipid-induced effects on the GLUTs remain poorly understood. We systematically examined the effects of biologically relevant phospholipids on glucose transport in liposomes containing purified GLUT4 and GLUT3. For both GLUTs, anionic phospholipids were found to be essential for functional activity. Phosphatidic acid, phosphatidylserine, phosphatidylglycine or phosphatidylinositol significantly increased transport activity in a dose-dependent manner. Although not essential, the conical lipids phosphatidylethanolamine and diacylglycerol enhanced transporter activity up to threefold in the presence of anionic phospholipids. Kinetic analyses revealed that anionic and conical lipids increase the k_{cat} of transport without changing the K_m. These results extend the field of known membrane protein-lipid interactions to the family of structurally and functionally related human solute carriers.

3.2 Introduction

Membrane proteins are embedded in a lipid bilayer that covers a large percentage of their exposed surface. Lipid bilayers in typical human cells consist of hundreds of different lipid types that modulate cell signaling and protein function[99]. Membrane lipid composition changes in several disease states and varies markedly over different cellular compartments. This influences the activity of transmembrane proteins by direct interactions with specific lipids or through changes in the biophysical properties of the membrane (e.g. fluidity, permeability, curvature, charge density and lateral pressure)[20,100]. Each membrane protein interacts with several lipid molecules at any given time, yet understanding the functional and structural effects of these contacts has been previously limited. With the advent of several methodological advances in isolating and studying membrane proteins, the significance of individual lipid components has begun to emerge. Human and bacterial ion channels, aquaporin Z, LacY and the nicotinic acetylcholine receptor are among the growing list of membrane proteins that have been shown to require specific lipids like anionic phospholipids, phosphatidylethanolamine (PE), cholesterol or signaling lipids like phosphatidylinositol bisphosphate (PIP_2) for optimal activity or proper folding[101–108].

The solute carriers (SLCs) consist of over 400 family members in humans. A quarter of these are associated with disease, making them excellent targets for clinical research[24]. Although highly important in nutrient uptake, drug transport and waste removal, this class of proteins remains relatively understudied[24]. Elucidation of the lipid requirement for activity of mammalian solute carriers remains of paramount interest for drug discovery and general understanding of transport mechanisms.

Members of the SLC2A family of facilitative hexose transporters are essential in regulating cellular metabolism by selectively transporting glucose down a concentration gradient without the use of energy. To date, 14 distinct human SLC2A isoforms (GLUTs) have been identified[109] and for several of these proteins the cellular function in health and disease has been established. Regulation of the insulin-responsive facilitative glucose transporter GLUT4 (SLC2A4), which is primarily responsible for mediating peripheral glucose disposal in insulin sensitive tissues such as skeletal and cardiac muscle as well as adipose tissue[110], has been intensively studied in relation to the pathophysiology of type 2 diabetes mellitus[111]. Under basal conditions, the majority of GLUT4 remains sequestered within the cytosol in specialized membrane vesicles. Upon stimulation by insulin, a complex signaling cascade is initiated which results in the translocation of GLUT4 to the cell surface[112]. In contrast, GLUT3 (SLC2A3), which has been classically defined as the neuronal glucose transporter due to the high level of expression and initial characterization in nervous tissue[113], is constitutively present on the cell plasma membrane. GLUT3 is also highly expressed in other tissues with high energy needs including sperm, embryonic tissue and leukocytes[114]. Despite the longstanding recognition of an association between changes in membrane lipid composition and glucose transport in human disease[115,116], the role of specific phospholipids on the functional activity of individual GLUT isoforms remains elusive. Although initial studies on the influence of lipids on the activity of GLUT1 isolated from erythrocyte membranes were performed nearly 30 years ago[117], until recently it was not possible to isolate and reconstitute other GLUT isoforms in a functional form to allow comprehensive evaluation of membrane lipids, alone or in combination, at physiologically relevant levels.

Here, for the first time we demonstrate that the glucose transport activity of GLUT4 and GLUT3 is controlled by the membrane phospholipid composition. Based on biochemical data and on crystal structures of GLUT3 and the close homologues GLUT1 and GLUT5 in multiple conformations, the currently accepted mechanism of action for these transporters is defined by interconversions between inward- and outward- facing conformations via a rocker-switch motion, governing the transport of solutes over the membrane barrier[25–27]. Our findings expand the current model by introducing the modulation of transporter activity by specific phospholipids, thereby highlighting the importance of two classes of phospholipids that might regulate the activity of other members of the SLC family.

3.3 Results

GLUT4 and GLUT3 show specific and saturable uptake of glucose in liposomes of defined phospholipid composition.

To study the effect of different phospholipids at specific concentrations on the activity of GLUT4 and GLUT3, we developed an assay system allowing us to measure uptake of radiolabeled glucose into liposomes that contained purified transporter embedded in a tightly controlled lipid environment. Both transporters showed saturable uptake over seconds to minutes of their primary substrate D-glucose over the non-transportable L-glucose in liposomes containing 70% egg phosphatidylcholine (eggPC), 15% phosphatidic acid (PA) and 15% PE (mol/mol) (**Supplementary Results**, **Supplementary Fig. 3.1**). Transport could be completely abolished using the GLUT-specific inhibitor cytochalasin B (**Supplementary Fig. 3.1a**). As expected for random insertion, the transporter incorporated into liposomes with roughly half in

an outward- and half in an inward- facing orientation. Evidence for this conclusion was obtained from western blot analysis of the transporter using anti-FLAG antibody before and after tobacco etch virus (TEV) protease cleavage of an engineered N-terminal FLAG tag. In detergent micelles, the protease has access to both faces of the transporter whereas in liposomes, it can only access transporters that orient with their N-terminus facing outward. We determined cleavage of the FLAG tag of ~100% in micelles, whereas only ~50% of all transporters in liposomes are cleaved by TEV protease.

Anionic phospholipids stabilize GLUT4 and are required for activity of GLUT4 and GLUT3.

We hypothesized that similar to several ion channels and receptor proteins, mammalian transporter function is regulated by its lipid environment. Several studies have shown that specific binding of annular lipids to various membrane proteins stabilize their structure and modulate their function[118–120]. For example Laganowsky *et al.* demonstrated the stabilizing effect of lipids directly binding to several membrane proteins by preventing gas-phase unfolding in ion-mobility mass spectrometry experiments at increasing voltage[119]. Similar to this approach, we devised a simple method to efficiently identify lipids that stabilize the transporter. Microgram amounts of LMNG detergent purified monomeric GLUT4 were incubated in the presence or absence of various lipids followed by thermal destabilization. The ability of specific lipids to stabilize the folded protein was assessed via SEC. We previously established that a single, symmetrical peak in the SEC elusion profile corresponds to monomeric, properly folded, active GLUT4 whereas multiple, asymmetric peaks that elute earlier are an indicator of a heterogeneous population of destabilized, unfolded or aggregated protein[121]. In the presence of anionic phospholipids, a monomeric peak of folded GLUT4,

comparable to unheated, folded GLUT4 in LMNG micelles, was retained on the SEC profile (**Fig. 3.1a**) whereas zwitterionic and non-bilayer phospholipids did not stabilize the transporter, similar to heated GLUT4 in LMNG micelles (**Fig. 3.1b**).

The observation that only anionic phospholipids stabilize the transporter structure prompts the question as to whether these lipids also modulate the function of GLUT4. We assessed the activity of the transporter in liposomes containing 100% eggPC or eggPC liposomes containing a second lipid at an 85:15, molar ratio. No specific GLUT4 mediated uptake was observed in the zwitterionic phospholipids PC, PE, or sphingomyelin (SM) (**Fig. 3.2a**). In contrast, the addition of the anionic phospholipids, PA or phosphatidylserine (PS) activated the transporter and resulted in specific D-glucose uptake (**Fig. 3.2b**). These results indicate a requirement for anionic phospholipids for transport activity and confirm our SEC results. To study the effect of the major naturally occurring anionic phospholipids in eukaryotic membranes in detail, we titrated palmitoyl-oleoyl-phosphatidic acid (POPA), palmitoyl-oleoyl-phosphatidylserine (POPS), palmitoyl-oleoyl-phosphatidylglycerol (POPG) and phosphatidylinositol (PI) into PC liposomes and measured GLUT4- mediated uptake of D-glucose (**Fig. 3.2c**). All four anionic phospholipids led to a dose-dependent activation of GLUT4 with PA exhibiting the strongest effect, PS the second, followed by PI and PG. Anionic phospholipids also activated GLUT3 but with important differences (**Fig. 2d**). Unlike GLUT4, GLUT3 possessed measurable, albeit low transport activity in the absence of anionic phospholipids. The addition of anionic phospholipids greatly enhanced GLUT3 activity, with PS having the most potent effect, followed by PA, then PG and PI. These results demonstrate that anionic phospholipids are required for optimal GLUT4 and

GLUT3 activity and suggest the presence of an anionic phospholipid binding site on the transporter with different affinities for anionic phospholipid headgroups.

Conical lipids stimulate glucose uptake in liposomes that contain anionic phospholipid.

Nonbilayer lipids like palmitoyl-oleoyl-phosphatidylethanolamine (POPE) have been shown to increase the activity of several membrane proteins in the presence of anionic phospholipids[103,122–124]. To assess the effects of POPE on GLUT4 activity, we measured glucose transport in liposomes containing 10 % POPA in eggPC, titrated with increasing amount of POPE. POPE significantly increased glucose uptake reaching a maximum effect of three-fold at 30% POPE (**Fig. 3.3a**). We next determined the effect of anionic phospholipids on GLUT4 activity in the presence of POPE. Glucose transport measured in liposomes containing 30% POPE in eggPC were titrated with POPA. As expected, POPA stimulated glucose uptake in a concentration-dependent manner and no specific uptake was observed in 30% POPE in the absence of anionic phospholipid (**Fig. 3.3b**). Unlike the other predominant mammalian zwitterionic lipids PC or SM, POPE is conically shaped with a small headgroup and one unsaturated acyl chain that occupies a larger volume than saturated chains. To determine whether the activating effect of POPE on GLUT4 is mediated through specific binding of the lipid to the transporter, as suggested for anionic phospholipids, or through altering the biophysical properties of the lipid bilayer, we compared the effect of the non-bilayer lipid palmitoyl-oleoyl-glycerol (DAG) to POPE. Both lipids share the same aliphatic tails but significantly differ in their headgroup with DAG completely lacking the phosphate group and therefore exhibiting an even stronger conical shape than POPE (**Fig. 3.3c**). In the presence of DAG, GLUT4 activity was increased in a dose-dependent manner, similar to POPE (**Fig. 3.3d**).

DAG showed a more pronounced effect on transporter activity with a maximal activation of 2.5-fold higher than POPE, correlating with its stronger conical shape. Although it is unlikely that DAG has a physiological role in activating GLUT4 as the amount in the PM is a small fraction of PE[125], this experiment demonstrates the activation of GLUT4 through a headgroup unspecific effect on the biophysical properties of the lipid bilayer. This effect was also observed for GLUT3 (**Fig. 3.3e**). The addition of 15% conical lipids (POPE) increased transporter activity by 2.7-fold in the presence of anionic phospholipids. Similar to GLUT4, conical lipids did not significantly increase transporter activity of GLUT3 in the absence of anionic phospholipids. These results establish that conical lipids are necessary but not sufficient for optimal GLUT4 and GLUT3 transport activity.

Anionic and conical lipid increase transporter activity in liposomes with physiological lipid composition.

Like DAG, the levels of PA in mammalian PMs are quite low (~1%) and therefore the more abundant anionic phospholipids PS and PI most likely contribute more significantly in terms of enhancing normal glucose transport activity. To determine whether the anionic and conical lipid effects are also observed in a more physiological environment, GLUT4 activity was measured in liposomes with a phospholipid composition comparable to that of a mammalian PM [125] (**Fig 3.4a**). Cell plasma membranes show trans-bilayer lipid asymmetry with anionic phospholipids being found exclusively and conical lipids preferentially on the cytoplasmic face (inner leaflet), a feature that distinguishes eukaryotic from prokaryotic membranes[99]. Due to the technical challenge of generating asymmetric vesicles that recapitulate native mammalian cell membranes, characterization of the major phospholipids was carried out in liposomes

comprised of lipid levels found in either the PM inner leaflet (**Fig. 3.4b**) or the total PM membrane (**Fig. 3.4c**). To assess the contribution of each individual phospholipid on glucose transport, we determined transporter activity in liposomes after subsequent additions of lipids to the previous mix, starting with eggPC. From left to right each bar represents an experiment in which an additional lipid was added to the previous lipid mix thereby reducing the molar amount of eggPC. The precise lipid compositions for each experiment can be found in **Supplementary Tables 3.1 and 3.2**. As expected, in the presence of only the zwitterionic, cylindrical lipid eggPC no specific uptake was detected while the addition of the anionic phospholipid PS significantly increased D-glucose uptake above background. Uptake was dramatically enhanced upon the further addition of the conical lipid PE. Adding the other zwitterionic lipid SM to the system had no effect on glucose uptake while the addition of physiological levels of PI further increased uptake. PA addition had no measurable effect on transport suggesting that either the lipid binding sites on GLUT4 are already saturated by the other anionic phospholipids PS or PI or that the levels of PA in the PM are indeed too low to have any contribution. As anticipated, liposomes resembling the inner leaflet lead to increased GLUT4 activity due to the higher concentrations of anionic and conical lipids compared to liposomes comprised of lipid compositions that approximate total PM.

Anionic and conical lipids increase the maximal activity of GLUT4 and GLUT3 but not their substrate binding affinity.

We used kinetic analysis to determine the mechanism of lipid-induced changes of glucose transporter function. By measuring zero-trans uptake of radiolabeled D-glucose into transporter containing liposomes at increasing substrate concentrations with different amounts of anionic

or conical lipids present, we determined the Michaelis constant K_M and the turnover number k_{cat}. For both GLUT3 and GLUT4, increasing concentrations of anionic or conical lipid increased the turnover number linearly but had no measurable effect on the Michaelis constant (**Fig. 5**). These data support a mechanism in which anionic and conical lipids increase the fraction of active transporters and/or the transporter interconversion rate without changing substrate binding affinity. Therefore, at saturating substrate concentration, anionic and conical lipids alter the rate-determining step in facilitative glucose transport. Similar to previous studies[126], the reconstituted transporter GLUT3 showed higher affinity for D-glucose than GLUT4 while it transported its substrate with a lower turnover number than GLUT4. The K_M for GLUT3 (11.9 ± 1.6 mM) and GLUT4 (33.3 ± 5.1 mM) reconstituted in liposomes was higher than reported when expressed in cells, which is consistent with previously published studies comparing transporter kinetics in cells versus reconstituted into liposomes[127–131]. Measuring transporter kinetics of GLUT4 expressed in HEK293 cells prior to purification and reconstitution, we observed a lower K_M of 7.1 ± 1.1 mM (**Supplementary Fig. 3.3**), similar to previously published studies[126,132]. These results indicate that additional cellular components, not present in the purified four-component liposome system, might play a role in altering the transporter's K_M.

The slope of the transporter k_{cat} plotted against the concentration of anionic or conical lipids correlated with the intensity of the lipid effect on transporter activity and allows direct comparison of isoform-selective lipid effects. For both the anionic phospholipid PA and the conical lipid PE, the kinetic data show a 5-fold higher slope for GLUT4 compared to GLUT3, indicating a significantly stronger dependence of GLUT4 on anionic and conical lipids for activity. As expected, extrapolation to 0% PA indicated a negligible turnover number for GLUT4

where very little specific transport was observed. However, GLUT3 retained minimal activity even in the absence of anionic phospholipids. This correlates with our earlier data in which transport activity was measured in liposomes containing only PC or PC plus PE (**Fig. 3.3e**).

3.4 Discussion

Taken together, our data demonstrate that anionic and conical lipids are essential for full activity of the mammalian glucose transporters GLUT4 and GLUT3 but activate the transporters through distinct mechanisms. In this first in-depth, systematic study of the lipid dependences of any mammalian solute carrier protein, a key finding is that anionic phospholipids are required for activity and mediate this effect through their headgroups (**Fig. 3.2c**). All activating anionic phospholipids tested share the same fatty acids and a negative charge on the phosphate group but differ in the headgroup substituents (**Fig. 3.2e**). The zwitterionic lipids that were examined also share the same fatty acid moieties but carry a positive charge on their headgroup substituent that neutralizes the negatively charged phosphate group, and do not activate the transporters (**Fig. 3.2a**). The anionic phospholipid POPA shows potent activation of the transporters but carries no headgroup substituent, suggesting that the negatively charged phosphate group mediates the activating effect as the only common denominator. Hinging on the fact that anionic phospholipids are found exclusively on the inner leaflet of mammalian PMs, we propose that the interaction partner of the negative charge on the lipid is a cationic residue on the cytoplasmic face of the transporters, forming an anionic phospholipid binding site (**Fig. 3.6a**), similar to inward rectifier channels[104]. The stabilizing effect of anionic phospholipids on GLUT4 protein (**Fig. 3.1**) provides supporting evidence for a direct interaction

of annular anionic phospholipids with the transporter in contrast to an effect mediated through changes of the lipid bilayer chemical properties by bulk lipids. Additionally, the differences in GLUT4 and GLUT3 activation through anionic phospholipids with chemically different headgroup substituents is most likely caused by a difference in binding affinities of the lipids to the anionic phospholipid binding site on the proteins (**Fig. 3.2c,d**).

Conversely, conical or non-bilayer lipids alone are not sufficient for GLUT4 or significant GLUT3 activity but increase transporter activity dramatically in the presence of anionic phospholipids (**Fig. 3.3a,e**). Interestingly, this effect is not mediated through the headgroup, charge or acyl chains but through their conical shape. The shape of a lipid is determined by the ratio of headgroup to tail cross sectional area. Conical lipids have large tails, often carrying single or multiple double bonds and small headgroups while cylindrical lipids have tails and headgroups of similar size. The conical lipid POPE and the cylindrical lipid palmitoyl-oleoyl-phosphatidyl choline (POPC), the main constitutent of eggPC, share the same tail and charge and only differ in the methylation of the ethanolamine headgroup substituent (**Fig. 3.2e**). POPE is primarily found on the inner leaflet of mammalian PMs, affecting its biophysical properties by introducing lipid packing defects, curvature frustration and lowering the lateral pressure at the aqueous-lipid interface. POPE increased transporter activity in a dose dependent manner in the presence of anionic phospholipid, while POPC showed no effect (**Fig. 3.3a,e**). Interestingly, at physiological concentrations of anionic and conical lipids (**Fig. 3.4a**), we observed maximal activity of GLUT4 in liposomes containing 10% POPA and 30% POPE (**Fig. 3.3a**). Even more strikingly, the DAG lipid tested, which shares the same acyl chains as POPE but completely lacks the phosphate headgroup, making it even more conically shaped than POPE (**Fig. 3.3c**) showed

a nearly three-fold greater activation of GLUT4 compared to POPE (**Fig. 3.3d**). Similarly, nonbilayer lipids stimulate the activity of several other integral membrane proteins in the presence of anionic phospholipids[103,122,124].

In summary, our results show that anionic and conical lipids influence the activity of GLUT4 and GLUT3 in different ways: Anionic phospholipids are required and sufficient for activity while conical lipids alone are not sufficient but increase activity significantly in the presence of anionic phospholipids. Additionally, the presence of anionic phospholipids increases the stability of GLUT4 as determined by SEC whereas conical lipids have no influence on protein stability, indicating direct binding of only anionic phospholipids to the transporter. Moreover, our kinetic analysis of both transporters revealed that anionic and conical lipids increase the k_{cat} linearly in a concentration dependent manner while the K_M remains unchanged. This suggests that both lipids do not change the affinity of the transporters for their substrate D-glucose but change either the turnover number of the transporters or the fraction of active transporters. Therefore, we propose the following model of lipid activation: According to recently published crystal structures of the GLUT isoforms GLUT1, GLUT3 and GLUT5 in inward and outward facing conformations[25–27], we assume that the transport of glucose is controlled by alternating between inward and outward facing conformations via a rocker-switch motion and by a gated-pore mechanism involving transmembrane helices 7 and 10. Alternation between inward and outward facing conformations is catalyzed by the equilibrium of formation and breaking of transient salt bridges at the cytoplasmic side of the transporter between the ends of several inter transmembrane helices as well as between intracellular and transmembrane helices[25]. Formation of these salt bridges stabilizes the outward conformation by decreasing total free

energy. We propose that anionic phospholipids present cationic residues involved in salt bridge formation with an alternative binding partner, thereby lowering the energy barrier between inward and outward conformations (**Fig. 3.6c**). Salt-bridge forming cationic amino acids would switch between intramolecular Coulomb interactions with cationic amino acids and intermolecular interactions with anionic phospholipid headgroups. In the absence of anionic phospholipids, the transporter would be essentially trapped in an inward or outward state, with a drastically reduced interconversion rate due to the absence of an alternative binding partner for cationic amino acids when breaking intramolecular salt bridges (**Fig. 3.6a**). Increasing amounts of anionic phospholipid lead to a greater occupancy of the anionic phospholipid binding site on the transport proteins allowing for the interconversion between both conformations. The positive correlation between concentration of anionic phospholipids and transporter turnover number (**Fig. 3.5a,b**) is therefore a result of an increased fraction of active transporters. Interestingly, a similar mechanism has been proposed in a recent MD simulation study of the β_2 adrenergic receptor in lipid bilayers[133]. In the active state, the phosphate group of an anionic phospholipid forms a salt bridge with an arginine residue, allowing the binding of the G-protein. Receptor deactivation occurs upon a conformational change that breaks the lipid-arginine salt bridge and leads to the formation of an intramolecular interaction between the arginine and a glutamate residue instead.

In contrast, conical lipids in the bilayer introduce lipid packing defects, decrease the interfacial lateral pressure and create curvature frustration (**Fig. 3.6b**) thereby leading to increased flexibility and movement of integral membrane proteins[99,100,134]. Consequently, in the absence of conical lipids, the glucose transporters are embedded into a bilayer of mainly cylindrical

lipids that provide tight packaging and create strong lateral pressure at the lipid-water interface, thus stabilizing the transporters' low energy conformations (**Fig. 3.6c**). In our model, we propose that the increase in membrane flexibility by conical lipids in combination with anionic phospholipid binding leads to a destabilization of the inward and outward open low energy states (**Fig. 3.6c**), thereby causing an accelerated rate of interconversion (**Fig. 3.6a**) consistent with a conical lipid concentration dependent increase of k_{cat} (**Fig. 3.5c,d**).

Although further work is required to determine the differences and similarities between GLUT4 and GLUT3 in detail, our findings establish that both transporters require anionic and conical lipids for full activity. Similar to the previously findings by Tefft *et al.* for GLUT1 in liposomes comprised of 100% anionic phospholipid[135], we determined that GLUT4 and GLUT3 show a strong headgroup preference among anionic phospholipids. Importantly, the observed effects of anionic phospholipid on GLUT4 and GLUT3 are observed at physiologically relevant lipid levels. GLUT4 is most active in the presence of PA (**Fig. 3.2c**) whereas GLUT3 and GLUT1 show highest activity with PS (**Fig. 3.2c**)[135]. In contrast to GLUT4, GLUT3 and GLUT1 showed small but measurable glucose transport activity in PC liposomes in the absence of anionic phospholipids. Anionic phospholipid effects on transporter kinetics are consistent for all three transporters, affecting only the turnover number but not the K_M[135]. The same observation was made for conical lipids in GLUT3 and GLUT4. The turnover number of GLUT4, however, was affected more strongly by anionic and conical lipids compared to GLUT3 (**Fig. 3.5**).

The lipid sensitivity of GLUT4 and GLUT3 may have biological implications. Mammalian lipid composition varies significantly in different tissues and also between cellular

compartments[20,136–138]. Concurrently, both transporters show tissue specific expression patterns with specialized functions in different cell types. Therefore, anionic and conical lipid concentrations in specific tissues or cellular compartments may coincide with transporter expression and their lipid requirements for activity. Furthermore, pathologic changes in lipid composition could affect transporter function and thereby contribute to disease progression, making lipid bilayer composition a promising pharmacological target. Considering the wide family of solute carriers implicated in human disease, GLUT4 and GLUT3 have significant sequence and structural homology to many transporters in this class. Therefore, it will be highly important to determine if the herein reported lipid dependence is a general phenomenon for the entire class of SLCs or specific for certain transporters and what the effect the lipid activation has in the biological function of specific transport proteins.

With markedly expanded understanding of the biophysical effects of lipids on membrane proteins, advanced techniques for mammalian membrane protein purification, a growing list of crystal structures for transport proteins, and emerging methodologies to investigate protein conformational dynamics, our current findings provide the starting point for exploring the lipid effects that modulate the structure and function of the entire family of solute carrier proteins.

3.5 Material and Methods

Materials. EggPC, POPE, POPS, POPA, POPG, liver PI, brain SM, and 16:0-18:1 DG (DAG) were purchased from Avanti Polar Lipids Inc. LMNG and OMNG detergent were obtained from Anatrace. All other reagents were purchased from Sigma-Aldrich or as otherwise indicated.

GLUT4 expression and purification. Stable tetracycline inducible HEK293S GnTI-cell lines expressing GLUT4 tagged at the amino and carboxy termini with FLAG and 9xHis respectively were generated as described previously[121]. Protein was purified as described in[121]. Briefly, frozen cell pellets were thawed in a 30°C water bath and resuspended in buffer B (50 mM potassium phosphate, 130 mM KCl, 15 % (vol/vol) glycerol, 3 mM EDTA, protease inhibitor, 1 µg/ml DNAse I (Roche) and 1mM PMSF (Fisher), pH 7.4) containing 0.75 % (w/v) LMNG. Cells were broken using a 15 ml Dounce homogenizer and then rotated at 4°C for 1h. Cell lysate was spun at 75,000 x g for 45 min at 4°C and the supernatant was filtered through a 0.45 µm filter to remove insoluble matter. The filtered supernatant was incubated with washed M2 anti-FLAG affinity gel (Sigma Aldrich) according to the manufacturer's instructions for 3h with rotation at 4 °C. GLUT4 bound FLAG affinity gel was collected in a column and subjected to extensive washing with 30 column volumes of buffer C (50 mM potassium phosphate, 350 mM KCl, 15 % (vol/vol) glycerol, 3 mM EDTA, complete protease inhibitor (Roche), 0.1% (w/v) LMNG, pH7.4). GLUT4 protein was eluted with six subsequent additions of 0.5 column volumes elution buffer (buffer C containing 200 µg/ml FLAG peptide, 100 µg/ml 3x FLAG peptide (ApexBio)). Tags were cleaved using TEV protease (plasmid purchased from Addgene) at a ratio of 1:20 TEV:GLUT4 overnight at 4°C in the presence of 1mM DTT. Based on SDS-PAGE and Blue BANDit protein stain (Ameresco), GLUT4 protein after FLAG elution was > 90 % pure.

GLUT3 expression and purification

The gene for SLC2A3 (GLUT3) was purchased from the Mammalian Gene Collection IMAGE:4396508. GLUT3 (N43A) was expressed using a construct consisting of the full length

deglycosylation mutant SLC2A3 gene with a C-terminal purification tag containing a TEV protease cleavage site, a 10xHis purification sequence and a FLAG tag in the expression vector pFB-CT10HF-LIC (available from the SGC). Baculoviruses were produced by transformation of DH10Bac cells. *Spodoptera frugiperda* (Sf9) insect cells in Sf-900 II SFM medium (Life Technologies) were infected with recombinant baculovirus and incubated for 72h at 27°C in shaker flasks.

Cell pellets (4 to 6 litres were used for each purification) from 1 litre of insect cell culture were resuspended in 50ml of lysis buffer (50mM HEPES, pH 7.5, 200mM NaCl, Roche protease inhibitor cocktail) and lysed by two passes through an EmulsiFlex-C5 homogenizer (Aventis). Protein was extracted from cell membranes by incubation of the crude lysate with 1% (octyl glucose neopentyl glycol) OGNG and 0.1% cholesteryl hemisuccinate (CHS) for 1h at 4^{O}C. Cell debris and unlysed cells were removed by centrifugation at 35,000g for 1h. Detergent-solubilized protein was purified by immobilized metal affinity chromatography by batch binding to Co^{2+} charged TALON resin (Clontech) at 4°C for 1h. The resin was washed with 20 column volumes of wash buffer (50mM HEPES, pH 7.5, 300mM NaCl, 5% glycerol, 20mM imidazole with 0.18% OGNG and 0.018% CHS) and eluted with lysis buffer supplemented with 250mM imidazole. Imidazole was immediately removed using a PD10 column (GE Healthcare Life Sciences) and elution buffer lacking imidazole and glycerol. The PD10 eluted protein was treated with 20:1 (w:w, protein:protease) TEV protease overnight at 4°C. The TEV protease-cleaved protein was separated from the 6xHis-tagged TEV protease and uncleaved SLC2A3 by incubation for 1h with TALON resin at 4°C. The resin was collected in a column and the flow-through and initial wash with SEC buffer (20mM HEPES, pH 7.5, 100mM NaCl 0.12% OGNG and

0.012% CHS) were concentrated in a 50kDa cut-off, 2ml PES concentrator (Corning) and further purified by SEC using a Superdex 200 10/300GL column (GE Life Sciences) equilibrated with SEC buffer collected at 2mg/ml. The molecular weight of each purified GLUT3 construct was confirmed using an MSD-ToF electrospray ionization orthogonal time-of-flight mass spectrometer (Agilent Technologies inc. Palo Alto, CA, USA).

SEC stability study. FLAG-purified GLUT4 was injected on to a Superdex 200 10/300 GL size exclusion column (GE Healthcare) pre-equilibrated with 50 mM sodium phosphate, 150 mM NaCl, 0.1 % LMNG, pH 7.4 to purify monomeric GLUT4. 40 µg of monomeric, SEC purified GLUT4 in 0.1% LMNG was then incubated in the absence and presence of various LMNG solubilized lipids (0.02% w/v) for 1.5h at 40^{o}C. Lipid dependent stabilization from heat induced destabilization of GLUT4 was monitored by SEC. All SEC experiments were conducted at a flow rate of 0.55 ml/min.

Liposome reconstitution. GLUT4 and GLUT3 containing liposomes were assembled according to Kraft *et al.* [121]. Briefly, lipids were mixed in chloroform, dried down under argon, and residual chloroform was removed under vacuum for 4h. The dried lipid film was resuspended in buffer D (50 mM potassium phosphate, 130 mM NaCl, 10 % (vol/vol) glycerol, complete protease inhibitor (Roche), pH 7.4) with rigorous vortexing under argon. Lipids were hydrated for 1 h at room temperature using a vortexer set to the lowest speed followed by five freeze/thaw cycles in liquid nitrogen and 37^{o}C. The resulting multilamellar vesicles were extruded eleven times through 200 nm polycarbonate filters (Whatman) using a mini extruder (Avanti Polar Lipids) according to the manufacturer's instructions to form large unilamellar vesicles. Triton X-100

destabilized liposomes were rotated with purified GLUT4 at a lipid to protein ratio of 100-125:1 (w/w) for 45 min 4°C. Amberlite XAD-2 beads were added to remove detergent at a wet weight of 15.5 mg beads per mg Triton X-100 and samples were then rotated at 4^{o}C for 1 h. Fresh beads were added 3 additional times for 1 h, once more overnight, and one additional time for 2 h the following day. After removal of all beads, liposomes were collected by ultracentrifugation at 4°C for 1 h at 267,000 x g and resuspended in buffer containing 50 mM potassium phosphate (pH 7.4), 130 mM KCl, pH 7.4 and complete protease inhibitor (Roche). Samples were flash frozen with liquid nitrogen before storing samples at -80°C.

Liposome ^{3}H-glucose uptake. Frozen liposomes containing purified GLUT4 or GLUT3 were thawed at room temperature and subjected to three freeze/thaw cycles (liquid nitrogen/room temperature) followed by extrusion through a 200 nm polycarbonate filter. Uptake was started by adding ^{3}H-D-glucose (1 µCi/ml, 200 µM cold D-glucose) (American Radiolabeled Chemicals) to GLUT4 or GLUT3 proteoliposomes at room temperature. Transport was stopped at different times with 5 ml ice-cold quench buffer (50 mM potassium phosphate (pH 7.4), 130 mM KCl, pH 7.4, and 100 µM phloretin) and then filtered by vacuum on a 0.2 µm mixed cellulose ester filters (Avantec). Filters were subsequently washed with an additional 10 ml of quench buffer. Scintillation fluid was added to the filters and the radioactivity counted. ^{3}H-L-glucose (1 µCi/ml, 200 µM cold L-glucose) was used to determine nonspecific transport. Specific uptake was calculated for all experiments by subtracting nonspecific ^{3}H-L-glucose from ^{3}H-D-glucose uptake. In single time point experiments, specific uptake was normalized to amount of transporter per reaction. The amount of transporter protein used in each uptake assay was determined by analyzing aliquots of transporter containing liposomes along with a BSA

standard curve on an SDS polyacrylamide gel stained with Blue Bandit protein stain and quantified using an Odyssey infrared imaging system (LI-COR Biosciences). Data were fitted by non-linear regression analysis using GraphPad Prism 6.0.

[^{3}H]-D-glucose uptake in HEK293 cells. Stably transfected, tetracycline inducible HEK293S GnTI- cells, expressing GLUT4 were grown on PEI treated 12-well plates to 90% confluency for uptake experiments. 72 hours prior, protein expression was induced by 2 µg/ml doxycycline hyclate and 5mM sodium butyrate while control cells were left uninduced. Cells were glucose-starved in HEPES-buffered saline at room temperature 30 min prior to uptake measurements. Uptake was initiated in HEPES-buffered saline at room temperature with the addition of [^{3}H]-D-glucose and then quenched after 40 s by washing rapidly in ice-cold PBS. Intracellular radioactivity was quantified by liquid scintillation counting and normalized to total protein (BCA Protein Assay, Pierce). GLUT4 specific uptake was calculated by subtracting uptake from uninduced cells from that of induced cells.

3.8 Figures

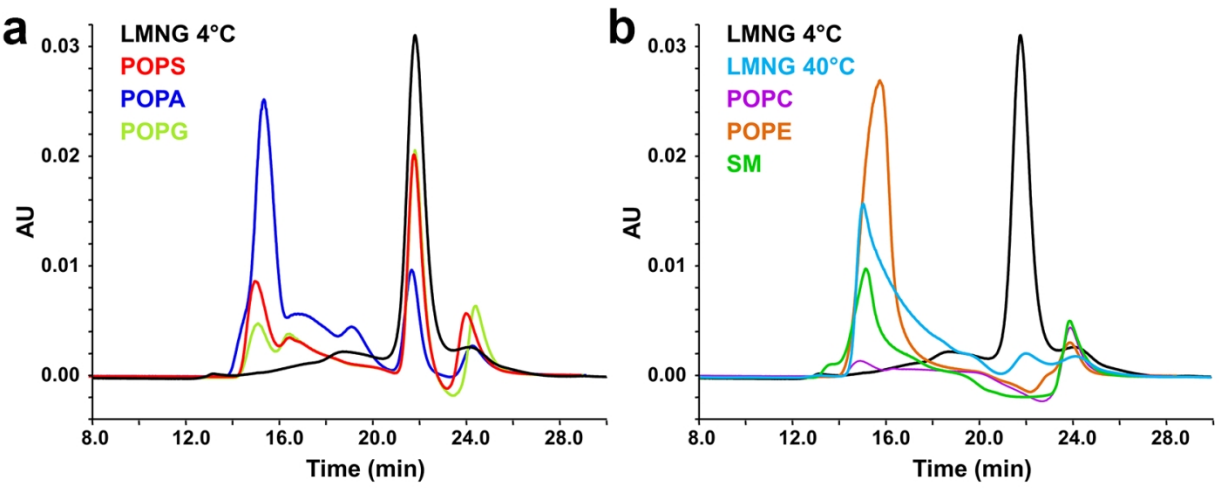

Figure 3.1. Protection of GLUT4 by anionic phospholipids from heat-induced destabilization. SEC elution profiles of GLUT4 before and after heating in the presence or absence of several anionic (**a**) and zwitteronic (**b**) lipids (0.02% w/v) as indicated by the color key. Protein absorption was monitored at 280nm at a flow rate of 0.55 ml/min. Results are representative of two independent experiments.

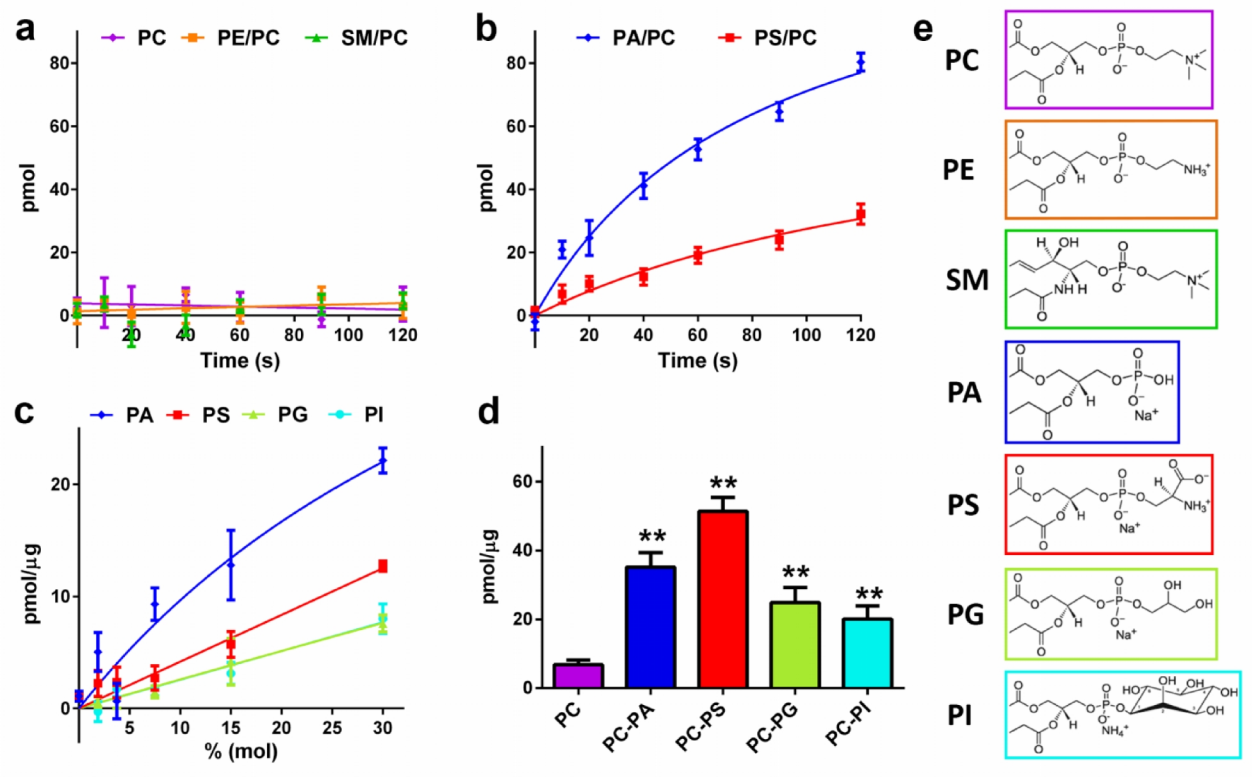

Figure 3.2. Anionic phospholipids are required for GLUT4 and GLUT3 mediated D-glucose uptake. (**a**,**b**) Time dependent specific uptake of ^{3}H-D-glucose into GLUT4 containing PC liposomes in the presence or absence of 15% (mol/mol) zwitterionic lipids (**a**) and anionic phospholipids (**b**). Data are the mean ± s.e.m. of three independent experiments. (**c**) Specific uptake of ^{3}H-D-glucose into GLUT4 containing PC liposomes with increasing concentrations of anionic phospholipids. Normalized uptake data (40s) are the mean ± s.e.m. of three independent experiments. (**d**) Specific uptake of ^{3}H-D-glucose into GLUT3 containing PC liposomes in the presence or absence of 15% (mol/mol) anionic phospholipids. Normalized uptake data (40s) are the mean ± s.e.m of four independent experiments. Asterisks denote statistically significant differences (**, $P \leq 0.01$) compared to PC control as determine by one-

way ANOVA plus *a posteriori* Holm-Sidak test. (**e**) The chemical structure of each of the lipid headgroups are colored coded for comparison.

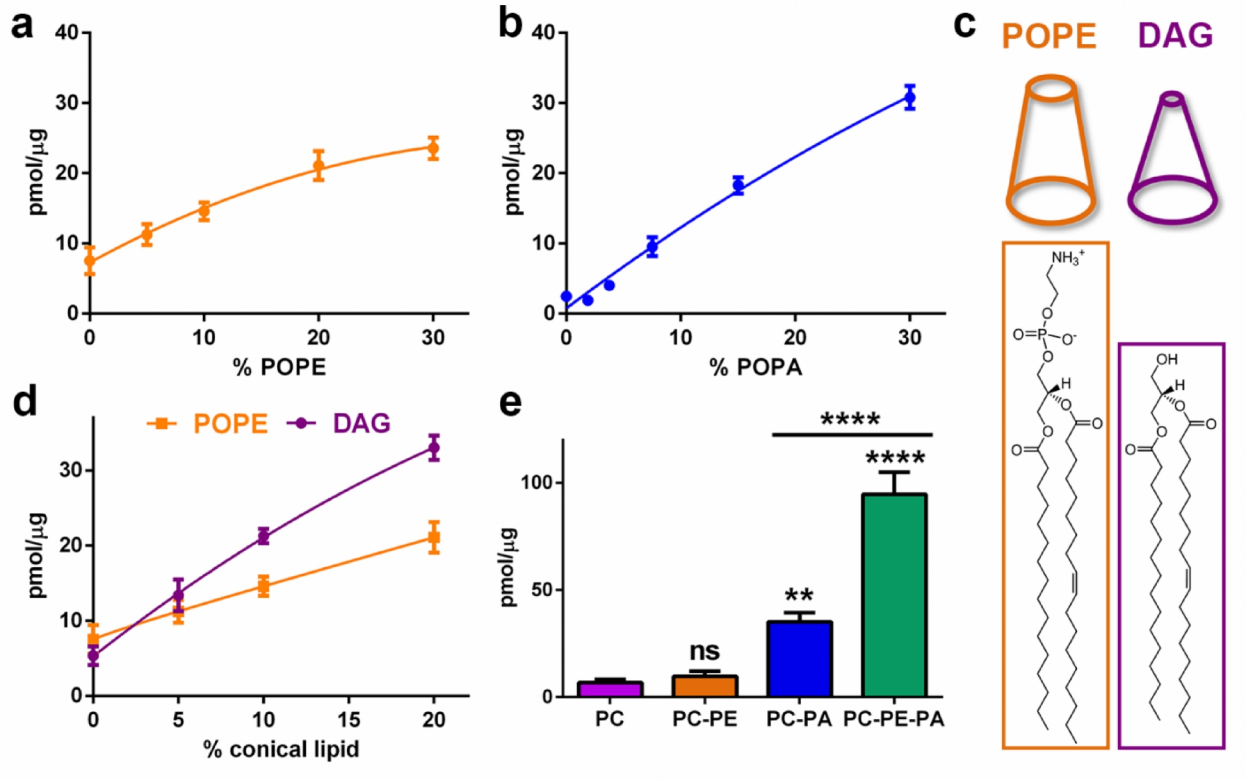

Figure 3.3. Conical lipids stimulate GLUT4 and GLUT3 mediated glucose uptake. (**a**) Specific uptake of ^{3}H-D-glucose into GLUT4 containing PC liposomes in the presence of 10% (mol/mol) POPA with increasing concentrations of POPE. Normalized uptake data (40 sec) are the mean ± s.e.m. of five independent experiments. (**b**) Specific uptake of ^{3}H-D-glucose into GLUT4 containing PC liposomes in the presence of 30% (mol/mol) POPE with increasing concentrations of POPA. Normalized uptake data (40 sec) are the mean ± s.e.m. of five independent experiments. (**c**) Chemical structures and overall shape of POPE and DAG. (**d**) Specific uptake of ^{3}H-D-glucose into GLUT4 containing PC liposomes in the presence of 10% (mol/mol) POPA with

increasing concentrations of DAG. POPE titration results are shown for comparison. Normalized uptake data (40 sec) are the mean ± s.e.m. of five independent experiments. (**e**) Specific uptake of ^{3}H-D-glucose into GLUT3 containing PC liposomes in the presence or absence of 15% (mol/mol) POPA and/or 15% (mol/mol) POPE. Normalized uptake data (40 sec) are the mean ± s.e.m. of five independent experiments. Asterisks denote statistically significant difference (ns, $P > 0.05$; **, $P \leq 0.01$; ****, $P \leq 0.0001$) compared to PC control (unless otherwise indicated) as determine by one-way ANOVA plus *a posteriori* Holm-Sidak test.

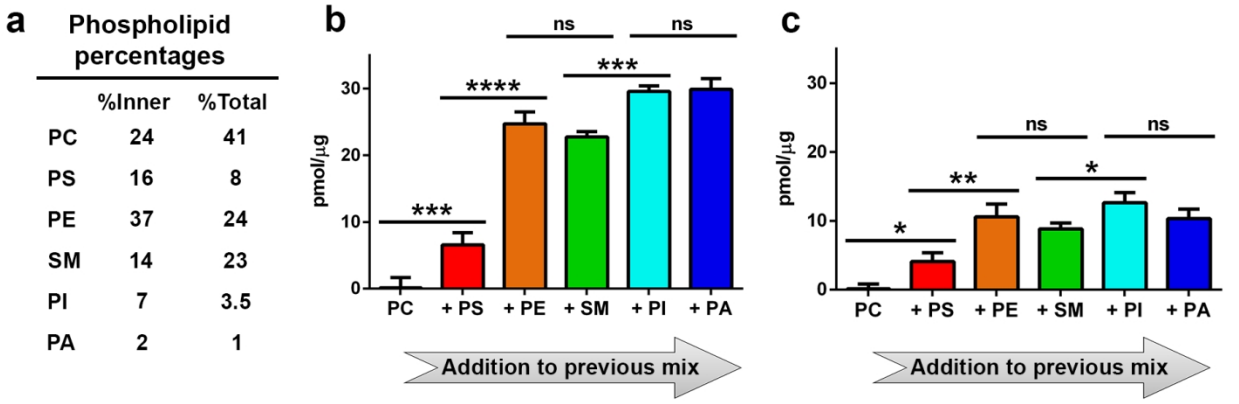

Figure 3.4. Anionic and conical lipid effects on GLUT4 mediated glucose uptake are observed in liposomes with a lipid composition comparable to that of the PM. (**a**) Phospholipid composition of an idealized mammalian PM[125]. (**b**,**c**) Specific uptake of ^{3}H-D-glucose into GLUT4 containing liposomes with lipid ratios reflecting the inner leaflet (**b**) or total PM (**c**) composition. From left to right each bar represents an experiment where an additional lipid was added to the previous lipid mix (**Supplementary Tables 1 and 2**). Normalized data (40s) are the mean ± s.e.m. of five independent experiments. Asterisks denote statistically significant difference (ns, $P > 0.05$; *, $P \leq 0.05$; **, $P \leq 0.01$; ***, $P \leq 0.001$; ****, $P \leq 0.0001$) as determine by one-way ANOVA plus *a posteriori* Holm-Sidak test.

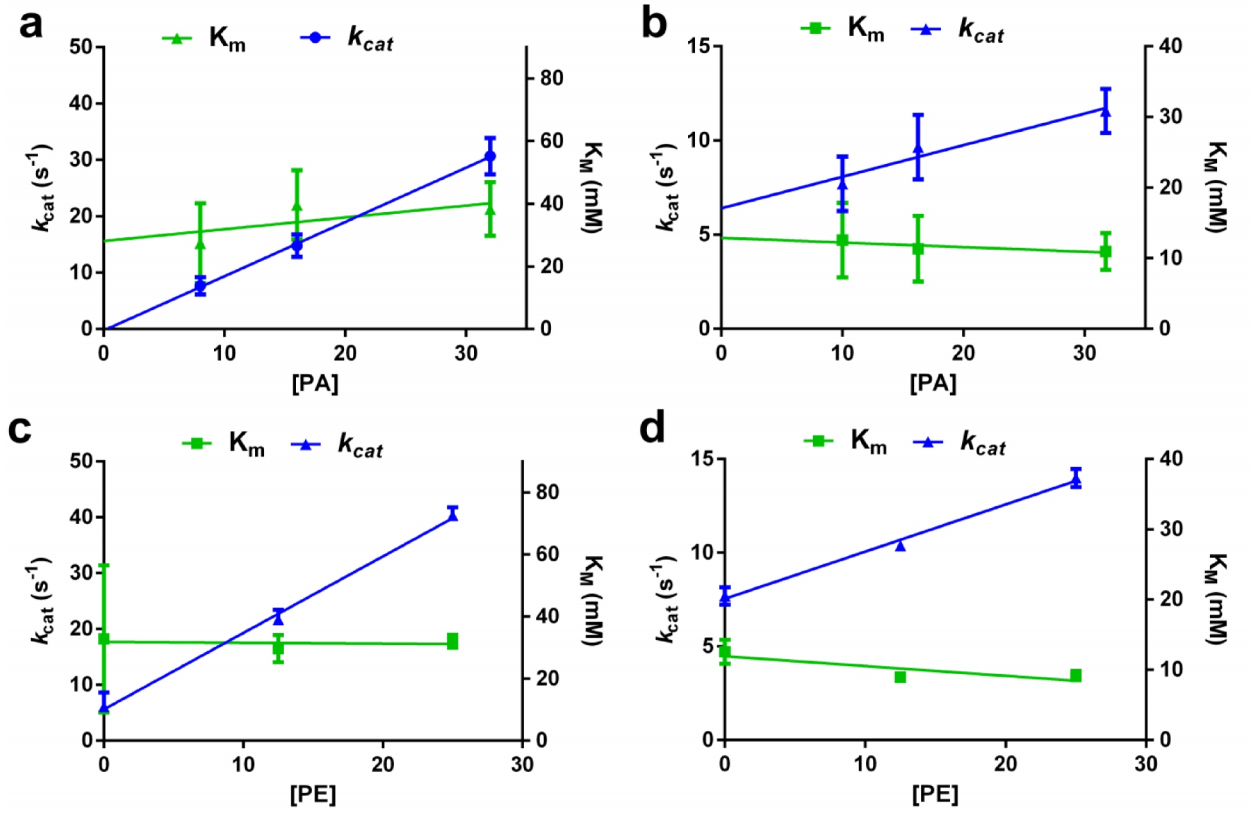

Figure 3.5. Anionic and conical lipids increase the k_{cat} but have no effect on the K_M of both GLUT4 and GLUT3. (**a**,**b**) POPA concentration dependent change of the kinetic parameters k_{cat} and K_M for GLUT4 (**a**) and GLUT3 (**b**). Data are expressed as mean ± s.e.m. of four independent experiments. (**c**,**d**) POPE concentration dependent change of the kinetic parameters k_{cat} and K_M for GLUT4 (**c**) and GLUT3 (**d**). Data are expressed as mean ± s.e.m. of four independent experiments. Kinetic parameters were determined from data shown in **Supplementary Fig. 2** by non-linear regression analysis and fitted using linear regression analysis.

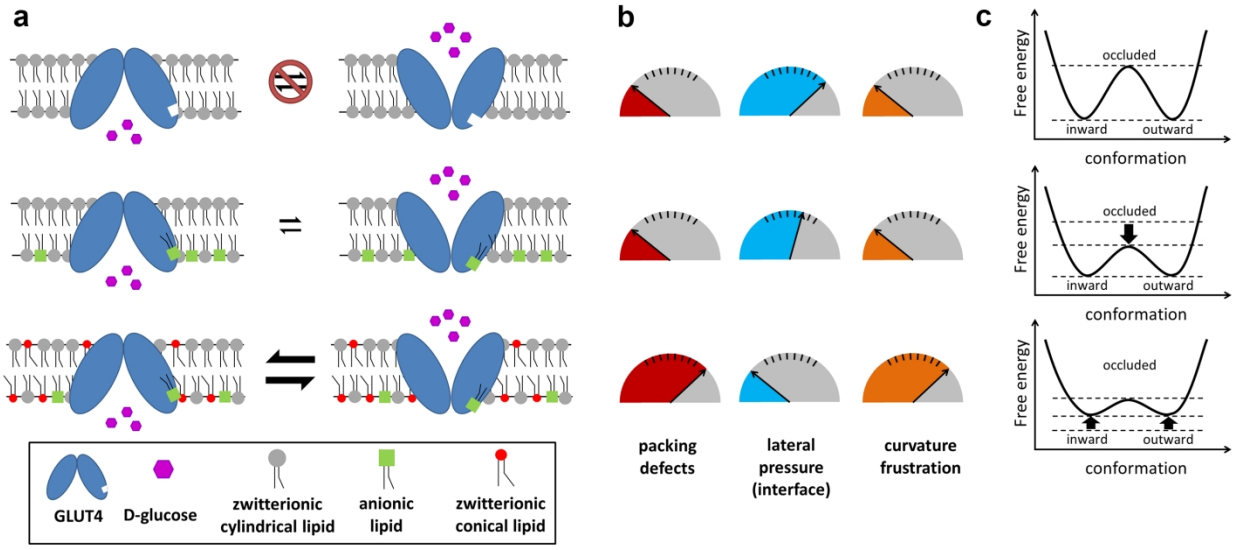

Figure 3.6. Mechanism of anionic and conical lipid effects on glucose transporters. (**a**) Model of GLUT transporter interconversion and glucose transport in the presence and absence of anionic and conical lipids. In the absence of anionic phospholipids, the transporter cannot interconvert between inward and outward facing conformations. Added anionic phospholipids bind to the transporter within the inner leaflet and trigger interconversion. Conical lipids lead to an increase in the interconversion rate of the transporter in the presence of anionic phospholipid. (**b**) Effect of anionic and conical lipids on lipid bilayer properties that influences transporter dynamics. (**c**) Energy diagrams of the free energy for different transporter conformations in the presence or absence of anionic and conical lipids.

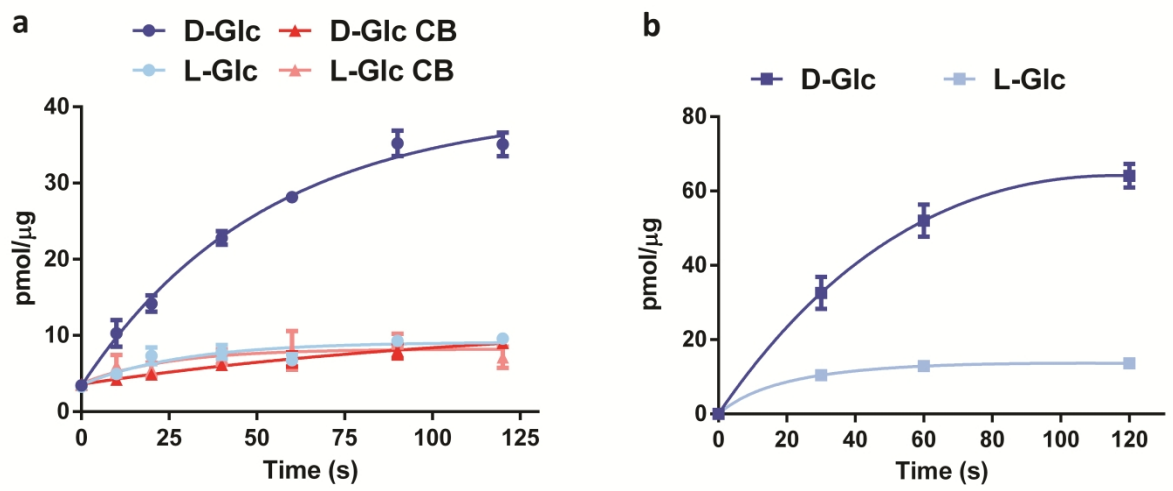

Supplementary Figure 3.1. Liposome reconstituted GLUT4 and GLUT3 transport D-glucose with high specificity over L-glucose. (**a**) Time dependent uptake of specific ^{3}H-D-glucose and nonspecific ^{3}H-L-glucose into GLUT4 containing PC:POPA:POPE (70:15:15) liposomes in the presence or absence of 20 µM of the GLUT specific inhibitor cytochalasin B. Data are the mean ± s.e.m. of three independent experiments. (**b**) Time dependent uptake of specific ^{3}H-D-glucose and nonspecific ^{3}H-L-glucose into GLUT3 containing PC:POPA:POPE (70:15:15) liposomes. Data are expressed as mean ± s.e.m. of three independent experiments.

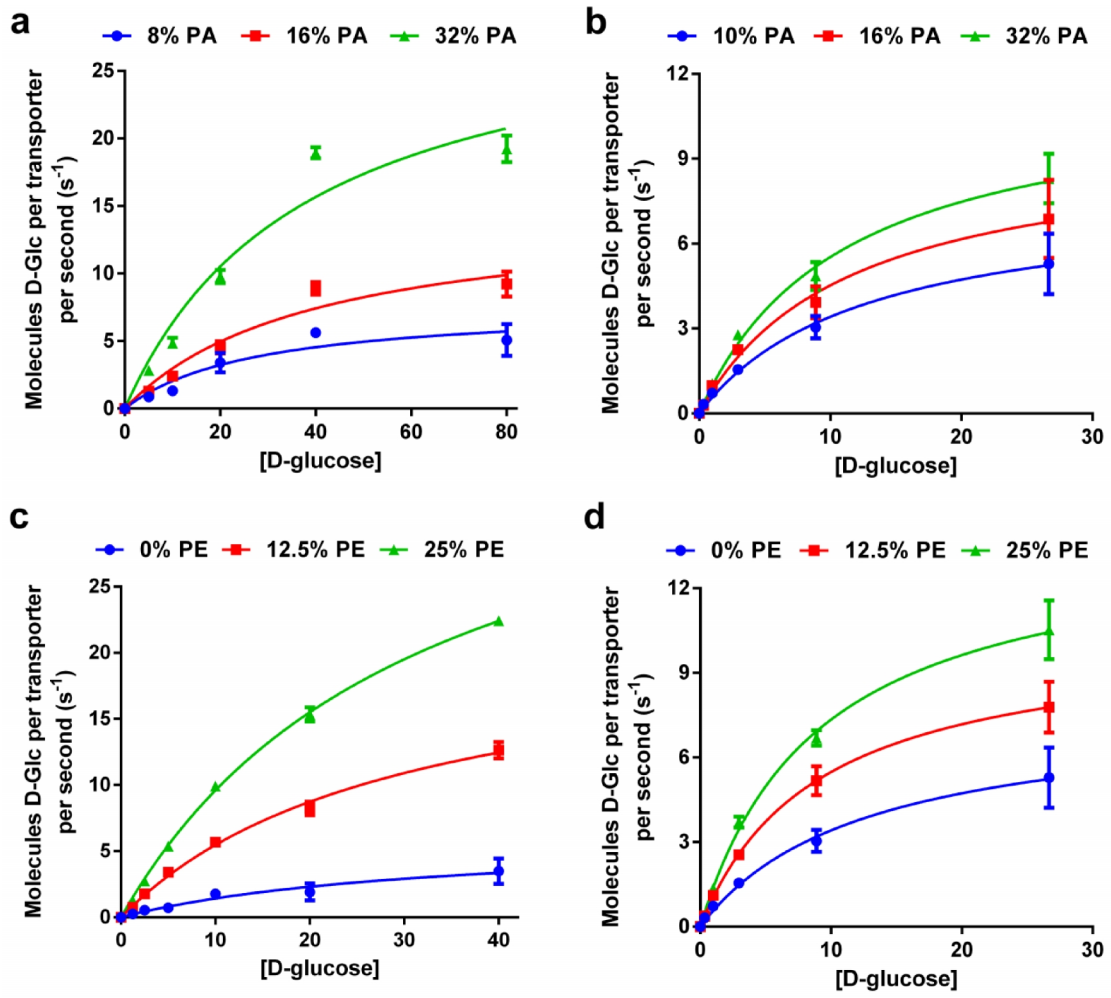

Supplementary Figure 3.2. Influence of anionic and conical lipids on transporter kinetics for GLUT4 and GLUT3. (**a**,**b**) D-glucose concentration dependent transport rate of GLUT4 (**a**) and GLUT3 (**b**) containing PC liposomes in the presence of several concentrations of POPA. Normalized data are expressed as mean ± s.e.m. of four independent experiments. (**c**,**d**) D-glucose concentration dependent transport rate of GLUT4 (**a**) and GLUT3 (**b**) containing PC liposomes in the presence of several concentrations of POPE. Normalized data are expressed as mean ± s.e.m. of four independent experiments.

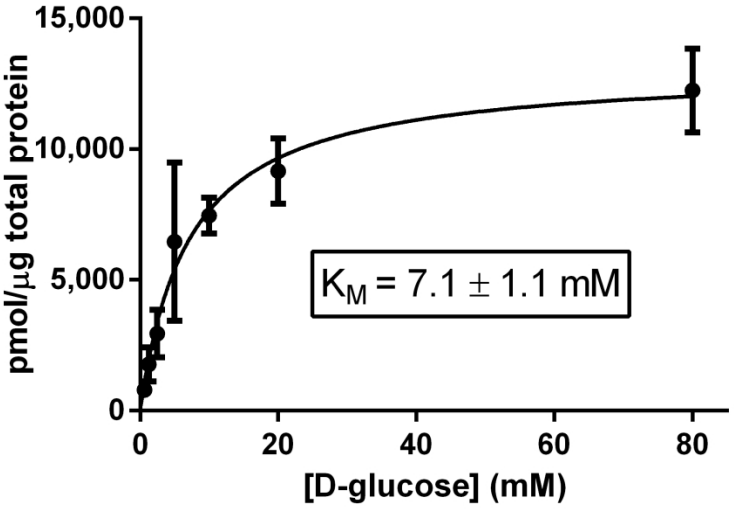

Supplementary Figure 3.3. D-glucose concentration dependent transport rate of GLUT4 in HEK293 cells. Normalized data are expressed as mean ± s.e.m. of four independent experiments. Michaelis constant K_M was determined by non-linear regression analysis using GraphPad Prism 6.0.

Supplementary Table 3.1. Total PM lipid composition (mole %)

	PC	+PS	+PE	+SM	+PI	+PA
eggPC	100	92	68	45	41.5	40.5
POPS	0	8	8	8	8	8
POPE	0	0	24	24	24	24
SM	0	0	0	23	23	23
PI	0	0	0	0	3.5	3.5
POPA	0	0	0	0	0	1

Supplementary Table 3.2. PM inner leaflet lipid composition (mole %)

	PC	+PS	+PE	+SM	+PI	+PA
eggPC	100	84	47	33	26	24
POPS	0	16	16	16	16	16
POPE	0	0	37	37	37	37
SM	0	0	0	14	14	14
PI	0	0	0	0	7	7
POPA	0	0	0	0	0	2

Chapter 4 - The Glucose Transporter PfHT is an Antimalarial Target of the HIV Protease Inhibitor Lopinavir

Thomas E. Kraft[a], Christopher Armstrong[a], Monique R. Heitmeier[a], Audrey R. Odom[a,c] and Paul W. Hruz[a,b,†]

[a]Department of Pediatrics, and [b]Department of Cell Biology and Physiology, [c]Department of Molecular Microbiology, Washington University School of Medicine, St Louis MO 63110

[†]corresponding author

4.1 Abstract

Malaria and HIV infection are co-endemic in a large portion of the world and remain a major cause of morbidity and mortality. Growing resistance of *Plasmodium* species to existing therapies has increased the need for new therapeutic approaches. The *Plasmodium* glucose transporter PfHT is known to be essential for parasite growth and survival. We have previously shown that HIV protease inhibitors (PIs) act as antagonists of mammalian glucose transporters. While the PI lopinavir is known to have antimalarial activity, the mechanism-of-action is unknown. We report here that lopinavir blocks glucose uptake into isolated malaria parasites at therapeutically relevant drug levels. Malaria parasites depend on a constant supply of glucose as their primary source of energy and decreasing the available concentration of glucose leads to parasite death. We identified the malarial glucose transporter PfHT as a target for inhibition by lopinavir that leads to parasite death. This discovery provides a mechanistic basis for the antimalarial effect of lopinavir and provides a direct target for novel drug design with utility beyond the HIV-infected population.

4.2 Introduction

Despite aggressive world-wide efforts to eradicate malaria, this life-threatening disease continues to affect over 200 million people per year, resulting in an annual death toll exceeding half a million, mostly among African children[139]. Currently, vaccination against malaria is not available, while resistance against all known therapeutics is spreading[139]. As a result, newer antimalarial agents with novel mechanisms-of-action are urgently needed.

The global prevalence of malaria and HIV infection largely overlap geographically. Combination antiviral therapy that includes the HIV protease inhibitor (PI) lopinavir has been found to dramatically decrease malaria incidence in a pediatric clinical population by 41%, suggesting a direct effect of PIs on parasite replication[45]. Indeed, lopinavir has demonstrated *in vitro* activity[49] against *Plasmodium falciparum*, the protozoan species responsible for most malaria deaths[48,139]. In addition, lopinavir reduces the malaria liver stage burden in infected rhesus monkeys *in vivo* at clinically relevant concentrations[140].

Despite ongoing efforts, the direct cellular target(s) of lopinavir responsible for its antimalarial properties against *P. falciparum* remains unclear. PIs were originally designed as antagonists of the viral aspartyl protease[141]. The malaria parasite requires a class of aspartyl proteases called plasmepsins, which are necessary to degrade host hemoglobin[142] and direct export of malaria export proteins[143]; however the antimalarial activity of PIs does not appear to be mediated through plasmepsin inhibition[47,50]. Identifying the antimalarial mechanism-of-action of PIs is imperative for finding a novel, clinically proven drug target and developing a new class of lopinavir-like antimalarial drugs.

In clinical populations, prolonged use of PIs is associated with insulin resistance. Recent studies have identified the molecular mechanism of this effect, which is mediated by direct binding of PIs to the insulin-responsive facilitative glucose transporter GLUT4[144–146]. The human glucose transporters share sequence homology with the essential *P. falciparum* glucose transporter, PfHT. Similar to GLUT1 and GLUT4, the predicted topology of PfHT comprises 12 transmembrane helices, forming a central glucose permeation path. Key residues that are

involved in glucose binding and transport are preserved between the human and malaria glucose transporters[44,147].

Intraerythrocytic malaria parasites depend on a constant supply of glucose as their primary source of energy[148]. Not surprisingly, infected erythrocytes show a ~100 fold increase in glucose consumption compared to uninfected erythrocytes[149]. PfHT (PF3D7_0204700) is the principal glucose transporter, transcribed from a single copy gene with no close paralogue[44]. PfHT has been genetically validated as essential in *Plasmodium* parasites[150] and has been independently chemically validated as a novel drug target against malaria[40,44].

Here we show that lopinavir inhibits glucose uptake into the *P. falciparum* parasite by blocking PfHT at therapeutically relevant concentrations. This establishes a direct molecular target for the antimalarial activity of lopinavir and validates the utility of targeting PfHT in novel drug development.

4.3 Results

We compared the effect of currently FDA-approved HIV protease inhibitors on the replication and survival of *P. falciparum* parasites in asexual erythrocyte cell culture. Consistent with prior reports[49,50] , all tested compounds inhibited parasite growth. Lopinavir was the most potent inhibitor with an IC_{50} of 1.9 µM (Fig. 4.1a). We previously determined the inhibitory effect of several HIV protease inhibitors on human glucose transport[68,144,146]. Since HIV PIs inhibit human glucose transport, we evaluated whether lopinavir might inhibit glucose uptake in isolated *P. falciparum* parasites. We compared the uptake of radiolabeled 2-DOG in live parasites, isolated from erythrocytes treated with vehicle, lopinavir, or the chemically unrelated PfHT inhibitor

3361 (Fig. 4.2a)[40]. The O-3-hexose derivative compound 3361 [3-O-((undec-10-en)-yl)-D-glucose)] has previously been shown to selectively inhibit PfHT relative to several mammalian sugar transporters and inhibit glucose uptake by the parasite, leading to inhibition of growth and proliferation *in vitro* and *in vivo*[40,43]. We found that high concentrations of lopinavir potently inhibited uptake of radiolabeled glucose by more than 70% compared to vehicle-treated control, similar to the effect observed by the known PfHT inhibitor compound 3361. In dose-response studies (Fig. 4.2b), we found that the inhibitory concentration (IC_{50})) of lopinavir was 16 ± 4.2 μM, which is within the range of average serum peak levels of both adult and pediatric patients treated with lopinavir/ritonavir[151–154].

To confirm that inhibition of malaria glucose transport was mediated through PfHT inhibition, we developed and tested the effect of this PI on glucose transport in a PfHT-overexpressing HEK293 cell line. HEK293 cells predominantly transport glucose using the facilitative transport protein GLUT1. Using a PfHT sequence codon-optimized for mammalian cell expression, we overexpressed the malarial hexose transporter protein and knocked down the expression of GLUT1 using shRNA. In this engineered cell line, PfHT was the predominant hexose transporter expressed (Fig. 4.3a). Glucose uptake in the PfHT overexpressing cell line was >5 times higher compared to background cells that did not overexpress PfHT but were transduced with GLUT1 shRNA (Fig. 4.3b). We quantified the amount of [^{3}H]-2-DOG accumulated in PfHT overexpressing HEK293 cells in the presence of varying concentration of lopinavir and determined an IC_{50} of 14 ± 2 μM. The IC_{50} values for the effect of lopinavir on glucose uptake in both *P. falciparum* parasites and PfHT-overexpressing HEK293 cells are closely correlated, consistent with a model in which inhibition of PfHT is responsible for decreased glucose uptake

and reduced parasite growth (Fig. 4.4). Supporting this model, blood stage *P. falciparum* is acutely sensitive to reduced extracellular glucose concentrations [149]. Since the measurement of 2-DOG uptake involves both the transport of this sugar and phosphorylation to 2-DOG-6-P, we cannot fully exclude the possibility that lopinavir also inhibits the malarial hexokinase. However, the observation that lopinavir inhibits 2-DOG uptake with different IC_{50}s when measured in HEK293 cells overexpressing different GLUTs (ranging from 3µM for GLUT4 to 32µM for GLUT1) suggests that hexokinase is not directly targeted.

To further investigate the mode of action of lopinavir on PfHT, we determined several parameters by Michaelis-Menten kinetics. As expected, uptake of glucose is saturated with increasing substrate concentration. The observed increase in K_m with constant V_{max} indicates that lopinavir acts as a competitive inhibition of glucose uptake (Fig. 4.5).

To investigate the binding site of lopinavir on PfHT, we generated a model of the transporter based on several crystal structures of homologous proteins using the I-TASSER webserver (Table 1). We selected a model with high cluster density in an inward conformation to determine the lopinavir binding site by docking analysis. We created a docking volume covering the entire protein to obtain unbiased results. Lopinavir was docked to the PfHT model using AutoDock VINA via rigid receptor, flexible ligand docking. All docked poses of lopinavir were bound to single binding pocket on the intracellular side of the glucose permeation path, preventing glucose from entering and reaching its binding site (Fig. 4.6a). These results could be replicated in several docking experiments using random seeds and different degrees of exhaustiveness, strongly supporting this position as the lowest energy binding site. We compared the PfHT-lopinavir putative binding site with the binding site of the structurally related protease inhibitor

indinavir in the PfHT homologue GLUT4, published by Hresko *et al.* (Fig. 4.6b)[68]. The docking experiments suggest that both indinavir and lopinavir bind to a structurally similar binding pocket in their respective glucose transporters. Lopinavir binding within the glucose permeation pathway is consistent with this drug acting as a competitive inhibitor of zero-trans glucose uptake (Fig. 4.5). Although inhibition of GLUT4 by Indinavir requires drug binding from the intracellular side of the transporter (35), lopinavir appears to have access to this domain from the exofacial side of PfHT. Similar to the observed differences in isoform-selectivity of HIV protease inhibitors for mammalian GLUTs (26), it is possible that steric influences of amino acid side chains lining the glucose permeation pathway contribute to the ability of these drugs to target PfHT.

4.4 Discussion

There is a compelling need for novel therapies for treatment of malaria. In particular, the emergence and spread of resistance to artemisinin-based compounds threatens malaria control efforts worldwide. Protease inhibitors, such as lopinavir, represent promising therapeutic leads for new antimalarial development. Lopinavir has potent antimalarial activity *in vitro* and in animal models[48,140], and human studies of lopinavir-treated individuals in endemic areas indicate antimalarial potency at clinically relevant doses[45]. Importantly, many of the pharmacologic challenges that slow antimalarial development have already been overcome with lopinavir, which is orally bioavailable, available in suspension form (for pediatric use), and suitable for once-daily dosing in combination with ritonavir.

Our studies provide substantial evidence that inhibition of the malaria hexose transporter, PfHT, is responsible for the antiparasitic effects of lopinavir. PfHT hexose transporter function is known to be required for *Plasmodium* parasite development in culture and in animal models[40,43,44,150,155]. We find that not only does lopinavir directly block glucose uptake into *P. falciparum* parasites, it also inhibits glucose uptake in human cells engineered such that majority of hexose transport is through heterologously expressed PfHT. Importantly, profound reductions of glucose uptake into parasites and into PfHT-expressing human cells are achieved at lopinavir concentrations well below therapeutically achieved drug levels[151–154].

Of note, even lower concentrations of both lopinavir and compound 3361 are required to inhibit parasite replication than are required to inhibit glucose transport[40]. This difference may be explained by the reliance of parasites on a constant glucose supply. *Plasmodium* infection increases cellular glucose consumption in erythrocytes nearly 100 fold, while parasite survival is highly sensitive to reduced extracellular glucose concentrations[149]. Thus, even partial inhibition of *Plasmodium* glucose transporters may lead to growth inhibition and eventually death of the parasite. PfHT may therefore represent a promising, parasite-specific "Achilles Heel" for target-based drug discovery efforts. We cannot rule out the possibility that there are additional targets of lopinavir in *P. falciparum* other than PfHT . The existence of additional drug targets, if present, could delay the development of drug resistance, a major problem for malaria drugs. However, observing this difference for both lopinavir and compound 3361, two structurally unrelated drugs that inhibit PfHT-mediated glucose transport decreases the likelihood that they would both also inhibit another secondary target.

As agents designed for long-term suppression of HIV replication, lopinavir and other protease inhibitors are well tolerated, with minor adverse events (mostly gastrointestinal) associated with short-term use[46]. During chronic HIV treatment regimens that include PIs, disturbances in glucose homeostasis and other metabolic changes that increase cardiovascular risk have been reported[156]. In this HIV-infected population, it has been challenging to dissociate the direct contributions of PIs from the influences of viral infection, other drug exposures (e.g. nucleoside reverse transcriptase inhibitors), and associated environmental factors. Nevertheless, the in vitro effects of PIs on the insulin-responsive facilitative glucose transporter GLUT4 correlate directly with in vivo changes in insulin sensitivity, both in rodent models[157] and in humans[158]. Fortunately, the effect of PIs on glucose tolerance is readily reversible following short-term drug exposure, as required for treatment of malaria[157,158]. However, the full spectrum of PI-mediated effects on the remaining GLUT isoforms remains unknown, and not all PIs appear to have the same effect on GLUT4 activity[159]. Ideally, the development of drugs that selectively target PfHT over mammalian GLUTs would provide highly selective inhibition of PfHT over the mammalian GLUTs, resulting in a superior safety profile.

The development of high-throughput screening protocols targeting the *Plasmodium* glucose transporter will help identify additional classes of PfHT antagonists. Several assays have been developed by expressing PfHT in yeast or *Leishmania*[44,150,160]. In combination with these prior studies, our current findings confirm that PfHT is an attractive, druggable target for malaria. Our development of a PfHT overexpressing HEK293 cell line and demonstration that this system can reliably test for drug-mediated inhibition of the malarial glucose transporter can significantly aid candidate drug screening. Complementing a high-throughput approach is the

opportunity for structure-based design. This can allow for higher affinity and selectivity to the plasmodium transporter while minimizing effects on mammalian glucose transporters (GLUTs). GLUT1 is the most extensively characterized of the human GLUTs and a crystal structure of this protein was recently reported[13]. In the absence of structural data for PfHT and the other known GLUTs, it has been necessary to rely upon molecular modeling based on the structures of related bacterial and mammalian transporter. Although, our docking results are consistent with the previously identified HIV protease inhibitor binding site in the closely related transporter GLUT4[68], we cannot exclude the possibility that lopinavir binds to a distinct binding site only accessible in an outward open conformation of PfHT. Testing this possibility will generate valuable data once a homologues transporter is crystallized in the outward open conformation. Future efforts to establish a comprehensive structure-activity profile for the inhibition of PfHT and the human GLUTs may provide valuable information about the feasibility of this approach. Investigation of potential additive or synergistic effects of PfHT inhibitors with existing anti-malarial agents or other compounds that inhibit parasite metabolism will also be of great interest.

In summary, the identification of lopinavir as a clinically meaningful inhibitor of the essential malaria hexose transporter PfHT provides a strong rationale and molecular basis for future antimalarial development efforts targeting this protein. Because PfHT inhibition retards both the liver and mosquito-stage development of rodent malaria parasites[42], novel PfHT inhibitors hold great promise for use in malaria treatment and as transmission-blocking agents. The existing pharmacokinetic and safety data for lopinavir should allow rapid assessment of the suitability and efficacy of this agent in non-HIV infected patient populations. Understanding the

molecular target of lopinavir in *P. falciparum* will be key to any necessary medicinal chemical optimization of lopinavir and related protease inhibitors, repurposed for use as antimalarials.

4.5 Material and Methods

Materials

[^{14}C]-2-deoxy- glucose (2-DOG) was purchased from PerkinElmer. [^{3}H]-2DOG was purchased from American Radiolabels Inc. PfHT DNA was codon optimized and synthesized by Life Technologies (Grand Island, NY). GLUT1 shRNA was obtained through the RNAi core at Washington University, School of Medicine. HEK293 cells were acquired from the American Type Culture Collection. HIV protease inhibitors were obtained through the NIH AIDS Reagent Program, Division of AIDS, NIAID, NIH. Compound 3361 was kindly donated by Sanjeev Krishna (Centre for Infection, Division of Cellular and Molecular Medicine, St. George's, University of London).

Malaria tissue culture

The *P. falciparum* strain strain 3D7 was obtained from the Malaria Research and Reference Reagent Resource Center (MR4, ATCC, Manassas, Virginia). Unless otherwise stated, *P. falciparum* strains were cultured at 37°C in a 2% suspension of human erythrocytes in RPMI-1640 medium (Sigma-Aldrich, SKU R4130) supplemented with 27 mM sodium bicarbonate, 11 mM glucose, 5 mM HEPES, 1 mM sodium pyruvate, 0.37 mM hypoxanthine, 0.01 mM thymidine, 10 µg/mL gentamicin, and 0.5% Albumax (Life Technologies) in a 5% O2/ 5% CO2 /

90% N2 atmosphere, as previously described[161,162]. Culture growth was monitored by microscopic analysis of Giemsa-stained blood smears.

Drug and glucose sensitivity of *P. falciparum*

Asynchronous *P. falciparum* cultures were diluted to 1% parasitemia and were treated at a range of concentrations of inhibitor or glucose. Growth inhibition assays were performed in opaque 96-well plates at 100 µL culture volume. After 3 days, parasite growth was quantified by measuring DNA content using Picogreen (Life Technologies), as previously described[163]. Picogreen fluorescence was measured on a FLUOstar Omega microplate reader (BMG Labtech) at 485 nm excitation and 528 nm emission. IC_{50} values were calculated by nonlinear regression analysis using GraphPad Prism software.

Stable expression of PfHT

HEK293 cells were stably transfected with codon optimized PfHT DNA in the pcDNA 3.1(-) hygro plasmid (Life Technologies) as described earlier[164]. After selection with hygromycin, 10 colonies were grown to near confluency in 4cm tissue culture dishes and the highest expresser of PfHT was selected using [^{3}H]-2DOG uptake and quantitative RT-PCR (as described below).

Short hairpin RNA lentiviruses for GLUT1 knockdown

293T packaging cells were cotransfected with VSVg and Delta 8.9 packaging plasmids plus shRNA lentiviral plasmids targeting GLUT1 (NM_006516.1-2310s1c1) using Optifect transfection reagent (Life Technologies). The media was changed 12 hours after transfection and supernatants (10 ml) were harvested every 24 hours for 72 hours and kept at 4°C until they were pooled, filtered through 0.45 µm syringe filters, aliquoted and stored at -80°C until use.

HEK293 wild-type cells or HEK293 cells stably expressing PfHT were infected by exposing them to viral supernatant for 48 hours, then replacing with selection media (containing 5 μg/ml puromycin).

Quantitative PCR analysis

Total RNA was isolated using the TRIzol Plus RNA Purification System (Life Technologies). RNA was reverse transcribed using the qScript cDNA SuperMix (Quanta Biosciences, Gaithersburg, MD). Quantitative RT-PCR was performed using the Power SYBR® Green PCR Master Mix (Applied Biosystems) as described previously[165].

2-DOG uptake into *P. falciparum* and HEK293 cells

Uptake of [^{14}C]-2DOG into isolated parasites was determined at room temperature using the methods described previously[43]. Lopinavir and compound 3361 were added 5min prior to the addition of [^{14}C]-2DOG (0.2 μCi/mL final concentration). Uptake of [^{3}H]-2DOG into HEK293 cells was measured in phosphate buffer at 37°C for 5min as described previously [68].

Statistical analyses

The data are reported as means ±SEM. Differences between control and experimental values were determined by one-way ANOVA analysis.

Modeling of PfHT and docking of lopinavir

PfHT structure was predicted using the I-TASSER webserver[90–92]. The webserver was amongst top scorers of the Server Section of the 7th (2006), 8th (2008), 9th (2010), 10th CASPs (2012), and 11th CASPs (2014), a community-wide experiment for testing the state-of-the-art of protein

structure predictions. We chose a model that resembled the inward open conformation. Docking was performed using AutoDock Vina[93]. The receptor was prepared using MGLTools version 1.5.6 and the ligand lopinavir was prepared using ArgusLab. The docking process was repeated with number of modes of 50 and increasing exhaustiveness of 25, 50 and 100. The results in each attempt were 20 similar docked poses. Docked poses were displayed using PyMOL version 1.7.4.0.

4.8 Figures

a

	IC_{50} (μM)
lopinavir	1.9 (1.7 - 2.1)
indinavir	8.2 (5.2 - 13.1)
nelfinavir	8.7 (8.1 - 9.4)
atazanavir	9.9 (8.5 - 11.6)
saquinavir	12.3 (10.8-14.1)
ritonavir	16.6 (14.7-18.7)
tipranavir	32.2 (25.9-40.1)
amprenavir	35.1 (28.8-42.7)
darunavir	64.3 (11.70-352.9)

b

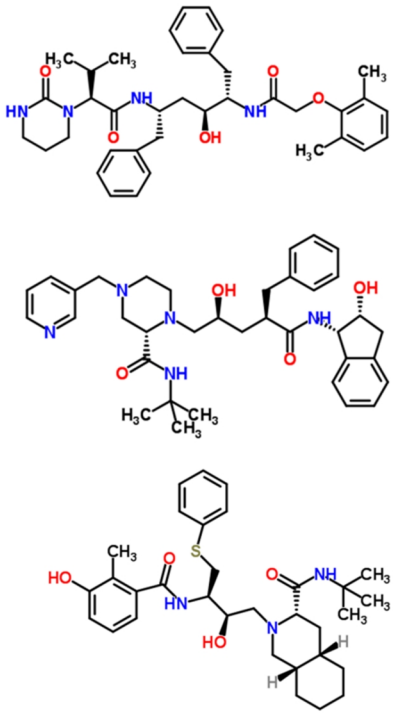

Figure 4.1. Comparison of HIV protease inhibitors' potency on P. falciparum growth inhibition

(a) IC_{50} comparison of HIV protease inhibitors on growth *P. falciparum* in blood culture. IC_{50} was calculated using non-linear regression analysis and is expressed as means with 95% confidence interval. **(b)** Chemical structures of the three most potent inhibitors HIV protease inhibitors of PfHT mediated glucose uptake.

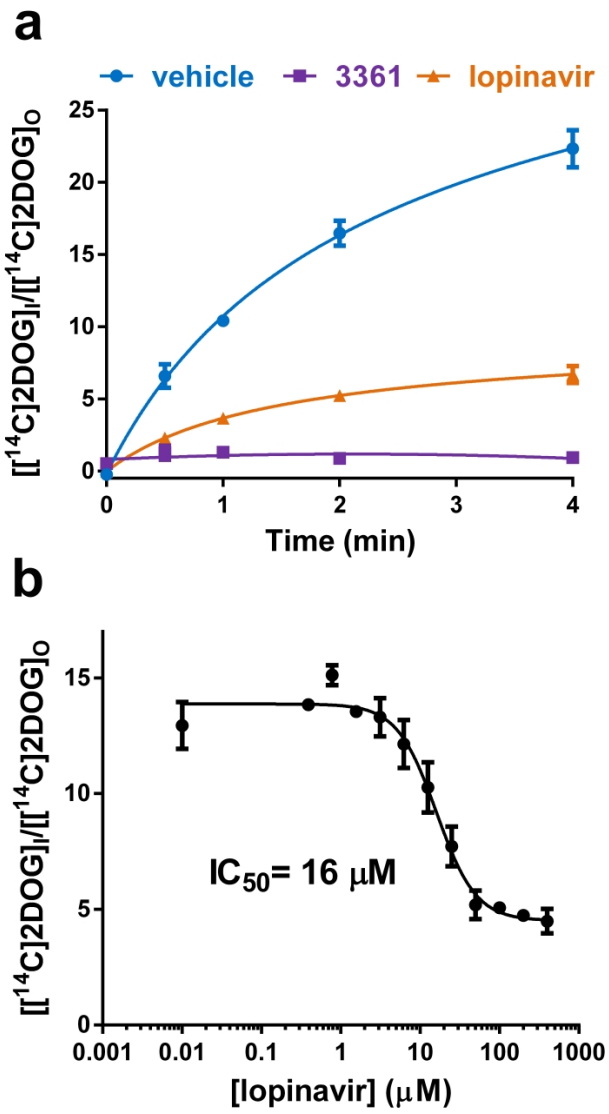

Figure 4.2. Uptake of [^{14}C]2DOG by isolated P. falciparum trophozoites (a) in the presence of lopinavir (100 µM), compound 3361 (200 µM) or vehicle or **(b)** at increasing concentrations of lopinavir. The uptake was quenched after 2 minutes. IC_{50} was calculated using non-linear regression analysis. Uptake data are expressed as means ±SEM. A 30sec or 1min time point would have been a more accurate measurement of initial rates however, we chose the longer time point to enhance the uptake signal as the degree of non-linearity will probably not greatly affect the calculated IC50 value.

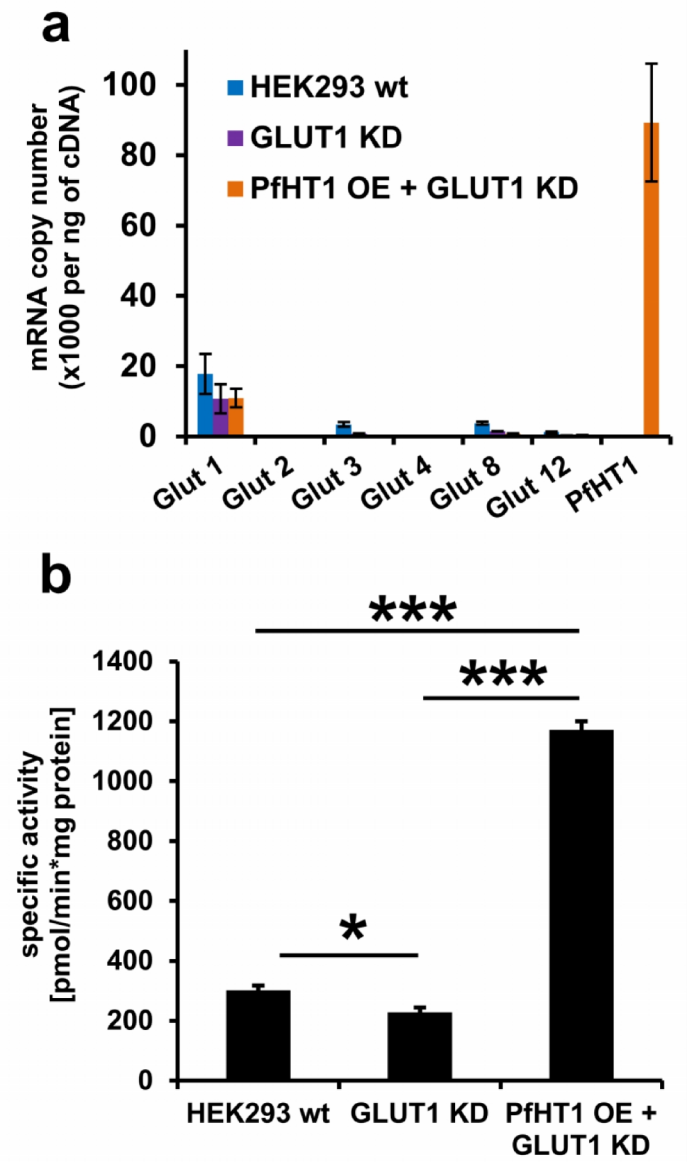

Figure 4.3. PfHT is the predominant transporter in engineered HEK293 cells. (**a)** mRNA expression levels of glucose transporter proteins in HEK293 wild-type (WT), GLUT1 knock-down (KD) and GLUT1 KD + PfHT overexpressing (OE) cells. mRNA levels were determined via quantitative PCR and levels are displayed in copy number per ng of cDNA. Data are expressed as means ±SEM. **(b)** Comparing specific activity of glucose uptake in HEK293 cells expressing GLUT1 shRNA and plus and minus overexpression of PfHT. Data are expressed as means ±SEM (*P<0.05, ***P<0.001; one-way ANOVA analysis).

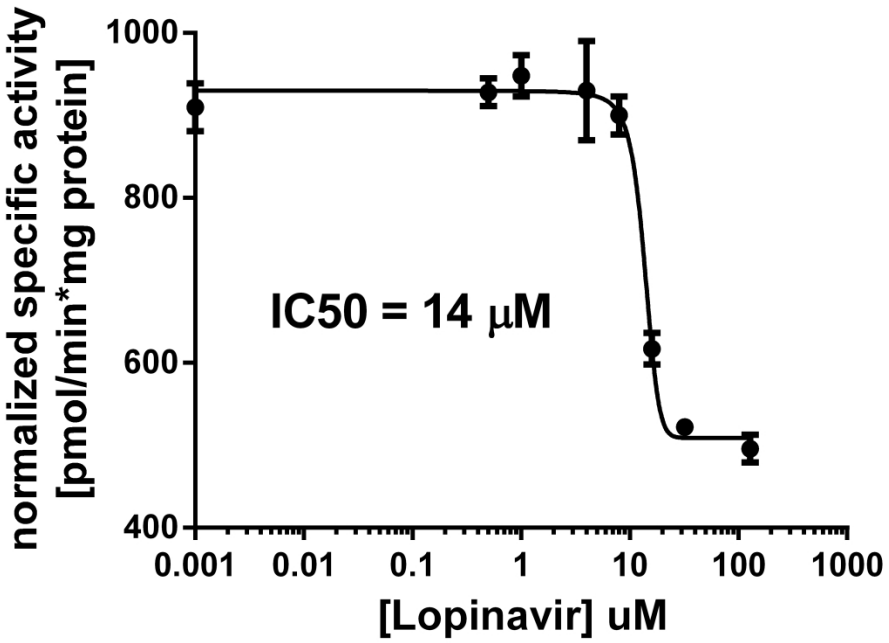

Figure 4.4. Specific activity of glucose uptake in HEK293 cells stably expressing PfHT and GLUT1 shRNA at different lopinavir concentrations. Glucose uptake was determined by quantifying the amount 2-DOG accumulated in HEK293 cells and normalizing to time and total protein. The experiment was repeated in an identical background cell line that does not overexpressing PfHT. Normalized specific activity of PfHT overexpressing cells was adjusted for non-PfHT specific glucose uptake by subtracting background uptake. Data are expressed as means ±SEM. IC_{50} was calculated using non-linear regression analysis.

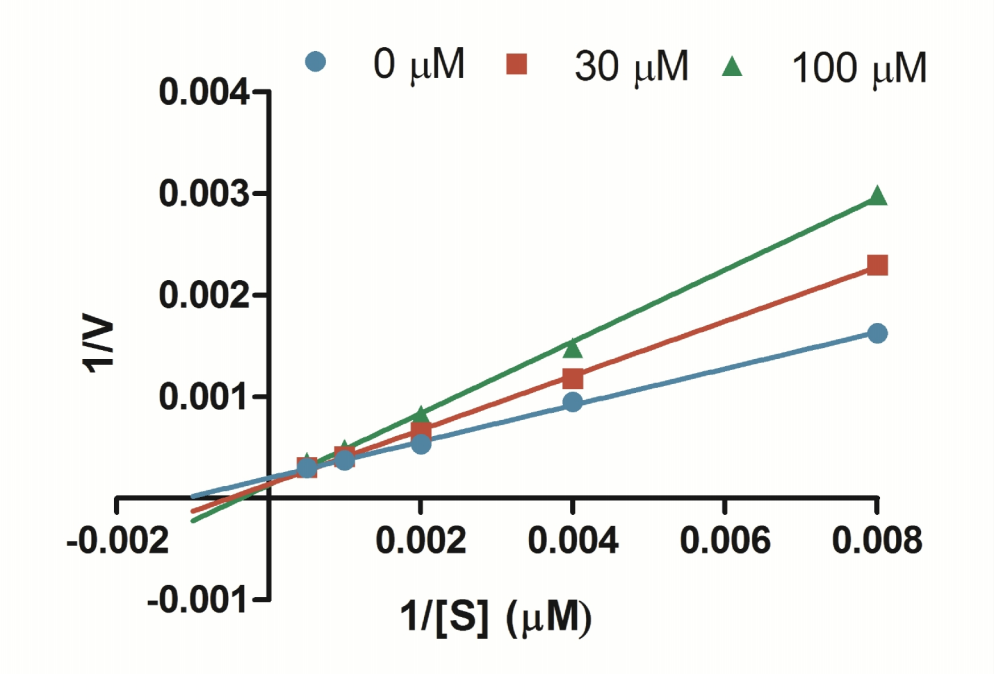

Figure 4.5. Kinetic analysis of inhibition of glucose uptake by PfHT by lopinavir. ^{3}H-2-DG uptake was determined in the presence of various concentrations of lopinavir and substrate. Uptake was quenched after 2 minutes. Data was fitted to the Michaelis-Menten equation by non-linear regression using GraphPad Prism 6 to obtain K_m and V_{max} values and was transformed and plotted as double-reciprocal Lineweaver-Burk plot using GraphPad Prism 6. Uptake data are expressed as means ±SEM (n=3).

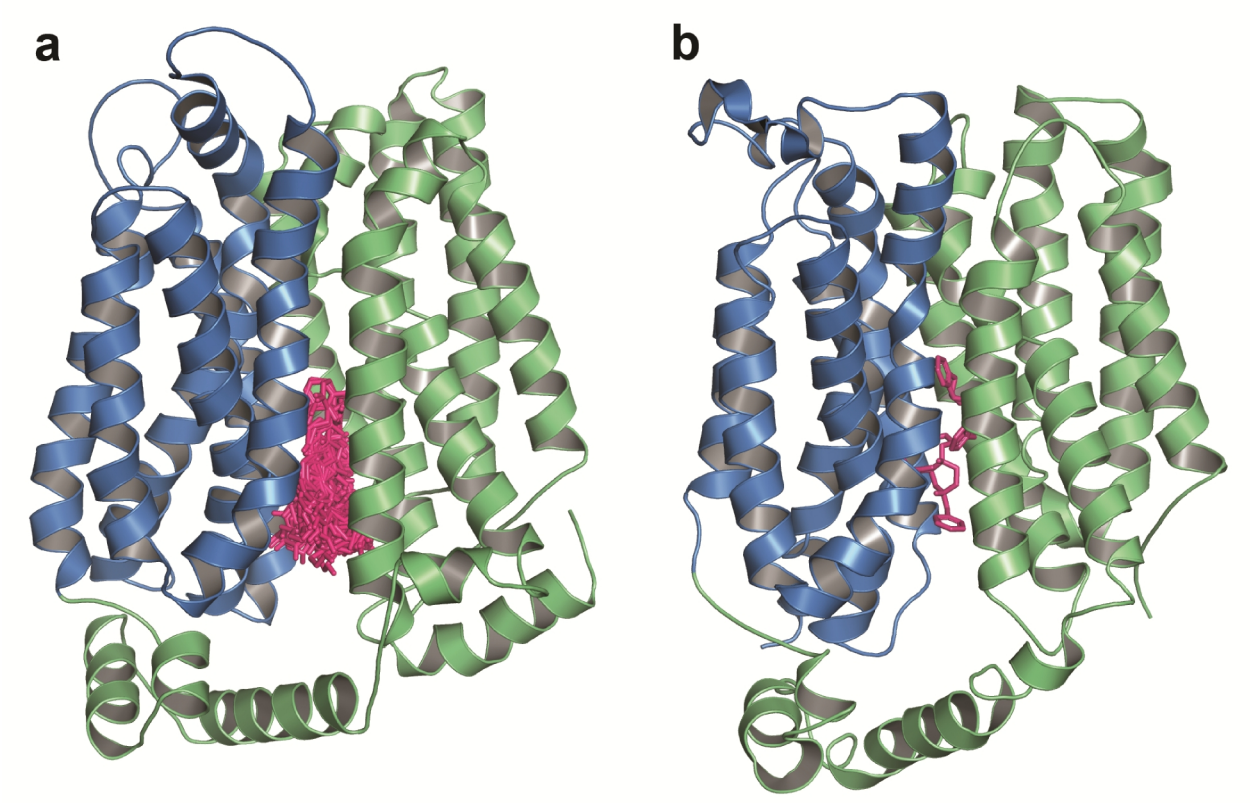

Figure 4.6. Docking analysis of HIV protease inhibitors with glucose transport proteins. (a) Lopinavir docked within the glucose permeation channel of PfHT. Lopinavir (pink) is docked in several poses to the inward open conformation of PfHT. The amino-terminal half of PfHT is colored blue and the carboxyl-terminal half is green. The depicted 40 poses occupy a single binding pocket and are representative of the results of several rounds of docking analysis. **(b)** Indinavir docked within the glucose permeation channel of GLUT4. Indinavir (pink) is docked to the inward open conformation of GLUT4 (published in [68]). The amino-terminal half of GLUT4 is colored blue and the carboxyl-terminal half is green.

Table 4.1. Top 10 templates used by I-TASSER. *Rank* of templates represents the top ten threading templates used by I-TASSER. *Ident1* is the percentage sequence identity of the templates in the threading aligned region with the query sequence. *Ident2* is the percentage sequence identity of the whole template chains with query sequence. *Cov*. represents the coverage of the threading alignment and is equal to the number of aligned residues divided by the length of query protein. *Norm. Z-score* is the normalized Z-score of the threading alignments. Alignment with a Normalized Z-score >1 mean a good alignment and vice versa.

Rank	PDB Hit	Iden1	Iden2	Cov.	Norm. Z-score
1	4pypA	0.28	0.26	0.87	3.85
2	4gbyA	0.26	0.26	0.88	5.79
3	4pypA	0.27	0.26	0.87	5.39
4	4gc0A	0.25	0.26	0.88	3.91
5	4gc0A	0.26	0.26	0.89	3.65
6	4pypA	0.28	0.26	0.87	5.35
7	4gc0A	0.26	0.26	0.89	4.83
8	4pypA	0.29	0.26	0.87	6.61
9	4pypA	0.28	0.26	0.87	4.68
10	4pypA	0.28	0.26	0.87	4.82

Chapter 5 – A novel, FRET-based high-throughput screen to identify inhibitors of malarial and human glucose transporters

Thomas E. Kraft[a,†], Monique R. Heitmeier[a], Marina Putanko[a], Rachel Edwards[a], Ma. Xenia G. Ilagan[b], Maria A. Payne[a], Audrey R. Odom[a,c] and Paul W. Hruz[a,d,†]

[a]Department of Pediatrics, [c]Department of Molecular Microbiology, and [d]Department of Cell Biology and Physiology, [b]High Throughput Screening Core, Washington University School of Medicine, St Louis MO 63110.

[†]corresponding author

5.1 Abstract

The glucose transporter PfHT is essential to the survival of the malaria parasite *Plasmodium falciparum* and has been shown to be a druggable target with high potential for pharmacological intervention. Identification of compounds against novel drug targets is crucial to combating resistance against current therapeutics. Here, we describe the development of a cell-based, high-throughput assay that directly measures the ability of a compound to inhibit glucose transport by PfHT. This assay determines the intracellular glucose concentration via an expressed glucose sensor protein that changes its fluorescence resonance energy transfer (FRET) intensity in a glucose-dependent manner. This allows for the direct assessment of the ability of a compound to inhibit glucose uptake with high accuracy (Z'-factor of >0.8), while eliminating the need for radiolabeled substrates. Furthermore, we have adapted this assay to counter screen PfHT hits against the human orthologues GLUT1, 2, 3 and 4. We report the identification of several hits after screening the Medicines for Malaria Venture (MMV) Malaria Box, a 400 compound library of known inhibitors of parasite blood stage growth. Hit compounds were verified and characterized by determining the IC_{50} for inhibition of radiolabeled glucose uptake into isolated *P. falciparum* parasites. One of our hits, compound MMV009085, shows high potency and ortholog selectivity, thereby successfully validating our assay for large-scale application.

5.2 Introduction

Malaria is estimated to have killed half of all the people who have ever lived and remains a major threat, affecting over 200 million people per year[139,166]. Beyond the staggering effect of

this disease on human life, malaria also cripples economic development and burdens the health care systems of malaria endemic countries[167]. The emergence of parasites with resistance to even the most potent existing anti-malarial drugs like artemisinins [168] has made paramount the development of novel drugs that target essential pathways for parasite survival. Glucose is the primary source of energy for blood-stage parasites as they almost exclusively rely on glycolysis for survival The malarial glucose transporter, *Plasmodium falciparum* hexose transporter (PfHT), first cloned by Woodrow *et al.* in 1999[147] and shown to be essential for parasite survival[155], is one highly promising molecular target. PfHT has been chemically validated as an antimalarial target, as a glucose analog (compound 3361) has been found to inhibit PfHT with high selectivity over the human orthologue GLUT1 and also inhibits asexual intraerythrocytic growth in culture [40]. Compound 3361 is also active against *P. berghei* liver and transmission stage parasites in infected mice[42]. However, while 3361 validates efforts to target PfHT, this compound is not itself considered drug-like and is therefore not a valid candidate for lead development [169]. We have recently extended these earlier findings by identifying PfHT as a direct molecular target of the HIV protease inhibitor lopinavir, thus providing a link between lopinavir use and decreased malarial transmission in areas where HIV and malaria are co-endemic [170]. However, lopinavir has a relatively high IC_{50} of 16 μM in parasites and shows higher selectivity for the human insulin responsive glucose transporter GLUT4 over PfHT [170]. Therefore, novel therapeutics targeting PfHT with improved potency and selectivity are required.

Results

Assay development

To develop a robust and efficient high-throughput assay to identify novel PfHT inhibitors, consideration was given to simplicity, sensitivity, scalability, cost, and reliability. Current assays for transporter inhibition in high-throughput format generally employ radiolabeled substrate or cell death of a transporter-overexpressing cell line as a readout[171,172]. Both formats have significant limitations. Although measuring the uptake of radiolabeled substrate generally yields quantitative, highly reproducible results and minimizes false positives (e.g. fluorescent compounds), the use and disposal of radiolabels are expensive and handling radioactive substances requires increased safety precautions. Alternatively, using cell death of an engineered cell line that requires transporter function for survival is an elegant way to simplify the readout. In both cases, these assays fail to discriminate between compounds that kill the cells through transporter inhibition and compounds that kill through other mechanisms, resulting in false positive results as high as 97.8% [160].

Our goal was to design an assay that would use transporter function as a direct, highly reproducible readout without the use of radiolabels. We therefore designed a cell line that transports glucose almost exclusively through PfHT and combined this with an intracellular glucose sensor protein that translates glucose concentration into a fluorescence signal as readout. We used the glucose sensor FLII[12]Pglu-700μδ6 (FLIP), initially developed and characterized in the laboratory of Wolf Frommer as readout for measuring cellular glucose influx[173]. This genetically encoded optical glucose sensor consists of three protein domains: A

central glucose-binding domain that is coupled terminally to a cyan fluorescent protein (CFP) and a yellow fluorescent protein (YFP). Upon excitation of CFP, energy is transferred to YFP through FRET. When glucose enters the cell, it binds to the glucose binding domain, leading to a conformational change that brings the two fluorescent proteins closer together and increases FRET (Fig. 5.1). Using the human embryonic kidney cell line HEK293, we created a reporter cell line, stably expressing PfHT in conjunction with FLIP (PfHT-FLIP cells). HEK293 cells are known to exhibit relatively low endogenous glucose uptake[173]. To further reduce background levels of glucose uptake, we knocked down the primary endogenous transporter isoform GLUT1 using siRNA, yielding a cell line that predominantly transports glucose through PfHT[170]. We tested the function of our engineered cell line by measuring the time course of glucose uptake via readout of the YFP/CFP ratio (FRET ratio) in the presence and absence of known PfHT inhibitors. Upon addition of the HIV protease inhibitor lopinavir (Fig. 5.2a), previously identified to block PfHT-mediated glucose uptake, the PfHT-FLIP cells showed decreased FRET ratio upon the addition of D-glucose, consistent with inhibition of radiolabeled D-glucose uptake in these cells[170]. Additionally, we confirmed concentration-dependent inhibition of glucose uptake in PfHT-FLIP cells by the glucose transport inhibitor cytochalasin B (CB) as previously shown in *Xenopus laevis* oocytes[147]. In PfHT-FLIP cells, CB causes a maximal decrease in FRET ratio of 75% at 50 µM consistent with radiolabeled uptake inhibition in oocytes[147] and complete inhibition of D-glucose uptake at 200 µM (Fig. 5.2b), making CB an ideally suited positive control for assay optimization and high-throughput screening.

Assay optimization

We optimized the assay for high-throughput application in a 96-well format using the Z'-factor and the coefficient of variation (CV) as measures of assay robustness [174]. For these measurements, half of the plate was treated with 200 µM CB as positive control and the other half with vehicle prior to the addition of D-glucose. Cells adhered tightly to the plate bottom after treatment of the plate with the highly branched polymer PEI that acted as adhesive, thereby preventing cells from dislodging during washing and buffer exchange steps. After optimization of assay temperature, fluorescence read mode, cell density and cell plating protocol we were able to routinely obtain a Z'-factor of >0.8 (a perfect assay would have a Z'-factor of 1.0) and CV of ~2% (Fig. 5.3).

Screening of the Malaria Box compound library

In order to test our assay system in an automated setting for high-throughput application, we selected the MMV Malaria Box, a small library of 400 compounds previously shown to have a cytotoxic effect on malaria parasites[175]. This library contains chemically diverse compounds with half of the compounds having drug-like properties and the other half having been selected as molecular probes. As this compound set was selected for their cytotoxic activity against blood-stage malaria parasites, the molecular drug targets remain to be determined. The rationale for choosing this library was to identify compounds that inhibit parasite growth mainly or partially through blockade of PfHT-mediated glucose uptake, since deorphanization of these compounds will aid in further PfHT-specific drug development.

We screened the Malaria Box at 10 µM drug concentrations in triplicate and selected hits that decrease the FRET ratio by more than 40% with vehicle-treated cells set to 100% and cells treated with 200 µM CB set to 0%. Since this assay is based upon changes in FRET, we reduced the number of fluorescent, false positive hits, by determining the FRET ratio of compounds without cells present. After false positive elimination, we identified 6 compounds as primary hits. Hit confirmation was ascertained by determining the IC_{50} for glucose uptake into isolated *P. falciparum* parasites from blood culture using radiolabeled D-glucose. Five of the six primary hits could be confirmed to inhibit glucose uptake into *P. falciparum* parasites in the low micromolar range (Table 1) with compound MMV665941 showing only partial maximal inhibition (Fig. 5.4). Comparison of the IC_{50} for glucose uptake inhibition with the IC_{50} for cytotoxicity in blood culture parasites indicates that only the most potent hit, MMV009085, inhibits parasite growth mainly through PfHT inhibition (Table 1). For the other confirmed hits, glucose uptake inhibition contributes to the cytotoxic effects of these compounds but is most likely not the main mechanism of action (Table 1).

To establish selectivity of these hits for PfHT over human orthologues, we cross-validated the inhibition of GLUTs 1, 2, 3 and 4 by the confirmed hits. Using the same HEK293-FLIP cell line, we overexpressed each of the individual class I transporters. With the exception of GLUT1-FLIP, the other GLUT cell lines were also treated with GLUT1 specific siRNA to reduce background glucose uptake. We confirmed that the overexpressed GLUT was the main glucose transporter expressed in each cell line by comparing the cDNA copy number of all human SLC2A genes via qPCR (Fig. 5.5). We determined the inhibitory effect of the five confirmed hits on all four human class I GLUTs at the IC_{50} concentration for PfHT-mediated glucose uptake inhibition. Only

compound MMV009085, the most potent hit with an IC_{50} of 1.8 µM for PfHT-mediated glucose uptake, showed significantly less inhibition of the human GLUTs compared to PfHT (Fig. 5.6a). Comparison of the IC_{50}s for glucose uptake inhibition, mediated by either the human GLUTs or PfHT, revealed a more than 10-fold higher selectivity of MMV009085 for PfHT over human orthologues (Fig. 5.6b). Although MMV009085 is considered a probe-like molecule, its high potency in inhibiting both glucose uptake and growth of the parasites as well as its high selectivity for PfHT over human orthologues makes this compound a potential candidate for lead optimization. Additionally, it demonstrates that our newly developed assay can identify glucose transporter-specific inhibitors and further distinguish compounds with high selectivity for their target over its orthologues or isoforms**.**

Discussion

We describe here the development of a new high-throughput screening assay that uses the ability of a compound to directly inhibit glucose uptake, mediated by either the malarial glucose transporter PfHT or a human GLUT transporter as readout to identify novel and selective anti-malarial agents. Our results show high reproducibility with a CV of ~2% and good separation of hits from background with a Z'-factor of >0.8, which is indicative of an excellent assay for high throughput screening[174]. Additionally, this assay does not require radioactive labels, thereby increasing throughput and ease-of-use while significantly decreasing cost. This is especially important in the field of infectious diseases affecting people in the developing world, where funding is generally provided by nonprofit organizations[176]. Our initial screen of a small, 400 compound library resulted in four verified hits. Although the rate of false positives (2) after the

initial round of screening is significantly lower than in similar assays[160] it can still be improved by selecting a higher threshold of FRET ratio reduction, especially when screening a larger library or using different detection methods like fluorescence lifetime[177,178]. The hits identified in this screen include three compounds (MMV009085, MMV020548, MMV665879) that were previously identified by Ortiz *et al.*[160] to selectively inhibit glucose uptake, but not proline transport, in PfHT-overexpressing *Leishmania mexicana*. Compound MMV009085 consistently exhibited the highest potency in inhibiting PfHT-mediated glucose uptake in both assays. In our screen, reduction in FRET ratio correlated well with inhibitory potency of the compound with the most potent inhibitor MMV009085 showing the strongest decrease in FRET ratio.

The quality of hits in drug discovery projects is crucial in improving the odds of developing a successful candidate for clinical application, especially as downstream investments into the hits that are selected for lead development are significant both in terms of funding and time[176]. Therefore, target-based screens are highly advantageous to phenotypic screens as they allow lead identification and optimization that are directed towards the malarial target protein versus human orthologues. We adapted our assay system to include cross-screening of PfHT-specific hits against human glucose transporters. The facilitative glucose transporters GLUT1-4 are fundamentally important for human glucose homeostasis as they are primary glucose transporters in most tissues[109]. PfHT and the human transporters share a common MFS fold and show a sequence similarity of close to 50%. The significance of the human GLUTs and their close homology to the malarial glucose transporter make it crucial, but potentially challenging to identify drugs with high orthologue selectivity. By replacing PfHT with human GLUTs, our HEK293 cell based assay system successfully distinguished PfHT specific from orthologue non-

specific inhibitors and identified a compound that showed a 19 to >250-fold high selectivity for PfHT over the human GLUTs.

An additional advantage of target-directed screening is the opportunity for structure-based rational drug design to aid in lead compound optimization. For the mammalian glucose transporters, recent progress has been made in solving the crystal structures of several isoforms in both inward and outward conformations[25–27]. Furthermore, our prior work has provided evidence for the binding pocket that mediates transporter inhibition by HIV protease inhibitors[81,170,179]. This has been used to model lopinavir binding to a model of PfHT[170]. Taken together, these data provide a framework for iterative structure activity analysis of compounds identified via our newly developed high-throughput screening assay.

In addition to using the GLUT-expressing FLIP cells lines for selecting orthologue-specific PfHT inhibitors, these cell lines can be used to identify GLUT-specific inhibitors with isoform selectivity with applications beyond anti-malarial therapy. Several types of tumors have been shown to overexpress specific GLUT isoforms that mediate the transport of high levels of glucose to malignant cells that have undergone metabolic rearrangement and primarily metabolize glucose through aerobic glycolysis (known as the Warburg effect)[29,31]. Many cancer cells express transporter isoforms that are not found in these tissues in non-malignant conditions. Among the class 1 facilitative glucose transporters, GLUT1 is most abundantly expressed in cancers from breast, brain, lung, colorectal, and bladder[30]. Inhibition of GLUT1 has already been shown to exert antineoplastic effects, both *in vitro* and *in vivo*[32,33] making it a promising target for cancer therapy. Expression of the glucose transporters GLUT2, GLUT3 and

GLUT4 is also upregulated in various tumors, among them several types that are difficult to treat and are associated with low survival rates like lung, pancreatic, and liver tumors[30,31,180]. Our cell-based, target-specific screen is designed to be easily adaptable to mediate glucose transport through selectively expressed transporter isoforms. This versatility combined with a robust, easily detectable readout significantly increases the feasibility of screening large compound libraries to identify isoform-specific GLUT inhibitors that can be further developed into drugs for either stand-alone or adjunct cancer therapy.

5.5 Material and Methods

Materials

[^{14}C]-2-deoxy- glucose (2-DOG) and [^{3}H]-2-DOG were purchased from American Radiolabels Inc. GLUT1 shRNA was obtained through the RNAi core at Washington University School of Medicine. HEK293 cells were acquired from the American Type Culture Collection (ATCC). Lopinavir was obtained through the NIH AIDS Reagent Program, Division of AIDS, NIAID, NIH.

HEK293 cell line generation

HEK293 cells were transfected with pcDNA3.1 FLII12Pglu-700uDelta6 (Addgene), containing the FRET glucose sensor (HEK293-FLIP) using Optifect Reagent (Life Technologies) according to manufacturer's specifications. Cells that stably integrated the gene were selected using G418 (Sigma Aldrich) and highest expressers were identified using Fluorescence Activated Cell Sorting (FACS). These cells were then stably transfected with PfHT, human GLUT1 (hGLUT1), human GLUT2 (hGLUT2), human GLUT3 (hGLUT3) or human GLUT4 (hGLUT4) DNA in the pcDNA 3.1(-)

hygro plasmid (Life Technologies) as described previously[170]. In all cell lines except for HEK293 overexpressing hGLUT1 cells, native hGLUT1 was knocked down using siRNA as described in[170]. mRNA transcript levels of all known human GLUTs were determined in the four GLUT overexpressing cell lines as described below using qPCR. PfHT expression levels in overexpressing cells were previously characterized[170].

RNA isolation and quantitative PCR

Total RNA was isolated using the TrizolW Plus RNA Purification System (Invitrogen), and one microgram of RNA was reverse transcribed using qScript cDNA Supermix (Quanta Biosciences). Quantitative RT-PCR was performed using Power SYBR Green PCR Master Mix (Applied Biosystems). Each reaction was run in triplicate using the primers listed in Table 2. Quantifications were performed with standard curves generated using plasmids containing each human GLUT (DNASU).

Assay optimization and high throughput screening

Several conditions were optimized to increase the sensitivity and reliability of the assay. PfHT-FLIP cells were plated 48 h prior to the assay in black opaque 96-well plates (Greiner Bio-One) at 30,000 cells/well. 96-well plates were pretreated with 25 µg/ml Polyethylenimine (PEI, 750 kDa, Sigma Aldrich) solution containing 150 mM NaCl to maintain cell adhesion during washing steps. After 20 min incubation at room temperature (RT), PEI was aspirated and wells were air dried for 5 min. After cell plating, plates were then left in the sterile hood at RT for 45 min before transfer to the incubator to reduce edge effects. Compound screening was performed using the integrated and automated screening system (Beckman Coulter) at the Washington

University High Throughput Screening Core. We used the SAMI EX software (Beckman Coulter) to design and execute the screening protocol. The Malaria Box (Medicines for Malaria Venture) compound library was prediluted in glucose-free HEPES buffered saline solution (HBSS) (146 mM NaCl, 4.7 mM KCl, 0.6 mM $MgSO_4$, 1.6 mM $NaHCO_3$, 0.13 mM NaH_2PO_4, 2.5 mM $CaCl_2$, 20 mM HEPES, pH 7.3) using the BiomekFX liquid handler (Beckman Coulter). We prepared a 1:100 dilution of 1 mM stock solution for 10 µM final concentration.

To start the high throughput assay, cells were washed twice with 150 µl HBSS per well using the ELx405 Plate Washer (Biotek). Cells were starved in HBSS for 30 min at RT followed by aspiration of the HBSS from cell plates using the ELx405 Plate Washer. Cells were treated with 45 µl of diluted compound using the BiomekFX (with 3 replicate cell plates for each library plate) and incubated for 6 min at RT. To start the uptake, 5 µl of 100 mM glucose was added to the wells (final concentration 10 mM) using a Multidrop384 dispenser (Thermo Fisher Scientific). After incubation at RT for 120 min, fluorescence was measured using the 2102 EnVision Multilabel Plate Reader (Perkin Elmer) at excitation 436 nm (CFP) and emissions 485 nm (CFP) and 535 nm (YFP).

***P. falciparum* culture**

P. falciparum strain 3D7 was obtained from the Malaria Research and Reference Reagent Resource Center (MR4). *P. falciparum* parasites were cultured in a 2% suspension of human erythrocytes and RPMI 1640 (Sigma Aldrich) medium supplemented with 27 mM sodium bicarbonate, 11 mM glucose, 5 mM HEPES, 1 mM sodium pyruvate, 0.37 mM hypoxanthine,

0.01 mM thymidine, 10 µg/ml gentamicin, and 0.5% albumax (Gibco) at 37°C, 5% O_2/ 5% CO_2 / 90% N_2 atmosphere as previously described [161,162].

P. falciparum growth inhibition assays

Asynchronous *P. falciparum* cultures were diluted to 1% parasitemia and were treated with compounds at concentrations ranging from 9.8 nM - 20 µM. Growth inhibition assays were performed in 100 µl cultures in opaque 96-well plates. Parasite growth was quantified after 3 days by measuring DNA content using PicoGreen (Life Technologies) [163]. Fluorescence was measured by a FLUOstar Omega microplate reader (BMG Labtech) at 485 nm excitation and 528 nm emission. IC_{50} values were calculated by nonlinear regression analysis using GraphPad Prism software.

Glucose uptake into *P. falciparum* parasites

P. falciparum strain 3D7 was cultured in 100 mm tissue culture dishes (Techno Plastic Products) in a 2% suspension of human erythrocytes and RPMI 1640 medium until reaching > 5% parasitemia. Cells were pelleted via centrifugation and resuspended in RPMI. Uptake of [^{14}C]-2-DOG into isolated parasites was determined at RT using the methods described previously[43]. Test compounds were added 5 min prior to the addition of [^{14}C]-2-DOG (0.2 µCi/ml final concentration). Uptake was quenched after 1 min. Data were fit by nonlinear regression analysis using GraphPad Prism software.

Glucose uptake into HEK293 cells

Uptake of [^{3}H]-2-DOG into HEK293-FLIP cell lines was measured in HEPES-buffered saline at RT for 4 min as described previously[81]. Data were fit by nonlinear regression analysis using GraphPad Prism software.

5.8 Figures

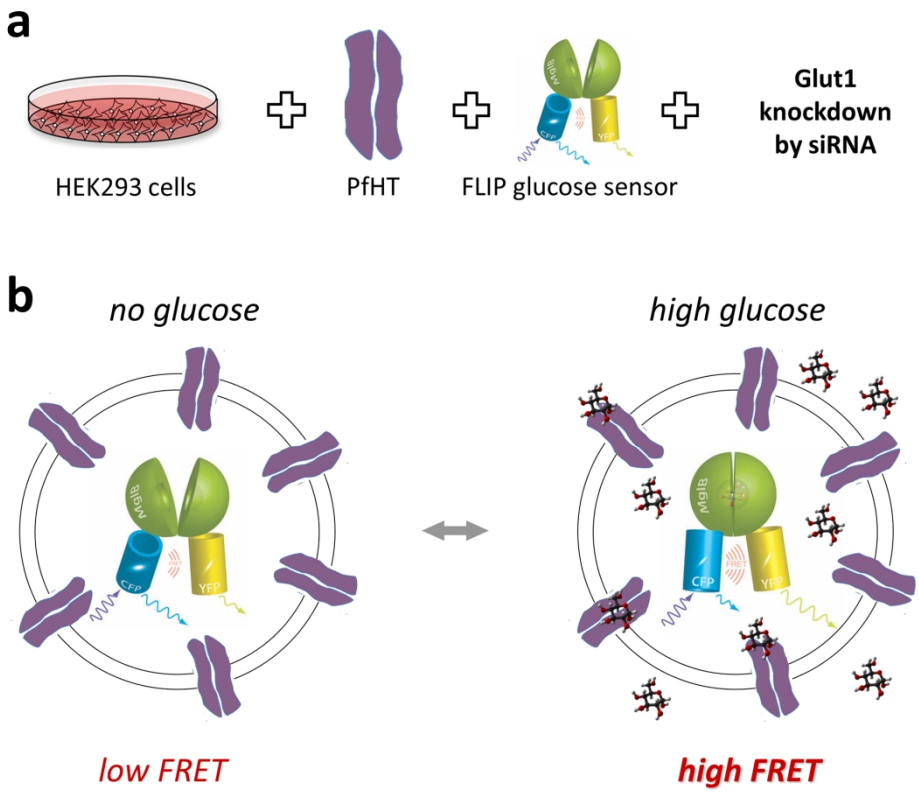

Figure 5.1. Generation of cell lines for high throughput screen. (**a**) HEK293 cells were stably transfected with the *P. falciparum* hexose transporter (PfHT), the glucose sensor FLII12Pglu-700uDelta6 and treated with siRNA directed at hGLUT1 to reduce background glucose uptake. (**b**) Glucose FRET sensor expressed in PfHT expressing cells. In the absence of glucose, CFP and YFP are further apart and the amount of energy transferred to from the donor CFP to the acceptor YFP that is emitted as light (FRET signal) is low. Glucose binding to the glucose/galactose binding domain (MglB) leads to a conformational change that brings CFP and YFP closer together, resulting in an increase FRET signal.

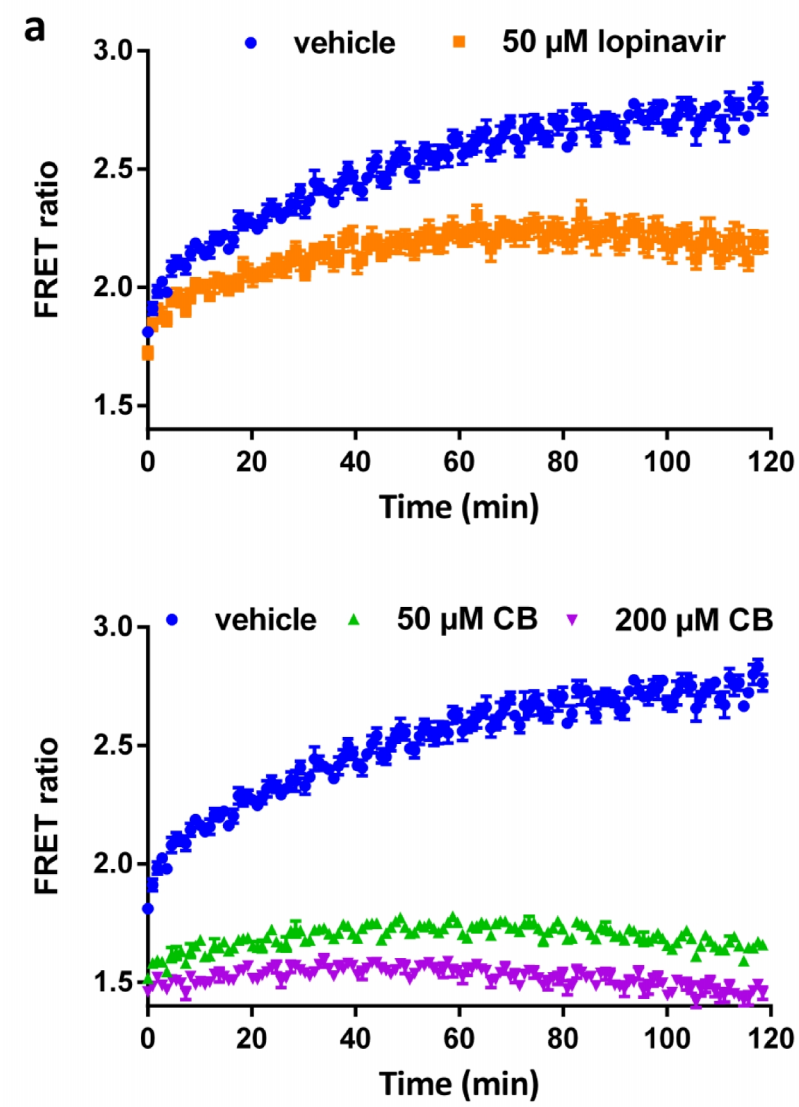

Figure 5.2. Time dependent change in FRET ratio (YFP emission/CFP emission) after addition of glucose to PfHT-FLIP cells (**a**) in the presence or absence of lopinavir or (**b**) in the presence or absence of cytochalasin B (CB).

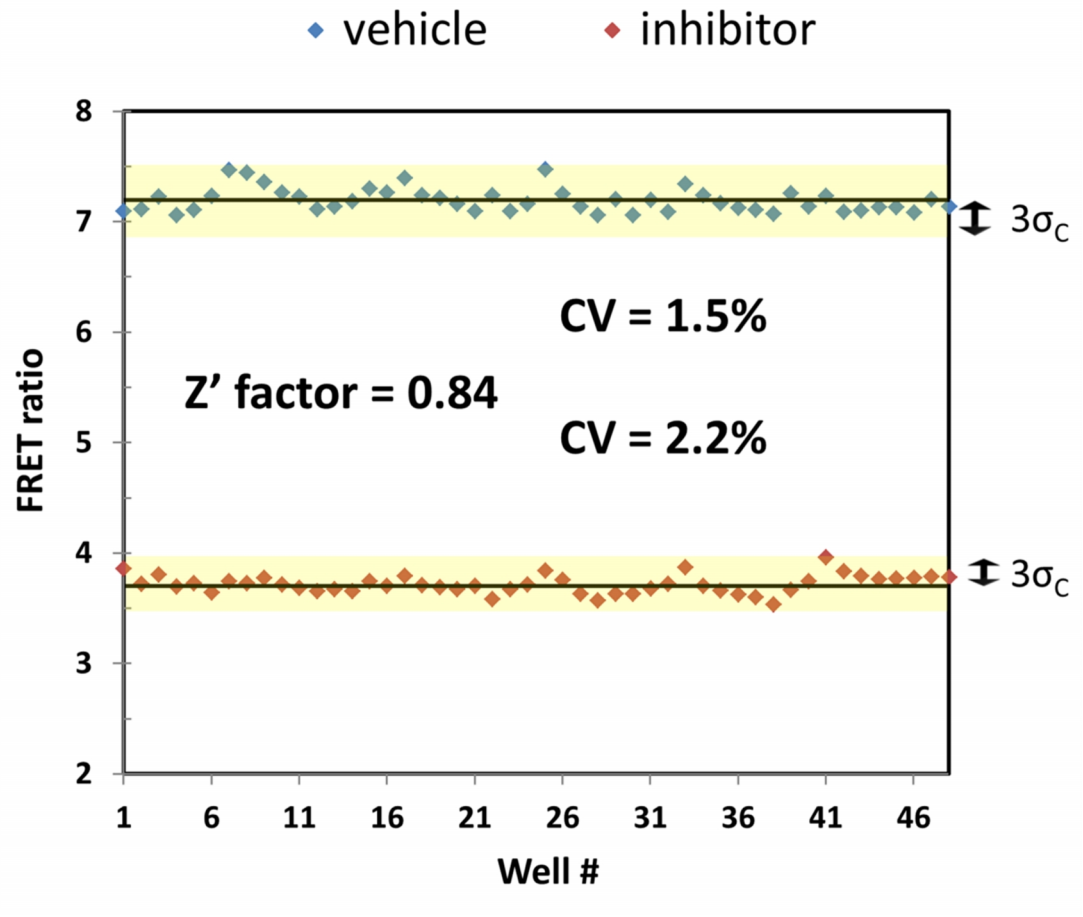

Figure 5.3. Z' factor determination. FRET ratio per well of 96-well plate, with 48 wells treated with 200μM CB (inhibitor) and 48 wells treated with vehicle. Z'-factor and the coefficient of variation (CV) as were determined from the average and standard deviation of each set of well according to[174].

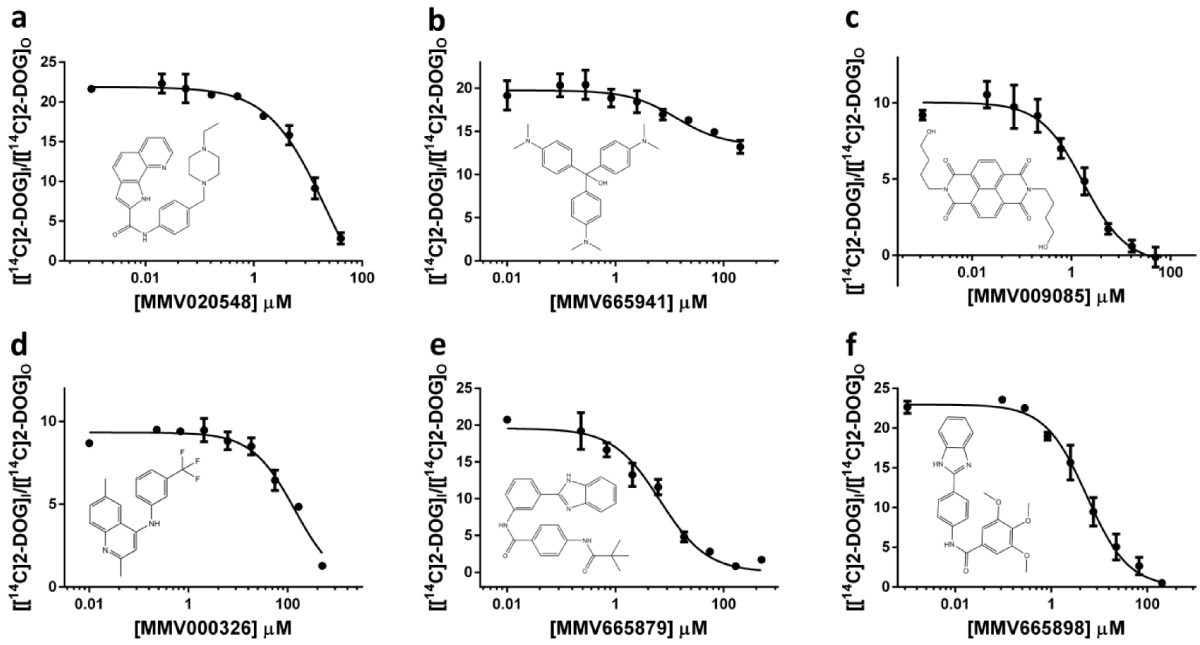

Figure 5.4. Uptake of [^{14}C]-2-DOG by isolated *P. falciparum* trophozoites at increasing concentrations of hit compounds. Distribution ratios (i.e., the ratio of intracellular concentration of radiolabel relative to the extracellular concentration) were calculated as described previously[43]. IC_{50} values were calculated using non-linear regression analysis and are tabulated in Table 1. Uptake data are expressed as means ±SEM. Chemical structures of the compounds tested are shown for comparison.

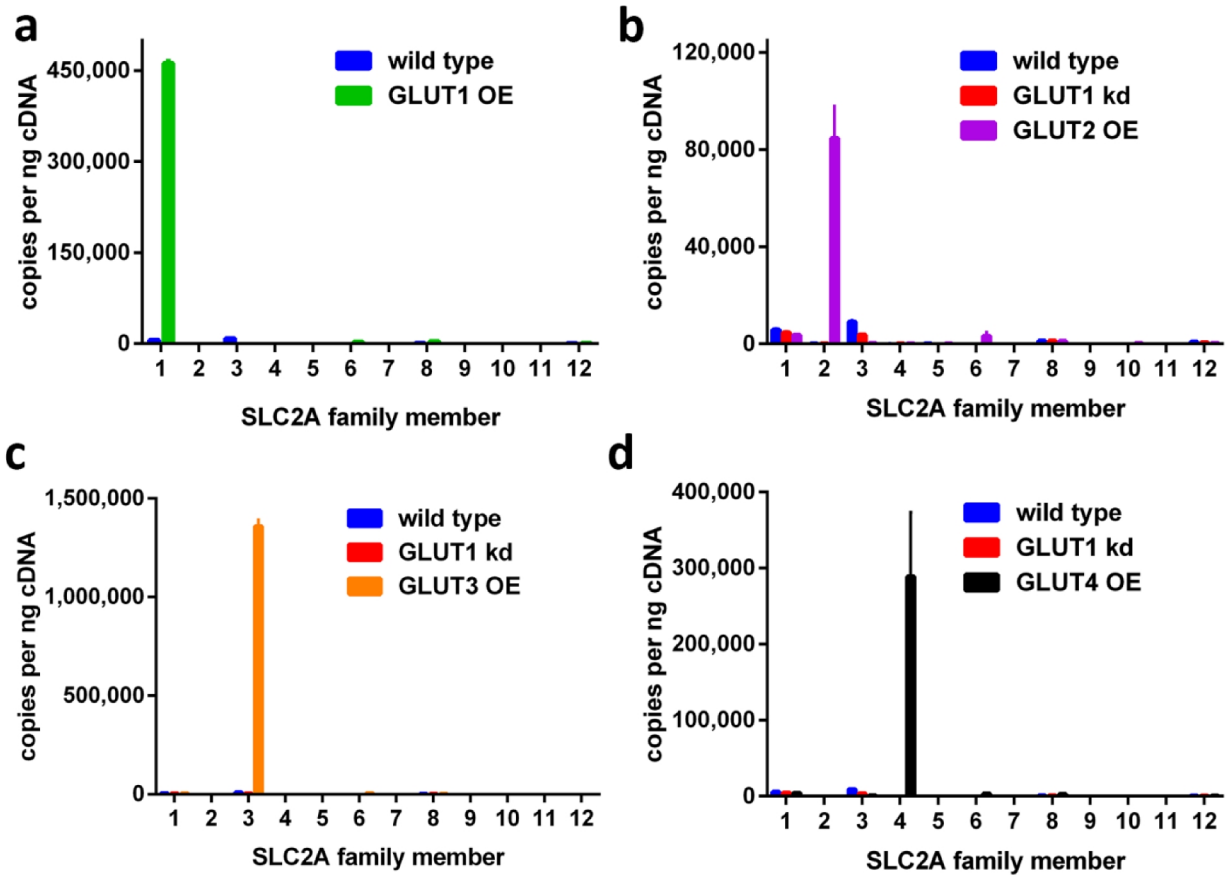

Figure 5.5. Copies of transcript per ng of cDNA for each glucose transporter SLC2A family member in HEK293-FLIP cells overexpressing (**a**) hGLUT1, (**b**) hGLUT2, (**c**) hGLUT3 and (**d**) hGLUT4 in comparison to HEK293 wild-type and/or HEK293 wild type cells treated with siRNA targeting hSLC2A1 (hGLUT1 kd).

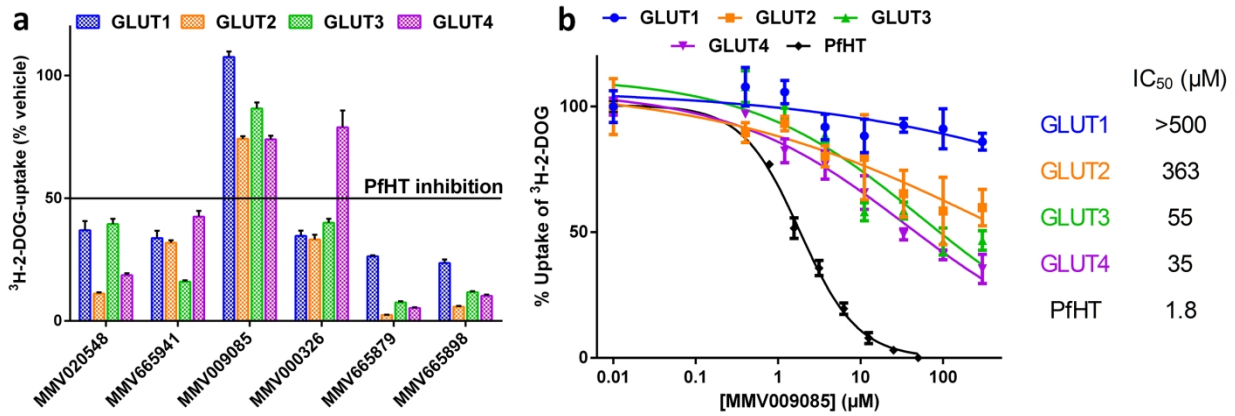

Figure 5.6. Specificity of hit compounds for PfHT over human orthologues. (**a**) Uptake of ^{3}H-2-DOG by HEK293 cells overexpressing hGLUTs 1-4 in the presence of hit compounds at their IC_{50} for PfHT (Table 1). (**b**) Uptake of [^{3}H]-2-DOG by HEK293 cells overexpressing PfHT or hGLUTs 1-4 at increasing concentrations of compound MMV009085. Uptake data are expressed as means ±SEM. IC_{50} values were calculated using non-linear regression analysis.

5.9 Tables

Table 5.1. Comparison of hit IC_{50} values for different assays. IC_{50} for PfHT in parasites were determined from dose-response curves shown in Fig. 5.4. IC_{50} values for inhibition of growth of *P. falciparum* strain 3D7 intraerythrocytic forms by each compound are also tabulated.

Compound ID #	IC_{50} 3D7 *in vitro* (µM)	IC_{50} PfHT in parasites (µM)
MMV020548	0.114	21.3
MMV665941	0.026	13.3
MMV009085	0.987	1.8
MMV000326	0.344	139
MMV665879	0.390	6.6
MMV665898	0.487	6.2

Table 5.2. Human glucose transporter primers for qPCR.

	Forward primer :	Reverse primer :	Amplicon size (bp)
GLUT1	AACTCTTCAGCCAGGGTCCAC	CACAGTGAAGATGATGAAGAC	140
GLUT2	TTTCAGGCCTGGTTCCTATG	GATGGCCAGCTGATGAAAAG	86
GLUT3	ACTTTGACGGACAAGGGAAATG	ACCAGTGACAGCCAACAGG	180
GLUT4	CATGCTGGTCAACAATGTCC	CCAATGAGGAATCGTCCAAG	105
GLUT5	GTCGGCCCCTTGGTGAATAA	AATGATGTGGCGACTCTGCT	110
GLUT6	GGCTGCTCATGTCTGAGGTC	GATGGCCGCGAAGAAGAAGAA	161
GLUT7	TGCAGGCATCTCCTACAGC	ACGAAAACCTCGGTCATTGTTC	96
GLUT8	CCATCTTTGAAGAGGCCAAG	ATGACCACACCTGACAAGACC	145
GLUT9	TGGCAAAGATCCCATACGTC	AGGTGCTCAATGACCAAACC	85
GLUT10	GCTGTCCTGCAATCCCTCAG	GTCCGGCCTCGCATGTTATC	173
GLUT11	GGAGTCAATGCAGGTGTGAG	CCAGAGCCGTAAAGATGGCTG	112
GLUT12	TGCTGGATTAAGCCACACTG	TGGCTAAGGACAGCCATTTC	83

Chapter 6 - Conclusions

With recognition of the fundamental importance of facilitative glucose transport in both health and disease together with major remaining gaps in understanding the molecular mechanisms responsible for mediating and regulating this process, initial effort was directed toward overcoming the most significant barrier to the study of integral membrane proteins. The first priority addressed was the development of a robust system for overexpression, purification and functional reconstitution of GLUT4 in artificial membranes. This work, described in detail in chapter 2 of this dissertation, has been successful in generating a reliable means to obtain milligram quantities of nearly homogeneous protein. It is notable that the newly developed inducible mammalian cell lines in suspension culture produced are capable of producing over 1.5 mg of GLUT4 protein per liter of culture media. In the process of developing these novel methods, several important insights regarding transporter stability and influences on maximal glucose transport rates were discovered. The application of FSEC to GLUT4 allowed the creation of a multi-step process to identify cell lines with high expression, to identify detergents that are harsh enough to solubilize the transporter from its membrane environment but still mild enough to keep its tertiary structure intact and to purify solubilized proteins. Of note, our two-step purification protocol is capable of yielding protein with >95% purity, allowing study of GLUT4 with a variety of established and newly emerging biophysical techniques such as smFRET and EPR DEER spectroscopy.

With this established purification framework in hand, tremendous opportunity remains for the extension of this approach to the investigation of other SLC2A family members. Ongoing modification and optimization of the procedures outlined in Chapter 2 are being used for the

expression and purification of several additional GLUT isoforms and other difficult-to-purify mammalian membrane proteins. This stream-lined approach is significantly reducing the time from DNA sequence to purified protein from greater than 2 years to less than 4 months.

The development of protocols for the reconstitution of GLUT4 in different membrane mimetics that significantly stabilize the protein compared to detergent micelles is also contributing to ongoing efforts to investigate structure and molecular dynamics. Building on our previous results, reconstituted GLUT4 and GLUT3 protein in liposomes were used to determine the influence of various phospholipids, found in mammalian PMs, on the activity of these transporters. We determined that anionic phospholipids are required for GLUT3 and GLUT4 activity while conical lipids increase transporter activity several fold in the presence of anionic lipids. We further investigated these effects to decipher the mechanism by which these lipids influence transporter function. Both types of lipids manipulate transporter interconversion between inward and outward facing conformations in different ways. According to our proposed model, anionic phospholipids bind to a specific anionic phospholipid binding site on the transporters, forming a salt bridge between the negative charge on the phosphate headgroup and a cationic amino acid on the transporter, thereby allowing the transporter to interconvert between conformations. Increasing concentrations of anionic lipids lead to an increase in the fraction of active transporters. Conical lipids, on the other hand, change the biophysical properties of the lipid membrane by introducing lipid packing defects, decreasing lateral pressure at the lipid-water interface and increasing curvature frustration. These changes lead to a dose-dependent increase in the interconversion rate of the transporters, caused by a destabilization of the inward and outward open states. These groundbreaking discoveries

prompted the question as to whether our model of transporter activation is applicable to other members of the GLUT family or even the entire superfamily of SLCs. Studies are currently ongoing to test the lipid dependence of several members of the class 1 and class 2 GLUTs. The differences and similarities of lipid effects on activity between different transporters will have a significant impact in understanding their role on health and disease.

Based on these successes, I expanded the focus of glucose transport as a drug target for several diseases. The malarial glucose transporter PfHT was chosen for its significance in malarial metabolism. We identified PfHT as a target for the clinically used HIV protease inhibitor lopinavir. This drug was reported to cause a reduction of malaria infection in children by over 40%[45] and was known to decrease viability of malarial parasites in different life stages but its mechanism of action was unknown[46–50]. Identification of PfHT as a target of lopinavir with potent effects *in vitro*, *in vivo*, and in patients stresses the importance of the malarial glucose transporter as an attractive drug target. Although, lopinavir is already approved for clinical use, due to its relative high IC_{50} for PfHT and higher selectivity for other human glucose transporters[170], further work is required to identify inhibitors with improved potency and selectivity. High throughput screens of large, chemically diverse compound libraries against molecular targets are commonly used for inhibitor identification. We developed an assay with high throughput capability that can identify PfHT inhibitors with high accuracy (Z' factor > 0.8) and high selectivity over human orthologues. Additionally, this assay can be used to identify isoform selective inhibitors of human GLUTs as potential therapeutics in cancer therapy. It uses a genetically encoded glucose sensor that changes its fluorescence signal with intracellular glucose concentration. Proof of concept screening of a small, targeted library revealed several

verified hits and signified several advantages of this assay compared to traditional radiolabeled uptake assays or cell-death based assays: As the screening assay doesn't involve radiolabeled chemicals while still directly measuring transporter function in comparison to cell death, it doesn't require expensive radiochemicals, avoids safety precautions and special waste removal while providing high accuracy and low false positive rates.

Chapter 7 - Future directions

7.1 Deciphering the effect of lipids and cholesterol on glucose transporter function

I believe that we only discovered the tip of the iceberg in our understanding of the impact of the PM composition on the activity of mammalian solute carriers. Open questions revolve around the effect of other molecules within the mammalian PM on transporter activity, especially signaling lipids and cholesterol. Although, signaling lipids like phosphorylated forms of PI (PIPs) or sphingosines are present at very low concentrations in the PM, they have a substantial effect on the activity and regulation of ion channels[181,182] but their effect on transporter proteins remains elusive. The sterol cholesterol is a major component of mammalian PMs, constituting about 20-50% of eukaryotic membranes while being universally absent in membranes of prokaryotes[20,183]. It has been shown to affect the structure, activity and regulation of several classes of integral membrane proteins like ion channels[184,185] or G-protein coupled receptors[186–188], either through direct interaction with the protein[187,189] or through changes of the membrane biophysical properties[186]. The effect of cholesterol is controversially discussed in the context of GLUT function in humans. Studies, highlighting the

increased activity of glucose transporters in cells after cholesterol removal using methyl-beta-cyclodextrin (MBCD)[190,191], are contradicted by data supporting decreased glucose transporter activity in multiple cell lines as a result of MBCD treatment or by the cholesterol lowering effects of statins[192]. Moreover, it remains unclear if the effect of cholesterol on the transporter is caused through a change in translocation or affecting transporter turnover, either through direct interaction with the protein or by affecting lipid bilayer properties. The purification and functional reconstitution system we established (described in Chapters 2 and 3) allows us to investigate the effect of each membrane component on the activity of individual GLUT isoforms. It uniquely positions us to systematically answer these and other questions which was not previously possible in a cellular system. We are able to measure kinetic parameters and thereby determine cholesterol's effect on the turnover number of different GLUT isoforms. Furthermore, a clear distinction can be made between a direct binding effect and an effect on the biophysical properties of the membrane by using the complete enantiomer of naturally occurring cholesterol which retains its effect on the lipid bilayer but cannot occupy a protein binding site of the natural enantiomer.

In our previous studies, the main focus was on the effect of the phospholipid headgroups on glucose transporter function. Interestingly, not only the headgroup but also differences in lipid acyl chain length and saturation have been linked to changes in glucose transport in patients with diabetes[115]. Deciphering their direct contributions and mechanism of action on glucose transporter activity will provide key indications for novel ways of improving the treatment of diabetes patients through dietary or pharmacological intervention.

7.2 Refining the mechanism of lipid effects on GLUT activity

In Chapter 3, we proposed a model for GLUT activation through anionic and conical lipids. Having already obtained a significant amount of data that supports this hypothesis, further investigation of specifically the anionic phospholipid binding site and the differential effect of anionic and conical lipids on transport rates and occupation of protein conformations will yield valuable information to refine our model. I propose several complimentary techniques to determine the location and the number of anionic phospholipid binding sites as well as the amino acids involved. Although, membrane protein crystallography is still challenging and success is not guaranteed, co-crystallization of GLUT3 with anionic lipids presents a worthwhile approach that could a yield high-resolution structure of the protein-lipid complex. This is especially true as the crystallization conditions for GLUT3 are already known (PDB accession number 56C5) and the protein which was used for structure determination showed headgroup dependent activation through anionic phospholipids (Chapter 3, Fig. 3.2d). Alternatively, MD simulations have previously been used to determine lipid binding sites and also the effect of lipid binding on transporter dynamics[133]. In order to fully understand the differences between anionic and conical lipids on the mechanism of transporter activation, it is necessary to depart from ensemble methods and employ single molecule techniques. We proposed that anionic lipids alter the fraction of active transporters in a dose-dependent manner while conical lipids increase the transport rate of every transporter molecule. When the turnover number k_{cat} is determined as readout for interconversion rate for both lipid classes using ensemble methods, both mechanisms yield the same phenotype and are indistinguishable (Chapter 3, Fig. 3.5). However, by determining the interconversion rate of individual transporters via single molecule

techniques, I expect to observe a change in the fraction of active transporters, interconverting at a similar rate with increasing concentration of anionic phospholipids (Fig. 7.1a). Conical lipids, on the other hand, would increase the interconversion rate for the entire transporter population in a dose-dependent manner (Fig. 7.1b). An ideally suited technique to test this hypothesis is smFRET. Here, two artificially introduced cysteine residues on the protein are labeled with fluorophores that transfer energy from the donor to the acceptor molecule through nonradiative dipole-dipole coupling upon excitation of the donor. The efficiency of this transfer is inversely proportional to the sixth power of the distance between donor and acceptor, making smFRET extremely sensitive to small changes in distance[193]. Labeled proteins are immobilized on a glass slide and changes in fluorescence intensity are recorded using ultrasensitive CCD or CMOS cameras via TIRF microscopy. Positions for fluorophore labeling on the GLUT transporter need to be carefully chosen to maximize the distance change between fluorophores in different conformations and to ensure high exposure of cysteine residues for covalent labeling with water soluble fluorophores to maximize labeling efficiency. We have already generated a cysteine free mutant of GLUT4 where all native cysteines were replace with serine residues. The cysteine free mutant showed similar activity when expressed in HEK293 cells compared to the native transporter. Using a protocol, developed previously (Chapter 2), we successfully reconstituted several versions of double-labeled GLUT4 protein into lipid nanodiscs and adhered them to a streptavidin coated glass slide via biotinylated lipids headgroups in lipid nanodiscs. Currently, efforts are ongoing to identify cysteine pairs whose distances, measured by smFRET, correspond to inward and outward facing conformations of GLUT4. FRET intensities will be correlated with conformational states using transporters locked

into single conformations via point mutations or small molecule inhibitors. The system described here offers several advantages including stabilization of a soluble, highly homogenous membrane protein population while embedding the protein in a near native lipid environment which can be precisely manipulated to determine the effect of various lipids on transporter dynamics and distribution of states.

7.3 Identification and development of potent and selective inhibitors of PfHT

The herein described high throughput assay was successfully tested on a small, directed compound library. The next steps involve screening large, chemically diverse library and further assay optimization. Increasing the throughput and sensitivity will make large screens more cost effective. Currently, the assay is optimized for a 96-well format. Increasing the number of wells per plate decreases the required amount of test compounds, cells and ultimately cost, while increasing throughput. Additionally, alternative detection methods like fluorescence lifetime can be explored to increase the sensitivity[177,178] and thereby the Z' factor.

Based on our previous results, I expect that a large, chemically unbiased screen will yield several diverse molecules with high potency against PfHT. These primary hits will be verified through uptake assays of radiolabeled substrate and structurally similar compounds of verified hits will be evaluated to identify a common backbone. Structure activity relationship (SAR) studies will use this information to modify the structure of verified hits by inserting new chemical groups into the biomedical compound and test the modifications for their biological effects. The resulting lead compounds should have high potency *in vitro* and in animal models (IC_{50} in the nanomolar range), good drug metabolism and pharmacokinetic (DMPK)

characteristics, show more than 10-fold higher selectivity for PfHT over its human orthologues, demonstrate good oral bioavailability in rodents and display no acute toxicity in in vivo efficacy studies[176].

The ultimate outcome of this screen, inhibitors with high selectivity for specific glucose transporters, together with currently emerging crystal structures of these transporters will help determine the structural requirements for designing highly selective, isoform or orthologue specific inhibitors, thereby minimizing off-target effects.

7.4 Figures

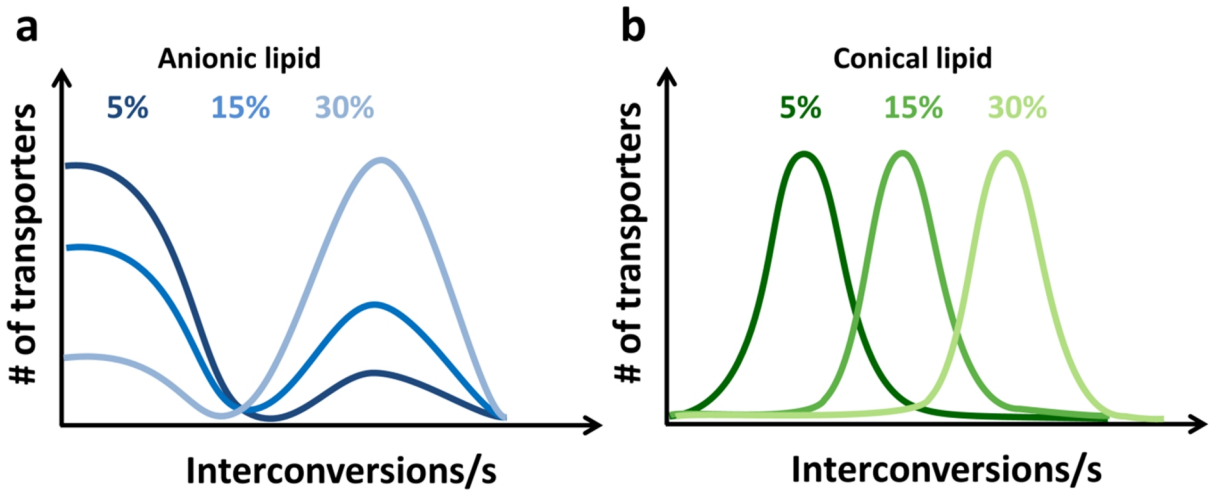

Figure 7.1. Prediction of the interconversion rate of glucose transporters measured via smFRET. (**a**) Anionic phospholipid dependent change in the interconversion rate of GLUT4 protein in nanodiscs. (**b**) Conical lipid dependent change in the interconversion rate of GLUT4 protein in nanodiscs.

References

1. Saier, M. H. Families of transmembrane sugar transport proteins. *Mol. Microbiol.* **35,** 699–710 (2000).

2. Valentine, V. The Role of the Kidney and Sodium-Glucose Cotransporter-2 Inhibition in Diabetes Management. *Clin. Diabetes* **30,** 151–155 (2012).

3. Jahreis, K., Pimentel-Schmitt, E. F., Brückner, R. & Titgemeyer, F. Ins and outs of glucose transport systems in eubacteria. *FEMS Microbiol. Rev.* **32,** 891–907 (2008).

4. Lalonde, S. *et al.* The dual function of sugar carriers. Transport and sugar sensing. *Plant Cell* **11,** 707–726 (1999).

5. Büttner, M. The monosaccharide transporter(-like) gene family in Arabidopsis. *FEBS Lett.* **581,** 2318–2324 (2007).

6. Sun, L. *et al.* Crystal structure of a bacterial homologue of glucose transporters GLUT1–4. *Nature* **490,** 361–366 (2012).

7. Iancu, C. V, Zamoon, J., Bum, S., Aleshin, A. & Choe, J. Crystal structure of a glucose / H + symporter and its mechanism of action. (2013). doi:10.1073/pnas.1311485110/-/DCSupplemental.www.pnas.org/cgi/doi/10.1073/pnas.1311485110

8. Ozcan, S. & Johnston, M. Function and regulation of yeast hexose transporters. *Microbiol. Mol. Biol. Rev.* **63,** 554–569 (1999).

9. Landfear, S. M. & Yan (ed.), Q. in *Membrane Transporters in Drug Discovery and Development* (ed. Yan, Q.) **637,** 245–262 (Humana Press, 2010).

10. Mueckler, M. & Thorens, B. The SLC2 (GLUT) family of membrane transporters. *Mol. Aspects Med.* **34,** 121–38

11. Abramson, J., Iwata, S. & Kaback, H. R. Lactose permease as a paradigm for membrane transport proteins (Review). *Mol. Membr. Biol.* **21,** 227–236 (2004).

12. Abramson, J. *et al.* Structure and mechanism of the lactose permease of Escherichia coli. *Science* **301,** 610–5 (2003).

13. Deng, D. *et al.* Crystal structure of the human glucose transporter GLUT1. *Nature* **510,**

121–5 (2014).

14. Guan, L. & Kaback, H. R. Lessons From Lactose Permease. *Annu. Rev. Biophys. Biomol. Struct.* **35,** 67–91 (2006).

15. Serebryany, E., Zhu, G. A. & Yan, E. C. Y. Artificial membrane-like environments for in vitro studies of purified G-protein coupled receptors. *Biochim. Biophys. Acta* **1818,** 225–233 (2011).

16. Cramer, W. a *et al.* Membrane proteins in four acts: function precedes structure determination. *Methods* **55,** 415–20 (2011).

17. Madej, M. G. Function, Structure, and Evolution of the Major Facilitator Superfamily: The LacY Manifesto. *Adv. Biol.* **2014,** e523591 (2014).

18. Cronan, J. E. Bacterial Membrane Lipids: Where Do We Stand? *Annu. Rev. Microbiol.* **57,** 203–224 (2003).

19. Glukhov, E., Stark, M., Burrows, L. L. & Deber, C. M. Basis for selectivity of cationic antimicrobial peptides for bacterial versus mammalian membranes. *J. Biol. Chem.* **280,** 33960–33967 (2005).

20. van Meer, G., Voelker, D. R. & Feigenson, G. W. Membrane lipids: where they are and how they behave. *Nat. Rev. Mol. Cell Biol.* **9,** 112–124 (2008).

21. Cura, A. J. & Carruthers, A. The role of Monosaccharide Transport Proteins in carbohydrate assimilation, distribution, metabolism and homeostasis. **2,** 863–914 (2013).

22. Wilson-O'Brien, A. L., Patron, N. & Rogers, S. Evolutionary ancestry and novel functions of the mammalian glucose transporter (GLUT) family. *BMC Evol. Biol.* **10,** 152 (2010).

23. De Vivo, D. C., Wang, D., Pascual, J. M. & Ho, Y. Y. Glucose transporter protein syndromes. *Int. Rev. Neurobiol.* **51,** 259–88 (2002).

24. César-Razquin, A. *et al.* A Call for Systematic Research on Solute Carriers. *Cell* **162,** 478–487 (2015).

25. Nomura, N. *et al.* Structure and mechanism of the mammalian fructose transporter GLUT5. *Nature* 1–7 (2015). doi:10.1038/nature14909

26. Deng, D. *et al.* Molecular basis of ligand recognition and transport by glucose transporters. *Nature* (2015). doi:10.1038/nature14655

27. Deng, D. *et al.* Crystal structure of the human glucose transporter GLUT1. *Nature* **510,** 121–125 (2014).

28. Huang, S. & Czech, M. P. The GLUT4 glucose transporter. *Cell Metab.* **5,** 237–52 (2007).

29. Galluzzi, L., Kepp, O., Heiden, M. G. Vander & Kroemer, G. Metabolic targets for cancer therapy. *Nat. Rev. Drug Discov.* **12,** 829–846 (2013).

30. Medina, R. A. & Owen, G. I. Glucose transporters: expression, regulation and cancer. *Biol. Res.* **35,** 9–26 (2002).

31. Szablewski, L. Expression of glucose transporters in cancers. *Biochim. Biophys. Acta* **1835,** 164–9 (2013).

32. Gautier, E. L. *et al.* HDL and Glut1 inhibition reverse a hypermetabolic state in mouse models of myeloproliferative disorders. *J. Exp. Med.* **210,** 339–53 (2013).

33. Liu, Y. *et al.* A Small-Molecule Inhibitor of Glucose Transporter 1 Downregulates Glycolysis, Induces Cell-Cycle Arrest, and Inhibits Cancer Cell Growth In Vitro and In Vivo. *Mol. Cancer Ther.* **11,** 1672–1682 (2012).

34. Barrett, M. P., Tetaud, E., Seyfang, A., Bringaud, F. & Baltz, T. Functional expression and characterization of the Trypanosoma brucei procyclic glucose transporter, THT2. *Biochem. J.* **312 (Pt 3,** 687–91 (1995).

35. Cazzulo, J. J. Aerobic fermentation of glucose by trypanosomatids. *FASEB J.* **6,** 3153–61 (1992).

36. Verlinde, C. L. *et al.* Glycolysis as a target for the design of new anti-trypanosome drugs. *Drug Resist. Updat.* **4,** 50–65 (2001).

37. Bringaud, F. & Baltz, T. Differential regulation of two distinct families of glucose transporter genes in Trypanosoma brucei. *Mol. Cell. Biol.* **13,** 1146–54 (1993).

38. Rodriguez-Contreras, D., Feng, X., Keeney, K. M., Bouwer, H. G. A. & Landfear, S. M. Phenotypic characterization of a glucose transporter null mutant in Leishmania

mexicana. *Mol. Biochem. Parasitol.* **153,** 9–18 (2007).

39. Burchmore, R. J. S. *et al.* Genetic characterization of glucose transporter function in Leishmania mexicana. *Proc. Natl. Acad. Sci. U. S. A.* **100,** 3901–6 (2003).

40. Joet, T., Eckstein-Ludwig, U., Morin, C. & Krishna, S. Validation of the hexose transporter of Plasmodium falciparum as a novel drug target. *Proc. Natl. Acad. Sci. U. S. A.* **100,** 7476–9 (2003).

41. Azema, L. *et al.* Interaction of substituted hexose analogues with the Trypanosoma brucei hexose transporter. *Biochem. Pharmacol.* **67,** 459–67 (2004).

42. Slavic, K. *et al.* Use of a selective inhibitor to define the chemotherapeutic potential of the plasmodial hexose transporter in different stages of the parasite's life cycle. *Antimicrob. Agents Chemother.* **55,** 2824–30 (2011).

43. Saliba, K. J., Krishna, S. & Kirk, K. Inhibition of hexose transport and abrogation of pH homeostasis in the intraerythrocytic malaria parasite by an O-3-hexose derivative. *FEBS Lett.* **570,** 93–96 (2004).

44. Slavic, K., Krishna, S., Derbyshire, E. T. & Staines, H. M. Plasmodial sugar transporters as anti-malarial drug targets and comparisons with other protozoa. *Malar. J.* **10,** 165 (2011).

45. Achan, J. *et al.* Antiretroviral agents and prevention of malaria in HIV-infected Ugandan children. *N Engl J Med* **367,** 2110–2118 (2012).

46. Chandwani, A. & Shuter, J. Lopinavir / ritonavir in the treatment of HIV-1 infection : a review. **4,** 1023–1033 (2008).

47. Hobbs, C. V *et al.* HIV treatments have malaria gametocyte killing and transmission blocking activity. *J. Infect. Dis.* **208,** 139–48 (2013).

48. Hobbs, C. V *et al.* HIV protease inhibitors inhibit the development of preerythrocytic-stage plasmodium parasites. *J. Infect. Dis.* **199,** 134–41 (2009).

49. Nsanzabana, C. & Rosenthal, P. J. In vitro activity of antiretroviral drugs against Plasmodium falciparum. *Antimicrob. Agents Chemother.* **55,** 5073–5077 (2011).

50. Parikh, S. *et al.* Antimalarial effects of human immunodeficiency virus type 1 protease

inhibitors differ from those of the aspartic protease inhibitor pepstatin. *Antimicrob. Agents Chemother.* **50,** 2207–2209 (2006).

51. Jiang, D. *et al.* Structure of the YajR transporter suggests a transport mechanism based on the conserved motif A. *Proc. Natl. Acad. Sci. U. S. A.* **110,** 14664–9 (2013).

52. Pao, S. S., Paulsen, I. T. & Saier, M. H. Major facilitator superfamily. *Microbiol. Mol. Biol. Rev.* **62,** 1–34 (1998).

53. Carruthers, A., DeZutter, J., Ganguly, A. & Devaskar, S. U. Will the original glucose transporter isoform please stand up! *Am. J. Physiol. Endocrinol. Metab.* **297,** E836–48 (2009).

54. Mueckler, M. *et al.* Sequence and structure of a human glucose transporter. *Science* **229,** 941–5 (1985).

55. Hruz, P. W. & Mueckler, M. M. Structural analysis of the GLUT1 facilitative glucose transporter. *Mol. Membr. Biol.* **18,** 183–193 (2001).

56. Mueckler, M. & Makepeace, C. Transmembrane segment 6 of the Glut1 glucose transporter is an outer helix and contains amino acid side chains essential for transport activity. *J. Biol. Chem.* **283,** 11550–5 (2008).

57. Alisio, A. & Mueckler, M. Purification and characterization of mammalian glucose transporters expressed in Pichia pastoris. *Protein Expr. Purif.* **70,** 81–7 (2010).

58. *Transporters As Targets for Drugs*. **4,** (Springer Berlin Heidelberg, 2009).

59. Chaudhary, S., Pak, J. E., Gruswitz, F., Sharma, V. & Stroud, R. M. Overexpressing human membrane proteins in stably transfected and clonal human embryonic kidney 293S cells. *Nat. Protoc.* **7,** 453–66 (2012).

60. Hresko, R. C., Murata, H., Marshall, B. A. & Mueckler, M. Discrete structural domains determine differential endoplasmic reticulum to Golgi transit times for glucose transporter isoforms. *J. Biol. Chem.* **269,** 32110–9 (1994).

61. Mitsumoto, Y. & Klip, A. Development regulation of the subcellular distribution and glycosylation of GLUT1 and GLUT4 glucose transporters during myogenesis of L6 muscle cells. *J. Biol. Chem.* **267,** 4957–62 (1992).

62. *Membrane proteins – Engineering, Purification and Crystallization*. (Elsevier Science, 2015). at <https://books.google.com/books?id=8vGcBAAAQBAJ&pgis=1>

63. Chae, P., Rasmussen, S., Rana, R. & Gotfryd, K. Maltose-neopentyl glycol (MNG) amphiphiles for solubilization, stabilization and crystallization of membrane proteins. *Nat. Methods* **7,** (2010).

64. Collins, T. *et al.* A nondetergent sulfobetaine prevents protein aggregation in microcalorimetric studies. *Anal. Biochem.* **352,** 299–301 (2006).

65. Expert-Bezançon, N., Rabilloud, T., Vuillard, L. & Goldberg, M. E. Physical-chemical features of non-detergent sulfobetaines active as protein-folding helpers. *Biophys. Chem.* **100,** 469–79 (2003).

66. Postis, V. L. G. *et al.* A high-throughput assay of membrane protein stability. *Mol. Membr. Biol.* **25,** 617–624 (2008).

67. Engel, C. K., Chen, L. & Privé, G. G. Stability of the lactose permease in detergent solutions. *Biochim. Biophys. Acta - Biomembr.* **1564,** 47–56 (2002).

68. Hresko, R. C., Kraft, T. E., Tzekov, A., Wildman, S. a. & Hruz, P. W. Isoform-selective inhibition of facilitative glucose transporters: Elucidation of the molecular mechanism of HIV protease inhibitor binding. *J. Biol. Chem.* **289,** 16100–16113 (2014).

69. Yano, Y. & May, J. M. Ligand-induced conformational changes modify proteolytic cleavage of the adipocyte insulin-sensitive glucose transporter. *Biochem. J.* **295 (Pt 1,** 183–188 (1993).

70. Boulter, J. M. & Wang, D. N. Purification and characterization of human erythrocyte glucose transporter in decylmaltoside detergent solution. *Protein Expr. Purif.* **22,** 337–48 (2001).

71. Haga, Y., Ishii, K. & Suzuki, T. N-Glycosylation Is Critical for the Stability and Intracellular Trafficking of Glucose Transporter GLUT4. *J. Biol. Chem.* **286,** 31320–31327 (2011).

72. Blot, V. & McGraw, T. E. Molecular mechanisms controlling GLUT4 intracellular retention. *Mol. Biol. Cell* **19,** 3477–87 (2008).

73. Leader, D. P. *et al.* Adipocytes Suggests Distinct Internalization Mechanisms Regulating

Cell. *Society* **543,** 535–543 (1999).

74. Firsov, D. *et al.* Cell surface expression of the epithelial Na channel and a mutant causing Liddle syndrome: a quantitative approach. *Proc. Natl. Acad. Sci. U. S. A.* **93,** 15370–5 (1996).

75. Voss, S. & Skerra, A. Mutagenesis of a flexible loop in streptavidin leads to higher affinity for the Strep-tag II peptide and improved performance in recombinant protein purification. *Protein Eng.* **10,** 975–82 (1997).

76. Crowe, J. *et al.* 6xHis-Ni-NTA chromatography as a superior technique in recombinant protein expression/purification. *Methods Mol. Biol.* **31,** 371–87 (1994).

77. Bornhorst, J. A. & Falke, J. J. Purification of proteins using polyhistidine affinity tags. *Methods Enzymol.* **326,** 245–54 (2000).

78. Cura, A. J. & Carruthers, A. Role of monosaccharide transport proteins in carbohydrate assimilation, distribution, metabolism, and homeostasis. *Compr. Physiol.* **2,** 863–914 (2012).

79. Yano, Y. & May, J. M. Ligand-induced conformational changes modify proteolytic cleavage of the adipocyte insulin-sensitive glucose transporter. *Biochem. J.* **295 (Pt 1,** 183–8 (1993).

80. Hu, X. *et al.* The abnormality of glucose transporter in the erythrocyte membrane of Chinese type 2 diabetic patients. *Biochim. Biophys. Acta - Biomembr.* **1466,** 306–314 (2000).

81. Hresko, R. C., Kraft, T. E., Tzekov, A., Wildman, S. a & Hruz, P. W. Isoform-selective inhibition of facilitative glucose transporters: elucidation of the molecular mechanism of HIV protease inhibitor binding. *J. Biol. Chem.* **289,** 16100–13 (2014).

82. Hresko, R. C. & Hruz, P. W. HIV Protease Inhibitors Act as Competitive Inhibitors of the Cytoplasmic Glucose Binding Site of GLUTs with Differing Affinities for GLUT1 and GLUT4. *PLoS One* **6,** e25237 (2011).

83. Privé, G. G. Detergents for the stabilization and crystallization of membrane proteins. *Methods* **41,** 388–97 (2007).

84. Tribet, C., Audebert, R. & Popot, J.-L. Amphipols: Polymers that keep membrane proteins soluble in aqueous solutions. *Proc. Natl. Acad. Sci.* **93,** 15047–15050 (1996).

85. Seddon, A. M., Curnow, P. & Booth, P. J. Membrane proteins, lipids and detergents: not just a soap opera. *Biochim. Biophys. Acta* **1666,** 105–17 (2004).

86. Bayburt, T. H. & Sligar, S. G. Membrane protein assembly into Nanodiscs. *FEBS Lett.* **584,** 1721–1727 (2010).

87. Liu, H. & Naismith, J. H. An efficient one-step site-directed deletion, insertion, single and multiple-site plasmid mutagenesis protocol. *BMC Biotechnol.* **8,** 91 (2008).

88. Reeves, P. J., Kim, J.-M. & Khorana, H. G. Structure and function in rhodopsin: a tetracycline-inducible system in stable mammalian cell lines for high-level expression of opsin mutants. *Proc. Natl. Acad. Sci. U. S. A.* **99,** 13413–8 (2002).

89. Kawate, T. & Gouaux, E. Fluorescence-detection size-exclusion chromatography for precrystallization screening of integral membrane proteins. *Structure* **14,** 673–81 (2006).

90. Zhang, Y. I-TASSER server for protein 3D structure prediction. *BMC Bioinformatics* **9,** 40 (2008).

91. Roy, A., Kucukural, A. & Zhang, Y. I-TASSER: a unified platform for automated protein structure and function prediction. *Nat. Protoc.* **5,** 725–738 (2010).

92. Yang, J. *et al.* The I-TASSER Suite: protein structure and function prediction. *Nat. Methods* **12,** 7–8 (2014).

93. Trott, O. & Olson, A. J. AutoDock Vina: improving the speed and accuracy of docking with a new scoring function, efficient optimization, and multithreading. *J. Comput. Chem.* **31,** 455–61 (2010).

94. Denisov, I. G., Grinkova, Y. V, Lazarides, a a & Sligar, S. G. Directed Self-Assembly of Monodisperse Phospholipid Bilayer Nanodiscs with Controlled Size Directed Self-Assembly of Monodisperse Phospholipid Bilayer Nanodiscs with Controlled Size. *Nano Lett.* 3477–3487 (2004). doi:10.1021/ja0393574

95. Knol, J., Sjollema, K. & Poolman, B. Detergent-mediated reconstitution of membrane proteins. *Biochemistry* **37,** 16410–5 (1998).

96. Tsirigos, K. D., Peters, C., Shu, N., Käll, L. & Elofsson, A. The TOPCONS web server for consensus prediction of membrane protein topology and signal peptides. *Nucleic Acids Res.* (2015). doi:10.1093/nar/gkv485

97. Inukai, K. *et al.* Replacement of both tryptophan residues at 388 and 412 completely abolished cytochalasin B photolabelling of the GLUT1 glucose transporter. *Biochem. J.* **302 (Pt 2,** 355–61 (1994).

98. Pawagi, a B. & Deber, C. M. Ligand-dependent quenching of tryptophan fluorescence in human erythrocyte hexose transport protein. *Biochemistry* **29,** 950–5 (1990).

99. Janmey, P. a. & Kinnunen, P. K. J. Biophysical properties of lipids and dynamic membranes. *Trends Cell Biol.* **16,** 538–546 (2006).

100. Bigay, J. & Antonny, B. Curvature, Lipid Packing, and Electrostatics of Membrane Organelles: Defining Cellular Territories in Determining Specificity. *Dev. Cell* **23,** 886–895 (2012).

101. Contreras, F., Ernst, A. M. & Wieland, F. Specificity of Intramembrane Protein − Lipid Interactions. *Cold Spring Harb. Perspect. Biol.* **3,** (2011).

102. daCosta, C. J. B., Dey, L., Therien, J. P. D. & Baenziger, J. E. A distinct mechanism for activating uncoupled nicotinic acetylcholine receptors. *Nat. Chem. Biol.* **9,** 701–707 (2013).

103. Kim, K.-H., Ahn, T. & Yun, C.-H. Membrane properties induced by anionic phospholipids and phosphatidylethanolamine are critical for the membrane binding and catalytic activity of human cytochrome P450 3A4. *Biochemistry* **42,** 15377–87 (2003).

104. Lee, S.-J. *et al.* Secondary anionic phospholipid binding site and gating mechanism in Kir2.1 inward rectifier channels. *Nat. Commun.* **4,** 1–12 (2013).

105. Marius, P. *et al.* Binding of Anionic Lipids to at Least Three Nonannular Sites on the Potassium Channel KcsA is Required for Channel Opening. *Biophys. J.* **94,** 1689–1698 (2008).

106. Rosenhouse-Dantsker, A., Mehta, D. & Levitan, I. Regulation of ion channels by membrane lipids. *Compr. Physiol.* **2,** 31–68 (2012).

107. Yeagle, P. L. Non-covalent binding of membrane lipids to membrane proteins. *Biochim. Biophys. Acta - Biomembr.* **1838,** 1548–1559 (2014).

108. Bogdanov, M. & Dowhan, W. Phospholipid-assisted protein folding: phosphatidylethanolamine is required at a late step of the conformational maturation of the polytopic membrane protein lactose permease. *The EMBO journal* **17,** 5255–64 (1998).

109. Thorens, B. & Mueckler, M. Glucose transporters in the 21st Century. *Am. J. Physiol. Endocrinol. Metab.* **298,** 141–145 (2010).

110. James, D. E., Brown, R., Navarro, J. & Pilch, P. F. Insulin-regulatable tissues express a unique insulin-sensitive glucose transport protein. *Nature* **333,** 183–5 (1988).

111. Bogan, J. S. Regulation of Glucose Transporter Translocation in Health and Diabetes. *Annu. Rev. Biochem.* (2012). doi:10.1146/annurev-biochem-060109-094246

112. Saltiel, A. R. & Kahn, C. R. Insulin signalling and the regulation of glucose and lipid metabolism. *Nature* **414,** 799–806 (2001).

113. Vannucci, S. J., Maher, F. & Simpson, I. A. Glucose transporter proteins in brain: delivery of glucose to neurons and glia. *Glia* **21,** 2–21 (1997).

114. Simpson, I. a *et al.* The facilitative glucose transporter GLUT3: 20 years of distinction. *Am. J. Physiol. Endocrinol. Metab.* **295,** E242–E253 (2008).

115. Weijers, R. N. M. Lipid composition of cell membranes and its relevance in type 2 diabetes mellitus. *Curr. Diabetes Rev.* **8,** 390–400 (2012).

116. Chem, J. B. & Field, J. Diet fat composition alters membrane phospholipid composition , insulin binding , and glucose metabolism in adipocytes from control and diabetic animals . C J Field , E A Ryan , A B Thomson and M T Clandinin Diet Fat Composition Alters Membrane Phospholip. *J. Biol. Chem* **265,** 11143–11150 (1990).

117. Tefft, R. E., Carruthers, A. & Melchior, D. L. Reconstituted human erythrocyte sugar transporter activity is determined by bilayer lipid head groups. *Biochemistry* **25,** 3709–18 (1986).

118. Pliotas, C. *et al.* The role of lipids in mechanosensation. *Nat. Struct. Mol. Biol.* 1–11

(2015). doi:10.1038/nsmb.3120

119. Laganowsky, A. *et al.* Membrane proteins bind lipids selectively to modulate their structure and function. *Nature* **510,** 172–175 (2014).

120. Bechara, C. *et al.* A subset of annular lipids is linked to the flippase activity of an ABC transporter. *Nat. Chem.* **7,** 255–262 (2015).

121. Kraft, T. E., Hresko, R. C. & Hruz, P. W. Expression, purification, and functional characterization of the insulin-responsive facilitative glucose transporter GLUT4. *Protein Sci.* **00,** n/a–n/a (2015).

122. Van Der Does, C., Swaving, J., Van Klompenburg, W. & Driessen, a. J. M. Non-bilayer lipids stimulate the activity of the reconstituted bacterial protein translocase. *J. Biol. Chem.* **275,** 2472–2478 (2000).

123. Hakizimana, P., Masureel, M., Gbaguidi, B., Ruysschaert, J. M. & Govaerts, C. Interactions between phosphatidylethanolamine headgroup and LmrP, a multidrug transporter: A conserved mechanism for proton gradient sensing? *J. Biol. Chem.* **283,** 9369–9376 (2008).

124. Vitrac, H., Bogdanov, M. & Dowhan, W. Proper fatty acid composition rather than an ionizable lipid amine is required for full transport function of lactose permease from Escherichia coli. *J. Biol. Chem.* **288,** 5873–5885 (2013).

125. Ingólfsson, H. I. *et al.* Lipid organization of the plasma membrane. *J. Am. Chem. Soc.* **136,** 14554–9 (2014).

126. Augustin, R. The protein family of glucose transport facilitators: It's not only about glucose after all. *IUBMB Life* **62,** 315–333 (2010).

127. Tamai, I. *et al.* Molecular and Functional Characterization of Organic Cation/Carnitine Transporter Family in Mice. *J. Biol. Chem.* **275,** 40064–40072 (2000).

128. Utsunomiya-Tate, N., Endou, H. & Kanai, Y. Cloning and functional characterization of a system ASC-like Na+-dependent neutral amino acid transporter. *J. Biol. Chem.* **271,** 14883–14890 (1996).

129. Oppedisano, F., Pochini, L., Galluccio, M. & Indiveri, C. The glutamine/amino acid transporter (ASCT2) reconstituted in liposomes: Transport mechanism, regulation by ATP

and characterization of the glutamine/glutamate antiport. *Biochim. Biophys. Acta - Biomembr.* **1768,** 291–298 (2007).

130. Pochini, L., Oppedisano, F. & Indiveri, C. Reconstitution into liposomes and functional characterization of the carnitine transporter from renal cell plasma membrane. *Biochim. Biophys. Acta* **1661,** 78–86 (2004).

131. Kobayashi, D., Irokawa, M., Maeda, T., Tsuji, A. & Tamai, I. Carnitine/organic cation transporter OCTN2-mediated transport of carnitine in primary-cultured epididymal epithelial cells. *Reproduction* **130,** 931–937 (2005).

132. Wieczorke, R., Dlugai, S., Krampe, S. & Boles, E. Characterisation of mammalian GLUT glucose transporters in a heterologous yeast expression system. *Cell. Physiol. Biochem.* **13,** 123–134 (2003).

133. Neale, C., Herce, H. D., Pomès, R. & Garcia, A. Can Specific Protein-Lipid Interactions Stabilize an Active State of the Beta 2 Adrenergic Receptor? *Biophys. J.* **109,** 1652–1662 (2015).

134. Brown, M. F. Curvature forces in membrane lipid-protein interactions. *Biochemistry* **51,** 9782–9795 (2012).

135. Tefft, R. E., Carruthers, A. & Melchior, D. L. Reconstituted human erythrocyte sugar transporter activity is determined by bilayer lipid head groups. *Biochemistry* **25,** 3709–18 (1986).

136. Ansell, G. B., Hawthorne, J. N. & Dawson, R. M. C. *Form and function of phospholipids*. (Elsevier Scientific Pub. Co., 1973).

137. Parrish, C. C., Myher, J. J., Kuksis, A. & Angel, A. Lipid structure of rat adipocyte plasma membranes following dietary lard and fish oil. *Biochim. Biophys. Acta - Biomembr.* **1323,** 253–262 (1997).

138. Ray, T. K., Skipski, V. P., Barclay, M., Essner, E. & Archibald, F. M. Lipid Composition of Rat Liver Plasma Membranes. *J. Biol. Chem.* **244,** 5528–5536 (1969).

139. World Health Organization. World malaria report 2014. 165–176 (2014). doi:10.1007/s00108-013-3390-9

140. Hobbs, C. V. *et al.* HIV treatments reduce malaria liver stage burden in a non-human primate model of malaria infection at clinically relevant concentrations in vivo. *PLoS One* **9,** e100138 (2014).

141. Nalam, M. N. L. & Schiffer, C. A. New approaches to HIV protease inhibitor drug design II: testing the substrate envelope hypothesis to avoid drug resistance and discover robust inhibitors. *Curr. Opin. HIV AIDS* **3,** 642–6 (2008).

142. Banerjee, R. *et al.* Four plasmepsins are active in the Plasmodium falciparum food vacuole, including a protease with an active-site histidine. *Proc. Natl. Acad. Sci.* **99,** 990–995 (2002).

143. Boddey, J. A. *et al.* An aspartyl protease directs malaria effector proteins to the host cell. *Nature* **463,** 627–631 (2010).

144. Hresko, R. C. & Hruz, P. W. HIV Protease Inhibitors Act as Competitive Inhibitors of the Cytoplasmic Glucose Binding Site of GLUTs with Differing Affinities for GLUT1 and GLUT4. *PLoS One* **6,** e25237 (2011).

145. Murata, H., Hruz, P. W. & Mueckler, M. The mechanism of insulin resistance caused by HIV protease inhibitor therapy. *J. Biol. Chem.* **275,** 20251–20254 (2000).

146. Murata, H., Hruz, P. W. & Mueckler, M. Indinavir inhibits the glucose transporter isoform Glut4 at physiologic concentrations. *AIDS* **16,** 859–863 (2002).

147. Woodrow, C. J., Penny, J. I. & Krishna, S. Intraerythrocytic Plasmodium falciparum expresses a high affinity facilitative hexose transporter. *J. Biol. Chem.* **274,** 7272–7 (1999).

148. Kirk, K. Membrane transport in the malaria-infected erythrocyte. *Physiol. Rev.* **81,** 495–537 (2001).

149. Mehta, M., Sonawat, H. M. & Sharma, S. Glycolysis in Plasmodium falciparum results in modulation of host enzyme activities. 95–103 (2006).

150. Blume, M. *et al.* A constitutive pan-hexose permease for the Plasmodium life cycle and transgenic models for screening of antimalarial sugar analogs. *FASEB J.* **25,** 1218–29 (2011).

151. Bergshoeff, A. S. *et al.* Increased dose of lopinavir/ritonavir compensates for efavirenz-induced drug-drug interaction in HIV-1-infected children. *J. Acquir. Immune Defic. Syndr.* **39,** 63–68 (2005).

152. Rosso, R. *et al.* Lopinavir/ritonavir exposure in treatment-naive HIV-infected children following twice or once daily administration. *J. Antimicrob. Chemother.* **57,** 1168–1171 (2006).

153. Best, B. M. *et al.* Lopinavir tablet pharmacokinetics with an increased dose during pregnancy. *J. Acquir. Immune Defic. Syndr.* **54,** 381–388 (2010).

154. Murphy, R. L. *et al.* ABT-378/ritonavir plus stavudine and lamivudine for the treatment of antiretroviral-naive adults with HIV-1 infection: 48-week results. *AIDS* **15,** F1–F9 (2001).

155. Slavic, K. *et al.* Life cycle studies of the hexose transporter of Plasmodium species and genetic validation of their essentiality. *Mol. Microbiol.* **75,** 1402–13 (2010).

156. Grunfeld, C. *et al.* Contribution of metabolic and anthropometric abnormalities to cardiovascular disease risk factors. *Circulation* **118,** e20–8 (2008).

157. Hruz, P. W., Murata, H., Qiu, H. & Mueckler, M. Indinavir Induces Acute and Reversible Peripheral Insulin Resistance in Rats. *Diabetes* **51,** 937–942 (2002).

158. Noor, M. A. *et al.* Metabolic effects of indinavir in healthy HIV-seronegative men. *AIDS* **15,** F11–8 (2001).

159. Noor, M. A., Flint, O. P., Maa, J.-F. & Parker, R. A. Effects of atazanavir/ritonavir and lopinavir/ritonavir on glucose uptake and insulin sensitivity: demonstrable differences in vitro and clinically. *AIDS* **20,** 1813–1821 (2006).

160. Ortiz, D. *et al.* Identification of Selective Inhibitors of the Plasmodium falciparum Hexose Transporter PfHT by Screening Focused Libraries of Anti-Malarial Compounds. *PLoS One* **10,** e0123598 (2015).

161. Zhang, B. *et al.* A second target of the antimalarial and antibacterial agent fosmidomycin revealed by cellular metabolic profiling. *Biochemistry* **50,** 3570–7 (2011).

162. Trager, W. & Jensen, J. B. Human malaria parasites in continuous culture. *Science* **193,** 673–5 (1976).

163. Corbett, Y. *et al.* A novel DNA-based microfluorimetric method to evaluate antimalarial drug activity. *Am. J. Trop. Med. Hyg.* **70,** 119–24 (2004).

164. Chaudhary, S., Pak, J. E., Gruswitz, F., Sharma, V. & Stroud, R. M. Overexpressing human membrane proteins in stably transfected and clonal human embryonic kidney 293S cells. *Nat. Protoc.* **7,** 453–66 (2012).

165. Aerni-Flessner, L., Abi-Jaoude, M., Koenig, A., Payne, M. & Hruz, P. W. GLUT4, GLUT1, and GLUT8 are the dominant GLUT transcripts expressed in the murine left ventricle. *Cardiovasc. Diabetol.* **11,** 63 (2012).

166. Wells, T. N. C., van Huijsduijnen, R. H. & Van Voorhis, W. C. Malaria medicines: a glass half full? *Nat. Rev. Drug Discov.* **14,** 424–442 (2015).

167. Sachs, J. & Malaney, P. The Economic and Social Burden of Malaria. *Nature* **415,** 680–685 (2002).

168. Ashley, E. A. *et al.* Spread of Artemisinin Resistance in *Plasmodium falciparum* Malaria. *N. Engl. J. Med.* **371,** 411–423 (2014).

169. Staines, H. M. *et al.* Exploiting the therapeutic potential of Plasmodium falciparum solute transporters. *Trends Parasitol.* **26,** 284–296 (2010).

170. Kraft, T. E., Armstrong, C., Heitmeier, M. R., Odom, A. R. & Hruz, P. W. The Glucose Transporter PfHT1 Is an Antimalarial Target of the HIV Protease Inhibitor Lopinavir. *Antimicrob. Agents Chemother.* **59,** 6203–6209 (2015).

171. Williams, J. B. *et al.* Development of a scintillation proximity assay for analysis of Na+/Cl−-dependent neurotransmitter transporter activity. *Anal. Biochem.* **321,** 31–37 (2003).

172. Gui, C., Obaidat, A., Chaguturu, R. & Hagenbuch, B. Development of a cell-based high-throughput assay to screen for inhibitors of organic anion transporting polypeptides 1B1 and 1B3. *Curr. Chem. Genomics* **4,** 1–8 (2010).

173. Hou, B.-H. *et al.* Optical sensors for monitoring dynamic changes of intracellular metabolite levels in mammalian cells. *Nat. Protoc.* **6,** 1818–33 (2011).

174. Zhang, J.-H. A Simple Statistical Parameter for Use in Evaluation and Validation of High

Throughput Screening Assays. *J. Biomol. Screen.* **4,** 67–73 (1999).

175. Spangenberg, T. *et al.* The open access malaria box: a drug discovery catalyst for neglected diseases. *PLoS One* **8,** e62906 (2013).

176. Katsuno, K. *et al.* Hit and lead criteria in drug discovery for infectious diseases of the developing world. *Nat. Rev. Drug Discov.* 1–8 (2015). doi:10.1038/nrd4683

177. Muretta, J. M. *et al.* High-performance time-resolved fluorescence by direct waveform recording. *Rev. Sci. Instrum.* **81,** 103101 (2010).

178. Petersen, K. J. *et al.* Fluorescence lifetime plate reader: Resolution and precision meet high-throughput. *Rev Sci Instrum* **85,** 113101 (2014).

179. Hresko, R. C. & Hruz, P. W. HIV Protease Inhibitors Act as Competitive Inhibitors of the Cytoplasmic Glucose Binding Site of GLUTs with Differing Affinities for GLUT1 and GLUT4. *PLoS One* **6,** e25237 (2011).

180. NIH National Cancer Institute. SEER Cancer Stat Fact Sheets. at <http://seer.cancer.gov/statfacts/>

181. Hansen, S. B. Lipid agonism: The PIP2 paradigm of ligand-gated ion channels. *Biochim. Biophys. Acta* **1851,** 620–8 (2015).

182. Rosenhouse-Dantsker, A., Mehta, D. & Levitan, I. Regulation of ion channels by membrane lipids. *Compr. Physiol.* **2,** 31–68 (2012).

183. Mouritsen, O. G. & Zuckermann, M. J. What's so special about cholesterol? *Lipids* **39,** 1101–13 (2004).

184. Levitan, I., Fang, Y., Rosenhouse-Dantsker, A. & Romanenko, V. Cholesterol and ion channels. *Subcell. Biochem.* **51,** 509–49 (2010).

185. Fürst, O. & D'Avanzo, N. Isoform dependent regulation of human HCN channels by cholesterol. *Sci. Rep.* **5,** 14270 (2015).

186. Paila, Y. D. & Chattopadhyay, A. Membrane cholesterol in the function and organization of G-protein coupled receptors. *Subcell. Biochem.* **51,** 439–66 (2010).

187. Hanson, M. A. *et al.* A specific cholesterol binding site is established by the 2.8 A

structure of the human beta2-adrenergic receptor. *Structure* **16,** 897–905 (2008).

188. Paila, Y. D., Tiwari, S. & Chattopadhyay, A. Are specific nonannular cholesterol binding sites present in G-protein coupled receptors? *Biochim. Biophys. Acta* **1788,** 295–302 (2009).

189. Prasanna, X., Chattopadhyay, A. & Sengupta, D. Cholesterol modulates the dimer interface of the β2-adrenergic receptor via cholesterol occupancy sites. *Biophys. J.* **106,** 1290–300 (2014).

190. Caliceti, C. *et al.* Effect of Plasma Membrane Cholesterol Depletion on Glucose Transport Regulation in Leukemia Cells. *PLoS One* **7,** e41246 (2012).

191. Barnes, K., Ingram, J. C., Bennett, M. D. M., Stewart, G. W. & Baldwin, S. a. Methyl-beta-cyclodextrin stimulates glucose uptake in Clone 9 cells: a possible role for lipid rafts. *The Biochemical journal* **378,** 343–351 (2004).

192. Nowis, D. *et al.* Statins impair glucose uptake in human cells. *BMJ open diabetes Res. care* **2,** e000017 (2014).

193. Ha, T. *et al.* Probing the interaction between two single molecules: fluorescence resonance energy transfer between a single donor and a single acceptor. *Proc. Natl. Acad. Sci. U. S. A.* **93,** 6264–8 (1996).